



# Final report

Project Title: Development of microemulsion-based gel from oil extracts of Plai (*Zingiber cassumunar* Roxb.) for anti-inflammatory activity

By Wantida Chaiyana

# **Final report**

Project Title: Development of microemulsion-based gel from oil extracts of Plai (*Zingiber cassumunar* Roxb.) for anti-inflammatory activity

Researcher Institute

1. Wantida Chaiyana Chiang Mai University

2. Rungsinee Phongpradist Chiang Mai University

This project granted by the Thailand Research Fund

Project Code: TRG 5780029

Project Title: Development of microemulsion-based gel from oil extracts of Plai

(Zingiber cassumunar Roxb.) for anti-inflammatory activity

Investigator: Wantida Chaiyana, Faculty of Pharmacy, Chiang Mai University

E-mail Address: wantida.chaiyana@gmail.com

Project Period: 2 years

#### **Abstract**

Zingiber cassumunar Roxb. (Plai) is an aromatic plant which is widely distributed in various parts of Thailand which has been used in folklore remedies for the treatment of many conditions especially rheumatism and muscular pain. The present study focused on the chemical constituents and anti-inflammatory effects of EO and HO. Moreover, microemulsions and microemulsion-based gel from EO and HO were developed to increase the stability of the oils and facilitate user's compliance in transdermal route of application.

EO was obtained by hydrodistillation. The major constituents determined by GC-MS were terpinen-4-ol (40.5±6.6%) and sabinene (17.4±1.4%). HO was obtained by hot infusion in coconut oil and the major constituent after TLC and HPLC analysis was curcumin. EO and HO were considered safe as they did not affect normal cell survival in human peripheral blood mononuclear cells, as determined by MTT assay. The native oils and major constituents were investigated for anti-inflammatory activities by albumin denaturation assay. Nuclear factor-kappa B expression in human leukemic monocyte lymphoma cell line (U937) and inhibition of interleukin-6 secretion in mouse monocyte macrophage cell line (RAW 264.7) was investigated using Western blotting and enzyme-linked immunosorbent assay, respectively. Both oils possessed anti-inflammatory effect. Terpinen-4-ol and sabinene were shown to be responsible for the anti-inflammatory effect of EO.

HLB values of HO and EO determined by external appearance inspection, droplet size analysis, and turbidimetric method were 6 and 10, respectively. Various factors affecting microemulsion region in the pseudoternary phase diagrams was investigated and the results indicated that surfactant type, co-surfactant type, and surfactant to co-surfactant ratio showed distinct effects on the microemulsion formation,

i

whereas, ionic strength and pH had no effect. Microemulsions from the system of "EO/Tween 20/propylene glycol/water" and "HO and oleic acid (1:1)/Triton X-114/propan-2-ol/water" were developed and characterized. The internal droplet size of EO microemulsion were in the range of 211.5 to 366.7 nm with medium polydispersity index (less than 0.38), whereas, the internal droplet size of HO microemulsion were in the range of 26.7 to 31.6 nm with small polydispersity index (less than 0.25). All formulation were transparent and showed Newtonian's flow behavior with low viscosity which were the characteristics of microemulsion. All microemulsion showed a good stability after the heating-cooling stability test and tended to protect EO from the evaporation, as well as, protect HO from the oxidation and reduce the occurrence of rancidity. Microemulsion of EO and HO were considered safe as the cell viabilities of human PBMCs after treatments were around 80%. The microemulsions of both EO and HO showed remarkable effect on NF-κB suppression.

Microemulsion-based gels, developed using carbopol 940 and sodium carboxymethylcellulose, had more aesthetic appearance than gels containing the native oils. The microemulsion-based gels containing EO showed the best characteristics with 2.5%w/w carbopol 940 and 2.5%w/w SCMC, whereas, those of HO showed the best characteristics with 1%w/w carbopol 940 and 2%w/w SCMC. However, there were significantly decrease in viscosity in the system of 2.5%w/w SCMC of microemulsion-based gel of EO. Moreover, the instability was observed in the formulations contained higher amount of corbopol 940 accompanied with higher content of water in the microemulsions. In conclusions, 2.5%w/w carbopol 940 is the best choice for microemulsion-based gel development of EO and 2%w/w SCMC is the best choice for microemulsion-based gel development of HO. The microemulsion-based gels would be the aesthetic formulation for the topical treatment of various inflammatory conditions, such as muscle pains, sprains, strains, arthritis, etc. It might be used for drug delivery system for topical application.

**Keywords:** Zingiber cassumunar, Anti-inflammation, Microemulsion, Microemulsion, based gel, Essential oil, Hot infused oil

รหัสโครงการ: TRG 5780029

หัวข้อ: การพัฒนาตำรับไมโครอิมัลชั้นเจลจากสารสกัดไพลที่มีฤทธิ์ต้าน

การอักเสบ

หัวหน้าโครงการ: ดร.วรรธิดา ชัยญาณะ คณะเภสัชศาสตร์ มหาวิทยาลัยเชียงใหม่

อีเมล์ : wantida.chaiyana@gmail.com

ระยะเวล: 2 ปี

# บทคัดย่อ

ไพล (Zingiber cassumunar Roxb.) เป็นพืชที่มีการปลูกทั่วไปในประเทศไทย ซึ่งมีการ ใช้ในการรักษาอาการต่างๆ เช่น ปวดข้อ ปวดกล้ามเนื้อ มาตั้งแต่สมัยโบราณ การศึกษานี้ มุ่งเน้นไปที่การศึกษาองค์ประกอบและฤทธิ์ต้านการอักเสบของน้ำมันหอมระเหย (EO) และ น้ำมันไพลสกัดร้อน (HO) นอกจากนี้ยังได้ทำการพัฒนาตำรับไมโครอิมัลชันและไมโครอิมัลชัน เจลที่มีองค์ประกอบของ EO และ HO เพื่อเพิ่มความคงตัวของน้ำมันและช่วยให้มีความสะดวก ในการใช้ทาภายนอกมากยิ่งขึ้น

EO ได้จากการกลั่นด้วยไอน้ำ โดยองค์ประกอบหลักที่วิเคราะห์ด้วยแก๊สโครมาโตกราฟิ ได้แก่ terpinen-4-ol ปริมาณร้อยละ 40.5±6.6 และ sabinene ปริมาณร้อยละ 17.4±1.4 ส่วน HO ได้จากการแช่ไพลสดในน้ำมันมะพร้าวที่ร้อน ซึ่งองค์ประกอบหลักที่วิเคราะห์ด้วยโครมาโตกราฟิสมรรถนะสูง คือ curcumin โดยทั้ง EO และ HO ที่ได้มีความปลอดภัยสูง เนื่องจากไม่มีผลต่อความอยู่รอดของเซลล์เม็ดเลือดขาวมนุษย์ ซึ่งทำการ วิเคราะห์ด้วยวิธี MTT ในการศึกษานี้ได้ทำการทดสอบฤทธิ์ต้านการอักเสบของทั้งน้ำมันจากไพลและองค์ประกอบหลักข้างต้น โดยการศึกษาการยับยั้งการสลายตัวของอัลบูมิน ศึกษาการ ยับยั้งการแสดงออกของ NF-kB ด้วยวิธีเวสเทิร์นบลอตในเซลล์มะเร็งต่อมน้ำเหลืองมนุษย์ (U937) ศึกษาการยับยั้งการหลังอินเตอร์ลิวคิน-6 (IL-6) ด้วยเทคนิคเอนไซม์-ลิงค์ อิมมูโนซอร์ เบนท์ แอสเซย์ ในเซลล์เม็ดเลือดขาวหนู (RAW 264.7) ซึ่งจากการศึกษาพบว่าน้ำมันท้ะงสอง ชนิดมีฤทธิ์ต้านการอักเสบ โดย terpinen-4-ol และ sabinene เป็นสารสำคัญที่มีผลต่อฤทธิ์ต้าน การอักเสบของ EO

จากการศึกษาค่า HLB ของ EO และ HO ด้วยวิธีการสังเกตลักษณะภายนอก การวัด ขนาดอนุภาคภายใน และการวัดความขุ่น พบว่า EO มีค่า HLB เท่ากับ 10 และ HO มีค่า HLB เท่ากับ 6 จากการศึกษาปัจจัยต่าง ๆที่ผลต่อการไมโครอิมัลชันในแผนผังวัฏภาคสามเหลี่ยมแบบ เทียม พบว่าชนิดของสารลดแรงตึงผิว ชนิดของสารช่วยสารลดแรงตึงผิว และสัดส่วนของสารลด แรงตึงผิวต่อสารช่วยสารลดแรงตึงผิว มีผลต่อการเกิดไมโครอิมัลชัน ในขณะที่ความเข้มขันของ ประจุและค่าความเป็นกรด-ด่างไม่มีผล ในการศึกษานี้ได้พัฒนาและศึกษาคุณลักษณะของไมโครอิมัลชันในแผนผังวัฏภาคสามเหลี่ยมแบบเทียมของ "EO / Tween 20 / propylene glycol / water" และ "HO and oleic acid (1:1) / Triton X-114 / propan-2-ol / water" ซึ่งพบว่าไมโคร

อิมัลชันของ EO มีขนาดอนุภาคภายในอยู่ในช่วง 211.5 ถึง 366.7 นาโนเมตร และมีการ กระจายขนาดอนุภาคปานกลาง (น้อยกว่า 0.38) ในขณะที่ไมโครอิมัลชันของ HO มีขนาด อนุภาคภายในเล็กกว่าอยู่ในช่วง 26.7 ถึง 31.6 นาโนเมตร และมีการกระจายขนาดอนุภาคปาน น้อย (น้อยกว่า 0.25) ไมโครอิมัลชันทุกตำรับที่ได้มีลักษณะใส มีการไหลแบบนิวโทเนียน และมี ความหนืดต่ำ ซึ่งเป็นคุณลักษณะของไมโครอิมัลชัน นอกจากนี้ยังมีความคงตัวทางกายภาพดี และสามารถป้องกันการระเหยของสารองค์ประกอบหลักของ EO ทั้งยังช่วยลดการเกิดปฏิกิริยา ออกซิเดชันของ HO ได้อีกด้วย ซึ่งจะช่วยลดปัญหาการเหม็นหืนของตำรับได้ ทั้งไมโครอิมัลชัน ของ EO และ HO มีความปลอดภัยสูง เนื่องจากเซลล์เม็ดเลือดขาวของมนุษย์มีความอยู่รอดสูง ถึงร้อยละ 80 นอกจากนี้ยังมีฤทธิ์ต้านการอักเสบที่ดี โดยสามารถลดการแสดงออกของ NF-<sub>K</sub>B อย่างมีนัยสำคัญทางสถิติ

ในการพัฒนาไมโครอิมัลชั้นเจล ได้ใช้สารก่อเจลสองชนิด คือ คาร์โบพอล 940 และ โซเดียมคาร์บอกซีเมทธิลเซลลูโลส ซึ่งพบว่าไมโครอิมัลชั้นเจลมีลักษณะทางกายภาพที่สวยงาม น่าใช้มากกว่าตำรับเจลที่ผสมน้ำมันโดยตรง ไมโครอิมัลชั้นเจลของ EO มีคุณลักษณะดีที่สุดเมื่อ ใช้ คาร์โบพอล 940 ร้อยละ 2.5 โดยน้ำหนัก และโซเดียมคาร์บอกซีเมทธิลเซลลูโลสร้อยละ 2.5 โดยน้ำหนักเป็นสารก่อเจล ในขณะที่ไมโครอิมัลชั้นเจลของ HO มีคุณลักษณะดีที่สุดเมื่อใช้ คาร์ โบพอล 940 ร้อยละ 1 โดยน้ำหนัก และโซเดียมคาร์บอกซีเมทธิลเซลลูโลสร้อยละ 2 โดย ้น้ำหนักเป็นสารก่อเจล แต่อย่างไรก็ตามตำรับไมโครอิมัลชั้นเจลของ EO ที่ใช้โซเดียมคาร์บอกซี เมทธิลเซลลูโลสร้อยละ 2.5 โดยน้ำหนักเป็นสารก่อเจลมีความหนืดลดลงอย่างมีนัยสำคัญทาง สถิติภายหลังจากการศึกษาความคงสภาพ และคาร์โบพอล 940 ในความเข้มข้นสูงมักเกิดความ ไม่เข้ากันกับตำรับไมโครอิมัลชั้นเจลของ HO ที่มีปริมาณน้ำในตำรับสูง ดังนั้นโดยสรุปแล้ว คาร์ โบพอล 940 ร้อยละ 2.5 โดยน้ำหนักมีความเหมาะสมที่สุดในการพัฒนาไมโครอิมัลชันเจลของ EO และโซเดียมคาร์บอกซีเมทธิลเซลลูโลสร้อยละ 2 มีความเหมาะสมที่สุดในการพัฒนาไมโคร อิมัลชั้นเจลของ HO และไมโครอิมัลชั้นเจลจากน้ำมันไพลเป็นตำรับที่มีความสวยงามน่าใช้ สำหรับการรักษาภาวะการอักเสบต่างๆ เช่น อาการปวดกล้ามเนื้อ เกร็ง เคล็ดขัดยอก หรือโรค ไขข้อ เป็นต้น นอกจากนี้ยังสามารถนำมาใช้เป็นระบบสำหรับนำส่งยาเพื่อการรักษาภายนอกได้ **อีกด้**วย

**คำสำคัญ :** ไพล, ต้านการอักเสบ, ไมโครอิมัลชัน, ไมโครอิมัลชันเจล, น้ำมันหอมระเหย, น้ำมันสกัดร้อน

Project Code: TRG 5780029

Project Title: Development of microemulsion-based gel from oil extracts of Plai

(Zingiber cassumunar Roxb.) for anti-inflammatory activity

Investigator: Wantida Chaiyana, Faculty of Pharmacy, Chiang Mai University

**E-mail Address :** wantida.chaiyana@gmail.com

Project Period: 2 years

# **Executive summary**

#### 1. Introduction

Zingiber cassumunar Roxb. (Plai) is an aromatic plant which is widely distributed in various parts of Thailand which has been used in folklore remedies for the treatment of many conditions especially rheumatism and muscular pain. The rhizome part has been used as a component in herbal compress balls and massage oil for muscular pain relief since the ancient time. Recently, there are many studies related to antiinflammatory activity of Z. cassumunar which is a pathogenesis of muscular pain and rheumatism. In those studies, Z. cassumunar were extracted by using solvent extraction or hydrodistillation. But the hot infusion has not been investigated. Therefore, the present study focused on anti-inflammatory activity of both essential oil (EO) and hot oil infusion (HO). However, the usage of the oil encountered with the stability problems. HO is easily rancid because of oxidation after a long time of heating in the extraction process, whereas, EO can easily evaporate even in a normal condition of storage. The rancidity of HO and evaporation of EO may alter the chemical compositions and affect the biological activities. Incorporation of these oils into the internal phase of microemulsion might be an alternative approach to solve the problems since microemulsions (isotropic, transparent, and thermodynamically stable colloidal systems) provided protective effect against oxidation and retarded the degradation rate of some active compound. Moreover, it was demonstrated that permeation rates from microemulsions were significantly higher than that of conventional formulations which leads microemulsion to be a useful vehicle to enhance transdermal drug permeability. Therefore, the present study aims to investigate the chemical constituents and antiinflammatory effects of EO and HO. Moreover, microemulsions and microemulsionbased gel from HO and EO were developed to increase the stability of the oils and facilitate user's compliance in transdermal route of application.

#### 2. Objectives

- 2.1 To construct fingerprints and characterize EO and HO for quality control applications
- 2.2 To determine anti-inflammatory activity and cytotoxicity of EO and HO
- 2.3 To reduce the rancidity of HO and evaporation of EO by incorporation into microemulsions
- 2.4. To develop microemulsion-based gel from EO and HO

#### 3. Method

#### 3.1. Oil extraction

The *Z. cassumunar* rhizome was subjected to hydrodistillation using a cleavenger type apparatus to obtain EO and fried in heated coconut oil to obtain HO.

#### 3.2. Characterization of HO

Acid value was determined by indirect titration method (Kardash and Tur'yan, 2005). Iodine value and saponification value were determined according to AOCS official method with slight modification (Official and Tentative Methods of the American Oil Chemists' Society, 1984).

#### 3.3. Chemical composition analysis

Chemical compositions of EO were analyzed by GC-MS, wherras, that of HO were analyzed by TLC and HPLC.

#### 3.4. Cell cytotoxicity

The effects of EO, HO, and microemulsion of both oils on cell viability of peripheral blood mononuclear cells (PBMCs) were determined by a colorimetric technique, which were MTT assay (Phongpradist et al., 2010).

# 3.5. Anti-inflammatory activity

The native oils and major constituents were investigated for anti-inflammatory activities by albumin denaturation assay. Nuclear factor-kappa B expression in human leukemic monocyte lymphoma cell line (U937) and inhibition of interleukin-6 secretion in mouse monocyte macrophage cell line (RAW 264.7) was investigated using Western blotting and enzyme-linked immunosorbent assay, respectively.

The anti-inflammatory activities of microemulsions were evaluated by inhibitory activities of albumin denaturation and NF-<sub>K</sub>B expression.

#### 3.6. Formulation Development

#### 3.6.1. Determination of required HLB

The required HLB values of EO and HO were determined by droplet size analysis and turbidimetric method.

#### 3.6.2. Pseudoternary phase diagram construction

Pseudoternary phase diagrams were constructed using a water titration method. Various co-surfactant and surfactant to co-surfactant ratio were involved in the study as the factors affecting microemulsion area existed in the phase diagram.

#### 3.6.3. Characterization of selected blank microemulsion

Microemulsions were characterized by means of particle size/size distribution, electrical conductivity, rheology profile and pH. To study the stability, the microemulsions were subjected to heating-cooling study and characterized again. The rancidity of HO microemulsions was determined by means of peroxidation value. The evaporation of EO microemulsions was determined by GC-MS.

#### 3.6.4. Microemulsion-based gel development

Gelling agents including carbopol 940 and sodium carboxymethylcellulose were used for the microemulsion-based gel development. The gel bases were previously prepared at the concentration of 2%w/w, 3%w/w, and 5%w/w. Then 50%w/w of microemulsion was incorporated into the gel base.

#### 3.6.5. Characterization of microemulsion-based gel

Microemulsion-based gels were characterized by means of rheology profile and pH. To study the stability, the microemulsion-based gels were subjected to heating/cooling study and characterized again.

#### 4. Results and discussion

The major constituents of EO were terpinen-4-ol (40.5±6.6%) and sabinene (17.4±1.4%), whereas, that of HO was curcumin. EO and HO were considered safe as they did not affect normal cell survival in human peripheral blood mononuclear cells, as determined by MTT assay.

Both EO and HO possessed significant anti-inflammatory activities in albumin denaturation assay with the  $IC_{50}$  values of 12±4 and 10±2  $\mu$ g/mL, respectively when

compared to indomethacin (6±3 µg/mL) as a positive control. Moreover, EO was more conspicuous to suppress NF-<sub>K</sub>B than HO by 42±3% and 36±4%, respectively. The activity of EO was correlated to the active compounds, terpinen-4-ol and sabinene that suppressed NF-<sub>K</sub>B by 47±5% and 78±8%, respectively. The terpinen-4-ol and sabinene significantly reduced IL-6 secretion levels to 82±2% and 80±7%, respectively.

HLB values of HO and EO were 6 and 10, respectively. Surfactant type, cosurfactant type, and surfactant to co-surfactant ratio showed distinct effects on the microemulsion formation, whereas, ionic strength and pH had no effect. Microemulsions from the system of "EO/Tween 20/propylene glycol/water" and "HO and oleic acid (1:1)/Triton X-114/propan-2-ol/water" were developed and characterized. The internal droplet size of EO microemulsion were in the range of 211.5 to 366.7 nm with medium polydispersity index (less than 0.38), whereas, the internal droplet size of HO microemulsion were in the range of 26.7 to 31.6 nm with small polydispersity index (less than 0.25). All formulation showed Newtonian's flow behaviour. The viscosity of EO microemulsions were in the range of 0.65 to 0.84 mPas, whereas, that of HO microemulsions were in the range of 0.015 to 0.024 mPas. The pH of each microemulsions was in the range of 3.9 to 5.5. All microemulsion showed a good stability after the heating-cooling stability test. Moreover, microemulsion tended to protect EO from the evaporation and protect HO from the oxidation and reduce the occurrence of rancidity. Microemulsion of EO and HO were considered safe as the cell viabilities of human PBMCs after treatments were around 80%. The microemulsions of both EO and HO showed remarkable effect on NF-<sub>K</sub>B suppression.

Microemulsion-based gels, developed using carbopol 940 and sodium carboxymethylcellulose, had more aesthetic appearance than gels containing the native oils. The formulations of EO showed the best characteristics with 2.5%w/w carbopol 940 and 2.5%w/w SCMC, whereas, the formulations of HO showed the best characteristics with 1%w/w carbopol 940 and 2%w/w SCMC. Microemulsion EO-1 to EO-4 and HO-1 to HO-3 could produce clear microemulsion-based gels. However, the instability was observed in some microemulsion-based gels. There were significantly decrease in viscosity in the system of 2.5%w/w SCMC of microemulsion-based gel of EO. According to microemulsion-based gel of HO, the instability was observed in the formulations contained higher amount of corbopol 940 accompanied with higher content of water in the microemulsions.

#### 5. Conclusion

EO possessed significantly higher anti-inflammatory activity than HO. The anti-inflammatory activity of EO was correlated to the presence of terpinen-4-ol and sabinene. Therefore, the anti-inflammatory activity of *Z. cassumunar* oil is mainly attributable to the volatile compounds and it is hence attractive for further application in the future. Microemulsion of EO significantly reduced the evaporation of sabinene and Microemulsion of HO tended to protect HO from the oxidation and reduce the occurrence of rancidity. Therefore, microemulsion show benefits in the term of stabilization.

# 6. Suggestions for future work

The release studies of active compounds from microemulsion-based gels in a comparison with the conventional formulations are needed to confirm the advantages of the formulations. *In vivo* anti-inflammatory assay or clinical test are needed to confirm the efficacy of the formulation.

# Content

|                                  | Page |
|----------------------------------|------|
| Abstract                         | i    |
| Executive summary                | V    |
| Table of content                 | x    |
| List of tables                   | xi   |
| List of figures                  | xii  |
| Chapter 1 Introduction           | 1    |
| Chapter 2 Literature review      | 3    |
| Chapter 3 Materials and methods  | 8    |
| Chapter 4 Results and discussion | 18   |
| Chapter 5 Conclusions            | 50   |
| References                       | 52   |
| Appendix                         | 59   |

# List of tables

|         |   | Page |
|---------|---|------|
| Table 1 | Acid value, iodine value, and saponification value of HO      | 18   |
| Table 2 | Percentage of constituents in EO identified by GC-MS analysis | 20   |

# List of figures

|           |  | Page |
|-----------|--|------|
| Figure 1  | External appearance of EO (left) and HO (right)                                  | 18   |
| Figure 2  | TLC chromatograms of curcumin (C) and HO after developing with thanol            | 22   |
|           | and hexane in the ratio of 2:8 (System I) and detected under visible light       |      |
|           | (A), short-wave (254 nm) UV light (B), and long-wave (366 nm) UV light           |      |
|           | (C) and after developing with ethanol and hexane in the ratio of 4:6             |      |
|           | (System II) and detected under visible light (D), short-wave (254 nm) UV         |      |
|           | light <b>(E)</b> , and long-wave (366 nm) UV light <b>(F)</b>                    |      |
| Figure 3  | HPLC chromatograms of curcumin standard (A) and HO (B)                           | 23   |
| Figure 4  | Dose-response curve of viability of PBMCs versus concentrations of EO            | 23   |
|           | (A) and HO (B) (n = 3)   |      |
| Figure 5  | Effect of various concentrations of indomethacin (■), EO (▲), and HO             | 24   |
|           | (●) on inhibition of BSA denaturation  |      |
| Figure 6  | Western blotting of NF- <sub>K</sub> B from U937 cells treated with indomethacin | 25   |
|           | (IND), control (CON), EO, and HO at 12 h (black), 24 h (white), and 48 h         |      |
|           | (grid) (n = 3, * denote $P$ < 0.05, ** denote $P$ < 0.01, *** denote $P$ <       |      |
|           | 0.001)   |      |
| Figure 7  | Western blotting of NF- <sub>K</sub> B from U937 cells treated with indomethacin | 26   |
|           | (IND), control (CON), curcumin (CUR), sabinene (SAB), terpinen-4-ol              |      |
|           | (TER), EO, and HO (n = 3, * denote $P$ < 0.05, ** denote $P$ < 0.01, ***         |      |
|           | denote $P < 0.001$ )   |      |
| Figure 8  | IL-6 secretion of RAW 264.7 cell line after treated with terpinen-4-ol and       | 28   |
|           | sabinene at the concentration of 5 $\mu g/mL$ (gray) and 50 $\mu g/mL$ (black)   |      |
|           | comparing to control (white) (n = 3, * denote $P < 0.05$ )                       |      |
| Figure 9  | External appearance of emulsion containing HO (A) and EO (B) using               | 29   |
|           | various HLB value of surfactant mixtures (Tween 20 and Span 20)                  |      |
|           | ranging from 5 to 16   |      |
| Figure 10 | Aqueous phase separation of emulsion containing HO (A) and EO (B)                | 29   |
|           | using various HLB value of surfactant mixtures (Tween 20 and Span 20)            |      |
|           | ranging from 5 to 16 after 1 day (●), 7 days (■), and 30 days (◆)                |      |

|           |  | Page |
|-----------|--|------|
| Figure 11 | Internal droplet size (●) and Turbidity (■) of emulsion containing HO (A) and EO (B) using surfactant mixtures (Tween 20 and Span 20) with HLB | 30   |
|           | ranging from 5 to 16 after 30 days   |      |
| Figure 12 | Pseudoternary phase diagram of EO/surfactant/ethanol/water when  | 30   |
|           | surfactant were Tween 20 and Span 80 (HLB = 10) (A), Triton X-   |      |
|           | 114+Span 80 (HLB = 10) (B), Tween 20 (C), and Triton X-114 (D),  |      |
|           | whereas, surfactant to co-surfactant ratio was 1:1   |      |
| Figure 13 | Pseudoternary phase diagram of EO/Tween 20/co-surfactant /water  | 31   |
|           | when the co-surfactant were ethanol (A), propan-1-ol (B), propan-2-ol  |      |
|           | (C), glycerin (D), propylene glycol (E), and polyethylene glycol 400 (F),  |      |
|           | whereas, surfactant to co-surfactant ratio was 1:1   |      |
| Figure 14 | Pseudoternary phase diagram of EO/Tween 20/ethanol/water when the  | 31   |
|           | surfactant to co-surfactant ratio were 2:1 (A), 1:1 (B), and 1:2 (C)   |      |
| Figure 15 | Pseudoternary phase diagram of EO/Tween 20/propylene glycol/water  | 32   |
|           | when the surfactant to co-surfactant ratio were 2:1 (A), 1:1 (B), and 1:2  |      |
|           | (C)  |      |
| Figure 16 | Pseudoternary phase diagram of EO/Tween 20/propylene glycol/water  | 32   |
|           | phase when the surfactant to co-surfactant ratio were 2:1 and the water  |      |
|           | phase were DI water (A), 0.1 M NaCl (B), 0.5 M NaCl (C), 1.0 M NaCl  |      |
|           | <b>(D)</b> , 0.1 M MgCl <sub>2</sub> <b>(E)</b> , 0.5 M MgCl <sub>2</sub> <b>(F)</b> , and 1.0 M MgCl <sub>2</sub> <b>(G)</b>                  |      |
| Figure 17 | Pseudoternary phase diagram of EO/Tween 20/propylene glycol/water  | 33   |
|           | phase when the surfactant to co-surfactant ratio were 2:1 and the pH of  |      |
|           | water phase were 4.0 <b>(A)</b> , 6.0 <b>(B)</b> , and 8.0 <b>(C)</b>  |      |
| Figure 18 | Pseudoternary phase diagram of EO/Tween 20/propylene glycol/water  | 33   |
|           | when the ratio of Tween 20 to propylene glycol was 2:1 (A), and the  |      |
|           | physical appearance of microemulsion number 1 to 6 from the left to  |      |
|           | right, respectively (B)  |      |
| Figure 19 | Internal droplet size ( $\square$ ) and polydispersity index ( $^ullet$ ) of microemulsions  | 34   |
|           | containing EO, Tween 20, propylene glycol, and water when the ratio of   |      |
|           | Tween 20 to propylene glycol was 2:1   |      |

|           |  | Page |
|-----------|--|------|
| Figure 20 | Electriical conductivity of microemulsions containing EO, Tween 20, propylene glycol, and water when the ratio of Tween 20 to propylene glycol was 2:1   | 34   |
| Figure 21 | Viscosity of microemulsions containing EO, Tween 20, propylene glycol, and water when the ratio of Tween 20 to propylene glycol was 2:1  | 35   |
| Figure 22 | pH of microemulsions containing EO, Tween 20, propylene glycol, and water when the ratio of Tween 20 to propylene glycol was 2:1   | 35   |
| Figure 23 | AUC of sabinene <b>(A)</b> and terpinen-4-ol <b>(B)</b> of EO solution in propyleneglycol <b>(EO)</b> and microemulsio number 1 <b>(EO-1)</b> before (■) and after (□) the heating-cooling stability test  | 36   |
| Figure 24 | Pseudoternary phase diagram of HO/surfactant/propan-2-ol/water when surfactant were Tween 20 and Span 80 (HLB = 6) (A), Triton X-114+Span 80 (HLB = 6) (B), Tween 20 (C), and Triton X-114 (D), whereas, surfactant to co-surfactant ratio was 3:2                                     | 37   |
| Figure 25 | seudoternary phase diagram of oil/Triton X-114/propan-2-ol/water when the oil were HO (A), HO and castor oil (1:1) (B), and HO and oleic acid (1:1) (C), whereas, surfactant to co-surfactant ratio was 3:2  | 37   |
| Figure 26 | Pseudoternary phase diagram of HO and oleic acid (1:1)/Triton X-114/co-surfactant/ water when the co-surfactant were absolute ethanol (A), 95% ethanol (B), propan-2-ol (C), polyethylene glycol 400 (D), and propylene glycol (E), whereas, surfactant to co-surfactant ratio was 3:2 | 38   |
| Figure 27 | Pseudoternary phase diagram of HO and oleic acid (1:1)/Triton X-114/propan-2-ol/water when the surfactant to co-surfactant ratio were 2:8  (A), 4:6 (B), 5:5 (C), 6:4 (D), and 8:2 (E)   | 38   |
| Figure 28 | Pseudoternary phase diagram of HO and oleic acid (1:1)/Triton X-114/propan-2-ol/water when the ratio of Triton X-114 to propan-2-ol was 3:2 <b>(A)</b> , and the physical appearance of microemulsion number 1 to 6  | 39   |
| Figure 29 | from the left to right, respectively <b>(B)</b> Internal droplet size (□) and polydispersity index (●) of microemulsions containing HO and oleic acid (1:1), Triton X-114, propan-2-ol, and water when the ratio of Triton X-114 to propan-2-ol was 3:2                                | 39   |

|           |  | Page |
|-----------|--|------|
| Figure 30 | Electrical conductivity of microemulsions containing HO and oleic acid (1:1), Triton X-114, propan-2-ol, and water when the ratio of Triton X-114 to propan-2-ol was 3:2   | 40   |
| Figure 31 | Viscosity of microemulsions containing HO and oleic acid (1:1), Triton X-114, propan-2-ol, and water when the ratio of Triton X-114 to propan-2-ol was 3:2   | 40   |
| Figure 32 | pH of microemulsions containing HO and oleic acid (1:1), Triton X-114, propan-2-ol, and water when the ratio of Triton X-114 to propan-2-ol was 3:2  | 41   |
| Figure 33 | Peroxidation value of native HO (HO) and microemulsions of HO before ( $\blacksquare$ ) and after ( $\square$ ) the heating-cooling stability test ( $P < 0.05$ )  | 41   |
| Figure 34 | Dose-response curve of viability of PBMCs versus concentrations of microemulsion containing EO (A) and HO (B) (n = 3)  | 42   |
| Figure 35 | BSA denaturation inhibition of indomethacin (IND), EO, microemulsion containing EO (EO-2, EO-4, EO-6), HO, and microemulsion containing HO (HO-2, HO-4, HO-6) at the concentration of 1.56%w/w (□), 3.13%w/w (□), and 6.25%w/w (□) | 43   |
| Figure 36 | Western blotting of NF- <sub>K</sub> B from U937 cells treated with control (CON), microemulsion control (ME), EO, microemulsion containing EO (EO-2, EO-4, EO-6), HO, and microemulsion containing HO (HO-2, HO-4, HO-6)          | 44   |
| Figure 37 | Microemulsion-based gel containing 1%w/w carbopol 940 (A), 1.5%w/w carbopol 940 (B), 2.5%w/w carbopol 940 (C), 1%w/w SCMC (D), 1.5%w/w SCMC (E), 2.5%w/w SCMC (F) and EO-1 to EO-6 from left to right, respectively                | 44   |
| Figure 38 | Microemulsion-based gel containing 1%w/w carbopol 940 (A), 1.5%w/w carbopol 940 (B), 2.5%w/w carbopol 940 (C), 1%w/w SCMC (D), 1.5%w/w SCMC (E), 2.5%w/w SCMC (F) and HO-1 to HO-6 from left to right, respectively                | 45   |
| Figure 39 | Gel containing HO (A) and microemulsion-based gel com containing HO (B)  | 45   |

|           |  | Page |
|-----------|--|------|
| Figure 40 | Rheogram of microemulsion-based gel containing 1%w/w carbopol 940 and HO-1   | 46   |
| Figure 41 | Viscosity of microemulsion-based gel containing 1%w/w gelling agent (■), 1.5%w/w gelling agent (■), and 2.5%w/w gelling agent (□) when the gelling agent was carbopol 940 (A and C) or SCMC (B and D)  | 46   |
| Figure 42 | Microemulsion-based gel containing 1%w/w carbopol 940 (A), 1.5%w/w carbopol 940 (B), 2.5%w/w carbopol 940 (C), 1%w/w SCMC (D), 1.5%w/w SCMC (E), 2.5%w/w SCMC (F) and EO-1 to EO-6 from left to right, respectively after the heating-cooling stability test | 47   |
| Figure 43 | Viscosity of microemulsion-based gel of EO containing 2.5%w/w carbopol 940 <b>(A)</b> and 2.5%w/w SCMC <b>(B)</b> before ( $\square$ ) and after ( $\blacksquare$ ) the heating-cooling stability test ( $P < 0.05$ )  | 48   |
| Figure 44 | Microemulsion-based gel containing 1%w/w carbopol 940 (A), 1.5%w/w carbopol 940 (B), 2.5%w/w carbopol 940 (C), 1%w/w SCMC (D), 1.5%w/w SCMC (E), 2.5%w/w SCMC (F) and HO-1 to HO-6 from left to right, respectively after the heating-cooling stability test | 48   |
| Figure 45 | Viscosity of microemulsion-based gel of HO containing 1%w/w carbopol 940 <b>(A)</b> and 2%w/w SCMC <b>(B)</b> before $(\Box)$ and after $(\blacksquare)$ the heating-cooling stability test $(P < 0.05)$   | 49   |

# Chapter 1

#### Introduction

Zingiber cassumunar Roxb. (Zingiberaceae) is widely distributed throughout Southeast Asia. Most members of this family are easily recognized by the characteristic aromatic leaves and fleshy rhizomes when both of them are crushed (Habsah et al., 2000). Plants in this genus contain essential oils within the oil glands that are commonly found in most plant parts. The rhizomes of *Z. cassumunar* are used in folk remedies for the treatment of many conditions, especially rheumatism and muscular pain (Pithayanukul et al., 2007; Sukatta et al., 2004). The plant has been used as a component in herbal compress balls and massage oils for pain relief (Nandhasri and Pawa, 2003). Massage oil from *Z. cassumunar* has been widely used by local people in Thailand and is now prescribed in some hospitals. During the past decade, a number of pure compounds isolated from *Z. cassumunar* have been reported for various biological activities, especially anti-inflammatory activity related to the relief of muscular pain (Tuntiwachwuttikul et al., 1981; Masuda and Jitoe, 1994; Pongprayoon et al., 1997; Panthong et al., 1997). However, the anti-inflammatory activity of *Z. cassumunar* extract made by local Thai people using hot infusion method has not been investigated. This study is thus the first report concerning the anti-inflammatory effects of hot infused oil (HO) from *Z. cassumunar*.

Inflammation is believed to be an aspect of the non-specific immune response that occurs in reaction to bodily injury. The cardinal signs of inflammation can be explained by increased blood flow, elevated cellular metabolism, vasodilatation, release of soluble mediators, extravasation of fluids, and cellular influx due to a complex array of enzyme activation, mediator release, fluid extravasations, cell migration, tissue breakdown, and tissue repair (Ryan and Majno, 1977; Ferrero-Miliani et al., 2007; Vane and Botting, 1995). Several complex pathways associated with persistent or chronic inflammation have been discovered. Denaturation of tissue protein is frequently associated with inflammation (Padmanabhan and Jangle, 2012). Therefore, protein denaturation inhibition has been widely used as an *in vitro* screening model for anti-inflammatory activity (Mizushima & Kobayashi, 1968).

Nuclear factor-kappa B (NF-<sub>K</sub>B) is a protein that acts as a switch to turn inflammation on and off in the human body (Maroon et al., 2005). After the detection of noxious stimuli, including infectious agents, free radicals, and other causes of cellular injury, NF-<sub>K</sub>B would turn on the particular genes that lead to the production of inflammatory cytokines (Gilroy et al., 1999). Normally, NF-KB is localized in the cytoplasm of the cell and is bound with I<sub>K</sub>B, which is

an inhibitory protein blocking the nuclear localization signal (Ghosh et al., 1998). A variety of cytokine stimuli can degrade the I<sub>K</sub>B resulting in the nuclear translocation of NF-KB (Maroon et al., 2005). Therefore, NF-<sub>K</sub>B is regarded as an important transcription factor for understanding the inflammation process (Lee et al., 2004).

Interleukin-6 (IL-6) is a pleiotropic cytokine involved in the regulation of immune responses. The cytokine is produced by a variety of cell stimulations, such as infection, trauma, or immunological challenge (Tilg et al., 1994). Investigation of IL-6 secretion level in macrophage cell after stimulation by lipopolysaccharide (LPS) can represent the anti-inflammation effect of the compounds (Mueller et al., 2010).

Therefore, the present study focused on anti-inflammatory activity of both EO and HO. However, the usages of the oils encounter with the stability problems. HO is easily rancid because of oxidation after a long time of heating in the extraction process, whereas, EO can easily evaporate even in a normal condition of storage. The rancidity of HO and evaporation of EO may alter the chemical compositions and affect the biological activities. Incorporation of these oils into the internal phase of microemulsion might be an alternative approach to solve the problems because microemulsions (isotropic, transparent, and thermodynamically stable colloidal systems) provided protective effect against oxidation for ascorbic acid, and therefore its degradation rate was retarded (Gallarate et al., 1999). Moreover, it was demonstrated that permeation rates from microemulsions were significantly higher than that of conventional formulations which leads microemulsion to be a useful vehicle to enhance transdermal drug permeability (Sintovand Botner, 2006; Sintov and Shapiro, 2004).

Therefore, the aims of the present study were to identify the chemical constituents and anti-inflammatory effects of essential oil (EO) and HO from *Z. cassumunar* rhizomes by evaluating albumin denaturation inhibition, NF-<sub>K</sub>B suppression using Western blot analysis, and IL-6 secretion level using enzyme-linked immunosorbent assay (ELISA). Moreover, microemulsions and microemulsion-based gel from HO and EO were developed to facilitate user's compliance in transdermal route of application.

# **Objectives**

- 1. To construct fingerprints and identify the chemical constituents of EO and HO
- 2. To determine anti-inflammatory activity and cytotoxicity of EO and HO
- 3. To reduce the rancidity of HO evaporation of EO by incorporation into microemulsions
- 4. To develop microemulsion-based gel from EO and HO

# Chapter 2

## Literature review

#### 2.1. Plai (Zingiber cassumunar Roxb.)

Z. cassumunar belongs to the Zingiberaceae family which is widely distributed throughout the tropics, particularly in Southeast Asia. Most members of this family are easily recognized by the characteristic aromatic leaves and fleshy rhizome when both of them are crushed (Habsah et al., 2000). Several species of Zingiberaceae are used as spices, medicines and flavoring agents. Z. cassumunar is used in folklore remedies as a single plant or as a component of herbal recipes for the treatment of various conditions including inflammation, sprains, rheumatism, muscular pain, wounds, and asthma (Jeenapongsa et al., 2003). It is also used as a mosquito repellant, an anti-dysenteric agent, a carminative, a mild laxative, and a cleansing solution for skin diseases (Bhuiyan et al., 2008). In Thailand, the rhizome part has been used as a component in herbal compress balls and massage oil for muscular pain relief (Nandhasri and Pawa, 2003).

A number of pure compounds isolated from Z. cassumunar have been shown to possess various biological activities, including antifungal (Tripathi et al., 2008), antibacterial (Pithayanukul et al., 2007; Habsah et al., 2000), antioxidation (Habsah et al., 2000; Masuda and Jitoe, 1994), and anti-inflammation (Tuntiwachwuttikul et al., 1981; Masuda and Jitoe, 1994; Pongprayoon et al., 1997; Panthong et al., 1997). It has been reported that the methanol extract of Z. cassumunar (p.o.) showed both anti-inflammatory activity and analgesic activity in rats with carrageenin-induced edema, mice with acetic acid-induced vascular permeability, and mice with writhing symptoms (Ozaki et al., 1991). The active compound responsible for these favorable effects was (E)-1-(3,4-dimethoxyphenyl)but-1-ene (Ozaki et al., 1991). This compound was also found as a major component in the essential oil of Z. cassumunar rhizome and was the most active compound exhibiting topical anti-inflammatory effect in the model of carrageenan-induced hind paw edema in rats (Pongprayoon et al., 1997). Moreover, it dose-dependently inhibited the rat edema induced by ethyl phenylpropiolate, arachidonic acid and ear tetradecanoylphorbol 13-acetate and it was more potent than any other standard drugs being used (Jeenapongsa et al., 2003).

Most of the previous studies focused on biological activities of essential oil from the rhizome part. Although both leaves and rhizome of *Z. cassumunar* contain volatile compounds, they are different in quality and quantity (Bhuiyan et al., 2008). However, essential oils from rhizomes isolated by hexane extraction and hydrodistillation were rather similar in their major

composition (Sukatta et al., 2009). The active compound from rhizome of *Z. cassumunar* can also be extracted by using hot oil extraction method. This method has been used to produce the massage oil which is currently in the national list of essential medicine of Thailand (นพมาศ สุนทรเจริญนนท์, 2555).

#### 2.2. Inflammation

The word 'inflammation' comes from the Latin 'inflammare' which means to set on fire (Ferrero-Miliani, 2007). The principal signs of an inflammation are redness, swelling with heat, and pain (Spencer, 1935). It is believed that inflammation is part of the non-specific immune response that occurs in reaction to any type of bodily injury and that the cardinal signs of inflammation can be explained by increased blood flow, elevated cellular metabolism, vasodilatation, release of soluble mediators, extravasation of fluids and cellular influx (Ryan and Majno, 1977; Ferrero-Miliani, 2007). In some disorders the inflammatory process, which under normal conditions is self-limiting, becomes continuous and chronic inflammatory diseases develop subsequently (Ferrero-Miliani, 2007). The mediators strongly implicated in the inflammation process are amines such as histamine and 5-hydroxytryptamine, short peptides such as bradykinin, long peptides such as interleukin-1, lipids such as prostaglandins and leukotrienes, enzymes released from migrating cells, complement, and so on (Vane and Botting, 1987). Cyclooxygenase-2 (COX-2) is a major contributor to the elevation of prostaglandin E2, which augment the processing of peripheral inflammation. After the discovery of the arachidonic/COX pathway, a number of additional pathways have been discovered that are associated with persistent or chronic inflammation. The discovery of nuclear Factor-Kappa B (NF-<sub>K</sub>B) is become an interesting transcription factor for understanding the inflammation process. NF-<sub>K</sub>B has been widely used as a biomarker in the anti-inflammatory activity determination (Rogerio et al., 2010; Tak and Firestein, 2001; Prajapati et al., 2010; Lawrens, 2009). It regulates the expression of several proteins, such as pro-inflammatory cytokines, inducible nitric oxide synthase, and COX-2 (Lee et al., 2004).

NF- $_K$ B molecule is a protein that acts as a switch to turn inflammation on and off in the body. The NF- $_K$ B proteins are localized in the cytoplasm of the cell and are associated with a family of inhibitory proteins as known as Nuclear Factor-Kappa B inhibitor ( $I_K$ B) (Barnes, 1997). The  $I_K$ B proteins are normally bound to NF- $_K$ B and block their nuclear localization signal. Many cytokine stimuli can degrade the  $I_K$ B and result in the nuclear translocation of NF- $_K$ B. The stimuli can include ultraviolet radiation, viral infection and the cytokines tumor necrosis factor  $\mathbf{C}$  (TNF $\mathbf{C}$ ) and interleukin-1B (IL-1B). The phosphorylation of  $I_K$ B protein and unbinding of the NF-

 $_{\rm K}$ B is the key step involved in the activation of NF- $_{\rm K}$ B. NF- $_{\rm K}$ B exists in the cytoplasm in the major of cell types as homodimer or heterodimers of a family of structurally related protein. Each member of this family contains a conserved amino-terminal region called the rel-homolgy domain which contains the DNA-binding and dimerization domains and the nuclear localization signal. In mammalian cell, there are five proteins that belonging to NF-KB family which are RelA, c-Bel, RelB, NF-<sub>K</sub>B1, and NF-<sub>K</sub>B2. RelA, c-Bel, and RelB are produced as transcriptionally active protein, whereas NF-<sub>K</sub>B1 and NF-<sub>K</sub>B2 are synthesized as longer precursor, which are further processed to transcriptionally active form. Naturally, NF-KB exists in the cytoplasm in an active form associated with the inhibitory protein named I-KB. I-KB family members share ankyrin-like repeat unit domain and regulate the DNA binding and subcellular localization. Binding sites for the transcription regulatory factor NF-<sub>K</sub>B present in the promoter regions of the proinflamatory cytokines and immunoregulatory mediators, which are important for induction of acute inflammatory response. NF-<sub>K</sub>B plays a crucial role in a variety of inflammatory diseases such as rheumatoid arthritis and asthma. In cell associated with these diseases, NF-<sub>K</sub>B has been found with aberrant, constitutively nuclear localization and enhanced transcriptional activity. NF-<sub>K</sub>B induces cyclooxygenase-2 which stimulates the synthesis of cyclopentanone prostaglandins result in the inhibition of I Kappa B kinase (I<sub>K</sub>K) activity. The anti-inflammatory cytokine IL-10 has been shown to inhibit I<sub>K</sub>K activity and NF-<sub>K</sub>B DNA binding mechanism (Maroon et.al, 2006).

As describe above, inflammation is a normal protective response to tissue injury and it involves a complex array of enzyme activation, mediator release, fluid extravasations, cell migration, tissue breakdown and repair (Vane and Botting, 1995). It is a complex process, which is frequently associated with pain and involves occurrences such as the increase in vascular permeability, increase of protein denaturation and membrane alteration (Padmanabhan and Jangle, 2012). Denaturation of tissue protein is one of well-documented causes of inflammation and arthritic disease. Production of auto antigens in certain arthritic disease may be due to denaturation of protein *in vivo*. Agents that can prevent protein denaturation, therefore, would be worthwhile for anti-inflammatory drug development (Chandra et al., 2012). A number of anti-inflammatory drugs are known to inhibit the denaturation of proteins. Mizushima and Kobayashi have employed protein denaturation as *in vitro* screening model for anti-inflammatory compounds (Mizushima and Kobayashi, 1968).

#### 2.3. Microemulsion

Microemulsions belong to the group of colloidal drug delivery systems (Krauel et al., 2007). Microemulsions are optically transparent, low viscosity and thermodynamically stable dispersions of oil, water, and surfactant, frequently in combination with a co-surfactant (Kogan and Garti, 2006; Kankkunen et al., 2002). The systems can be differentiated from a coarse emulsion by visual inspection (microemulsion = clear, coarse emulsion = white). The differentiation from a liquid crystal can be undertaken by polarizing light microscope (microemulsion = isotropic/non birefringent, liquid crystal = usually anisotropic /birefringent) and by viscosity determination (microemulsion = low, Newtonian viscosity, liquid crystal = high, non-Newtonian viscosity) (Krauel et al., 2007). Depending on their microstructure, microemulsions can be categorized into droplet or bicontinuous type. In a droplet type, the dispersed oil or water is surrounded by surfactant molecules forming micelles or reverse micelles in the continuous component whereas bicontinuous microemulsions are characterized by a sponge-like microstructure, with comparatively large oil and water domains intertwining, separated by a surfactant layer (Kreilgaard et al., 2000).

Phase diagram is used to provide a means of characterizing emulsions. Generally, ternary diagrams are employed to depict mixtures of three components which are oil, water, and surfactant. In case of microemulsion development, the diagrams are called pseudoternary phase diagrams since microemulsions are complex systems of oil, water, and emulsifiers (surfactant and co-surfactant). Surfactant and co-surfactant is prepared in defined mixtures and presented on one axis in the ternary phase diagram. Contrary to submicron emulsions, microemulsions are formed spontaneously without the input of energy as soon as the required ratio of components has been reached. Microemulsions are optically transparent and isotropic liquids, which are in thermodynamic equilibrium. Apart from single-phase ranges, such mixtures also have two- and three-phase regions and are usually only formed in narrow specific concentration ranges of the ingredients. Pseudoternary phase diagrams enable homogeneous or heterogeneous regions to be depicted (Schmidts et al., 2009).

The use of microemulsions in pharmaceutics is advantageous not only due to the low cost and ease of preparation (zero interfacial tension and almost spontaneous formation), but also because of the improved bioavailability, stability (long shelf-life), high surface area (high solubilization capacity), very small droplet size (5-200 nm) and good appearance (Kogan and Garti, 2006; Boonme et al., 2006). The small droplets have better chance to transport bioactive molecules in a more controlled fashion (Kogan and Garti, 2006). Using the microemulsion vehicles, water-soluble and oil-soluble components from different plant extracts can be co-

solubilized in order to attain synergistic effect for a specific therapeutic goal (Kogan and Garti, 2006). Microemulsions were also found as protecting medium for the entrapped of drugs from degradation, hydrolysis and oxidation (Kogan and Garti, 2006).

It was demonstrated that permeation rates from microemulsions were significantly higher than that of conventional emulsions and other formulations. Both, increase in solute concentration and the tendency of the drug to favor partitioning into the stratum corneum make the microemulsion a useful vehicle to enhance transdermal drug permeability (Sintov and Botner, 2006; Sintov and Shapiro, 2004). By far, it has been shown in many studies that microemulsion formulations possessed improved transdermal and dermal delivery properties. Recently many drugs such as lidocaine, diclofenac, 5-Fluorouracil and ascorbic acid using microemulsion for transdermal delivery had been reported (Kreilgaard, 2002; Sintov and Botner, 2006; Gupta et al., 2005; Gallarate et al., 1999) Kreilgaard et al., have reported that the transdermal flux of lidocaine from a microemulsion is up to four times higher than that from a conventional O/W emulsion (Kreilgaard, 2002). In addition, Sintov and Botner found that the transdermal administration of the microemulsion containing diclofenac to rats resulted in 8-fold higher drug plasma levels than those obtained after application of Voltaren Emulgel (Sintov and Botner, 2006). Moreover, Gupta et al., indicated that incorporation of 5-Fluorouracil into microemulsions increased the flux of the drug 2-6 fold in comparison to the aqueous solution (Gupta et al., 2005). Since microemulsions were also found as protecting medium from degradation (Kogan and Garti, 2006), Gallarate et al., found that microemulsion systems provided protection against oxidation for ascorbic acid, and therefore its degradation rate was slower than in aqueous solutions (Gallarate et al., 1999).

Microemulsion can be used as a template for developing many formulations such as hydrogel and nanoparticles. Gasco and Trotta indicated that the use of a microemulsion instead of a coarse or submicron emulsion frequently used as a template for nanoparticles preparation and offers advantages in terms of enhanced physical stability of the system, the minimal need of energy input to form the polymerization template, their small and uniform droplet size that is reflected in the size of the nanoparticles produced (Gasco and Trotta, 1986). Watnasirichaikul et al., developed a method for producing *poly*(alkylcyanoacrylate) (PACA) nanoparticles from biocompatible microemulsions in a simple one-step process thereby omitting the need of having to separate the resulting nanoparticles after polymerization and retaining a high yield of encapsulated peptide (Watnasirichaikul et al., 2000). In another hand, Chen et al. developed the microemulsion-based hydrogel formulation containing ibuprofen with a suitable viscosity for topical administration by swelling xanthan gum in microemulsion system (Chen et al., 2006).

# Chapter 3

#### Materials and methods

#### 3.1. Materials

#### 3.1.1. Plant material

Zingiber cassumunar Roxb. or Zingiber montanum (J.Koenig) Link ex A.Dietr. has been known as 'Cassumunar ginger'. In Thailand, the common local name of this plant is 'Plai'. However, different names are used in different regions; e.g. 'Wan-Fai' by Northeastern people and 'Bpu-lai' is called by Northern people.

The rhizomes of *Z. cassumunar* were collected from Chiang Mai, Thailand. Specimens were authenticated and a voucher specimen (number 22126) was deposited in the official Herbarium of the Faculty of Pharmacy, Chiang Mai University, Thailand.

#### 3.1.2. Chemical materials

Indomethacin, oleic acid, bovine serum albumin (BSA), 3-(4,5-dimethylthiazolyl-2)-2,5diphenyl tetrazolium bromide (MTT), phenolphthalein TS, sodium deoxycholate, phenolphthalein TS, triethanolamine, carbopol 940, sodium methylcellulose (SCMC), Triton X-114, and Tween 20 were purchased from Sigma-Aldrich (St. Louis, MO, USA). Fetal calf serum and fetal bovine serum (FBS) were purchased from Biochrom AG (Berlin, Germany). Ficoll-paque plus was purchased from Lymphoprep Axis-Shield PoC AS (Oslo, Norway). Anhydrous sodium sulphate, disodium hydrogen phosphate, dipotassium hydrogen phosphate, sodium hydroxide, potassium hydroxide, sodium chloride, potassium iodide, iodobromide, hydrochloric acid, and sodium thiosulfate were purchased from Fisher Chemicals (Loughborough, UK). Tris base was purchased from Fisher Chem Alert (Fair Lawn, NJ, USA). RPMI 1640, dulbecco modified eagle medium (DMEM) penicillin, streptomycin, L-glutamine, and trypan blue were purchased from GIBCO Invitrogen (Grand Island, NY, USA). Hydrochloric acid was AR grade and purchased from Merck (Darmstadt, Germany). Ethanol, methanol, propan-2-ol, dimethyl sulfoxide (DMSO), chloroform, hexane, ethyl acetate, and ether were AR grade and purchased from Labscan (Dublin, Ireland). Coconut oil were purchased from a local market in Chiang Mai province, Thailand. Acetone and acetronitrile were HPLC grade and purchased from Merck (Darmstadt, Germany). Horseradish peroxidase (HRP)-conjugated sheep anti-rabbit IgG antibody was obtained from Promega (Madison, WI, USA). RIPA buffer was purchased from Thermo scientific (Rockford, IL, USA). Sodium dodecyl sulfate (SDS) was purchased from EMD Millipore Corporation (Billerica, MA, USA). Polyvinylidine fluoride transfer membrane was purchased from Pall Corporation (Pensacola, FL, USA). GAPDH antibody, lipopolysaccharide (LPS), and NF-kB antibody were purchased from Cell Signaling (Boston,MA). SuperSignal West Pico Chemiluminescent was purchased from Pierce (Rockford, IL, USA). Coconut oil was purchased from a local market in Chiang Mai province, Thailand.

#### 3.2. Oil extraction

#### 3.2.1. Essential oil distillation

The *Z. cassumunar* rhizome was subjected to hydrodistillation for 3 h using a cleavenger type apparatus. The essential oil (EO) obtained was dried over anhydrous sodium sulphate and stored in a refrigerator and protected from light until further use. The yield of EO was recorded and density was analyzed by using pycnometer.

#### 3.2.2. Hot infused oil preparation

The *Z. cassumunar* rhizomes were sliced into small pieces and fried in heated coconut oil for 3-4 h until their color change to brown. The fried pieces of *Z. cassumunar* were then removed. And the HO was filtered through filter cloth after cooling down. HO was stored in well-closed container and protected from light until further use.

### 3.3. Characterization of HO

#### 3.3.1. Acid value determination

Acid value will be determined by indirect titration method (Kardash and Tur'yan, 2005). Briefly, about 10 g of oil will be weighted and mixed with 50 mL of ethanol/ether mixture (1:1). The mixture was then shaken until homogeneous. Phenolphthalein TS will be added as an indicator in the titration with 0.1 N NaOH. End point of the titration will be indicated at the first permanent pink color which was persisted for at least 10 s. The acid value which is expressed as the amount of NaOH (in milligrams) necessary to neutralize free fatty acids contained in 1 g of oil will be then calculated. The experiments will be done in triplicate.

#### 3.3.2. lodine value determination

Determination of iodine value will be conducted according to AOCS official method with slight modification (Official and Tentative Methods of the American Oil Chemists' Society, 1984). Briefly, about 0.2 g of oil will be weighted and dissolved in 10 mL of chloroform. After that the mixture is shaken until homogenous. Then 25 mL of iodobromide will be added, and

the reaction will be carried out in the dark for 30 min. KI solution (30 mL of KI in 100 mL of water) will be then added to stop the reaction. The remaining iodine was titrated using 0.1 N sodium thiosulfate ( $Na_2S_2O_3$ ) solution. The iodine value which is expressed as grams of halogen (calculated as iodine) absorbed by 100 g of substance will be then calculated. The experiments will be done in triplicate.

### 3.3.3. Saponification value determination

Saponification value will be determined according to AOCS official method with slight modification (Official and Tentative Methods of the American Oil Chemists' Society, 1984). Briefly, about 2 g of oil will be weighted and dissolved in 25 mL of alcoholic KOH. After 30 min of reflux with the assistance of heating from water bath, 1 mL of phenolphthalein TS will be added as an indicator for the titration. The sample will be then titrated with 0.5 N HCl and end point will be indicated at the appearance of amber yellow color. The saponification value which is expressed as the milligrams of KOH necessary to neutralise the free acids and to saponify the esters present in 1g of substance will be then calculated. The experiments will be done in triplicate.

#### 3.4. Chemical composition analysis

#### 3.4.1. Gas chromatography-mass spectrometry (GC-MS) of EO

EO was analyzed for its compositions by GC-MS. The GC-MS analysis was performed on an Agilent 6890 gas chromatograph (Agilent Technologies, CA, USA) coupled to an electron impact (EI, 70 eV) with HP 5973 mass selective detector (Hewlett Packard, CA, USA) fitted with a fused silica capillary column (HP-5MS) supplied by Hewlett Packard, USA (30.0 m × 250 mm, i.d. 0.25 mm film thickness). The analytical conditions were as follows; carrier gas: helium (ca. 1.0 mL/min), injector temperature: 260°C, oven temperature: 3 min isothermal at 100°C (No peaks before 100°C after first injection), then at 3°C/min to 188°C and then at 20°C/min to 280°C (3 min isothermal), and detector temperature was 280°C. The identification of individual compounds was based on their retention times relative to those of authentic samples and matching spectral peaks available with Wiley, NIST and NBS mass spectral libraries. The Kováts retention indices (KI) were obtained by GC-MS analysis of an aliquot of the volatile oil spiked with an n-alkanes mixture containing each homologue from n-C8 to n-C20. Identification of the compounds was based on a comparison of their mass spectra database (WILEY&NIST) and spectroscopic data (Adams, 2001). The experiments were done in triplicate.

#### 3.4.2. Thin layer chromatography (TLC) of HO

HO was diluted in a mixture of chloroform and acetone (50:50) before spotting on the TLC plate. The plate was then developed in two developing solvent systems, ethanol and hexane in the ratios of 2:8 (System I) and 4:6 (System II). Curcumin standard was used as a marker in this study. The developed plate was then observed in daylight, UV light at 254 nm, and UV light at 366 nm. Retardation factor ( $R_f$ ) were then calculated using the following equation:  $R_f = D_s/D_p$  whereas,  $D_s$  is the distance that the sample travelled before dropping out of the solution and  $D_f$  is the distance that the solvent travelled. The experiments were done in duplicate.

#### 3.4.3. High performance liquid chromatography (HPLC) of HO

Briefly, HPLC analyses were performed using an HP1100 system with a thermostatically controlled column oven and a UV detector set at 420 nm (Hewlett-Packard, Palo Alto, CA). A reversed phase column Eclipse XDB-C18 (4.6  $\times$  150 mm, 5-micron, Agilent, USA) was connected with an Eclipse XDB-C18 guard column (4.6  $\times$  12.5 mm mm, 5-micron, Algilent, USA). A mixture of acetonitrile and acetone in the ratio of 80:20 was used to elute samples at ambient temperature at a flow rate of 1 mL/min and 20  $\mu$ L of sample were injected. Curcumin standard was used as a marker. Samples and mobile phases were filtered through a 0.45 mm Millipore filter, type GV (Millipore, Bedford, MA) prior to HPLC injection. The experiments were done in duplicate.

# 3.5. Cell cytotoxicity

The effect of EO, HO, and microemulsion of both oils on cell viability of peripheral blood mononuclear cells (PBMCs) were determined by a colorimetric technique, which are 3-(4,5-dimethylthiazol-2-yl)-2,5-diphenyl tetrazolium bromide (MTT) assay (Phongpradist et al., 2010).

#### 3.5.1. PBMCs isolation

Peripheral blood mononuclear cells (PBMCs) were isolated from whole blood that was collected from the same healthy donor throughout the research. The whole blood sample was diluted with the same volume of phosphate buffer saline (PBS), pH 7.4. After that, the diluted blood sample was carefully layered onto a Ficoll-Paque Plus. The mixture was centrifuged at 5,000 × g for 30 min at room temperature. The undisturbed mononuclear cell layer was then carefully transferred out. The cells were washed and pelleted down with three volumes of PBS two times each and resuspended in RPMI-1640 media with 100 IU/mL penicillin, 100 µg/mL

streptomycin, and 10% FBS. The viable PBMC number was counted with an equal volume of trypan blue solution.

#### 3.5.2. Cell viability assay

The effects on cell viability of peripheral blood mononuclear cells (PBMCs) were determined by a colorimetric technique using MTT assay (Phongpradist et al., 2010). Briefly, 100  $\mu$ L of cell lines and PBMCs at a cell concentration of  $10^5$  cells/mL were added into each well of a 96-well plate and incubated at 37°C, 5% CO<sub>2</sub> and 90% humidity for 24 h. Then 100  $\mu$ L of various concentrations of samples were added to the cells compared with untreated cells and incubated again in the same conditions for 48 h. After the corresponding period, 100  $\mu$ L of media were removed and 25  $\mu$ L of MTT (5 mg/mL) were added into each well and incubated for 4 h. All media were then removed by turning the 96-well plate upside down. Then 200  $\mu$ L of DMSO were added into each well to solubilize the formazan crystals. The plate was then read at 540 nm by using a microplate reader (Bio-Rad Laboratories Ltd., Japan). All the experiments were done in triplicate.

#### 3.6. Anti-inflammatory activity

#### 3.6.1. Determination of albumin denaturation inhibition

Determination of albumin denaturation inhibition was used to evaluate the anti-inflammation activity (Rahman et al., 2015). Briefly, BSA aqueous solution (0.5% w/v) was mixed with various concentrations of test solution and incubated at  $37^{\circ}$ C for 20 min. Then the temperature was increased to  $57^{\circ}$ C and kept for 3 min. After cooling, PBS (pH 6.3) was added and the absorbance was measured using UV-Visible spectrophotometer (Shimadzu, japan) at 255 nm. The percentage inhibition was calculated using the following equation: % Inhibition = 1-[(S-C)/S], where S is the turbidity in the presence of a certain concentration of the test sample and C is the turbidity in absence of the test sample. Indomethacin was used as a positive control. All the experiment was done in triplicate.

# 3.6.2. NF-<sub>K</sub>B inhibition

# 3.6.2.1. U937 cells and culture conditions

U937 (human leukemic monocyte lymphoma) cells were grown in RPMI-1640 culture medium supplemented with 100 IU/mL penicillin, 100  $\mu$ g/mL streptomycin, 10% FBS, and 2 mM L-glutamine. The cells were incubated at 37°C in a humidified atmosphere of 5% CO<sub>2</sub> (Balsinde and Mollinedo, 1988).

#### 3.6.2.2. Western blot analysis

The immunoblotting assay was used to determine the level of NF-<sub>K</sub>B. The U937 cells were incubated with indomethacin, EO, and HO for 12, 24, and 48 h to determine the timedependent effects. The cells were also incubated with curcumin, terpinen-4-ol, and sabinene for 48 h to determine the NF-<sub>K</sub>B suppression of the major constituents of EO and HO. The cells were lysed in RIPA buffer (25 mM Tris+HCl, pH 7.6, 150 mM NaCl, 1% NP-40, 1% sodium deoxycholate, 0.1% SDS) containing protease inhibitors. Cell lysates were collected by centrifugation at 7,826 × g for 15 min, at room temperature. The protein concentrations were measured by the Folin-Lowry method and standardized with BSA. Whole protein lysate (50 µg) was separated by SDS-PAGE and transferred to a polyvinylidene fluoride (PVDF) membrane. The membrane was blocked for nonspecific binding by 5% non-fat dry milk in PBS containing 0.1% Tween 20 for 2 h and probed by anti-NF-κB, for 2 h. GAPDH was used as an internal control. The secondary antibody conjugated with horse radish peroxidase (HRP) was added. Peroxidase activity was detected using chemiluminescence reagents (Shishodia et al., 2005). The protein band levels were quantified by a scan densitometer and Quantity One software, version 4.6.3 (Bio-Rad laboratories, Hercules, CA, USA). The density value of each band was normalized to GAPDH band.

#### 3.6.3. Determination of IL-6 secretion inhibition

IL-6 secretion levels of RAW 264.7 cells after treated with EO and HO were determined by using enzyme-linked immunosorbent assay (ELISA).

#### 3.6.3.1. RAW 264.7 cells and culture conditions

RAW 264.7 cells (American Type Culture Collection, ATCC-TIB-71) were grown in DMEM culture medium supplemented with 10% FBS. The cells were incubated at 37°C in a humidified atmosphere of 5% CO<sub>2</sub> (Mueller, *et al.*, 2010).

#### 3.6.3.2. Enzyme-linked immunosorbent assay (ELISA)

LPS stimulated RAW 264.7cell was used to examine the effect of EO and HO on inflammation. The cell culture was performed following the method used in the previous study of Mueller, et al. with slight modifications (Mueller, et al., 2010). Briefly, RAW 264.7 cells were seeded at a density of  $2 \times 10^6$  cells per well in 24 well plates, and incubated at  $37^{\circ}$ C, 5% CO<sub>2</sub> and 90% humidity for 24 h. On the following day, test compound in ethanolic solution in DMEM were added, and further incubated in the same condition for 2 h. After that LPS was added to

let the final concentration be 1  $\mu$ g/mL and further incubated in the same condition for 24 h. On the third day, the media was removed and centrifuged at 13,500 × g for 10 min to remove cells. Supernatant was aliquoted and analyzed by ELISA. Cells which were not treated with LPS served as a negative control and cells incubated with ethanol and LPS served as a positive control. The IL-6 in cell supernatant (100  $\mu$ L) was determined by ELISA according to the manufacturer's protocol (R&D Systems). All incubation steps were performed at room temperature. The optical density at 450 nm, corrected by the reference wavelength 570 nm, was measured with a Genios Pro microplate reader (Tecan, Crailsheim, Germany).

#### 3.6.3.3. MTT assay

Simultaneous with the ELISA, the viability of LPS-stimulated cells was assessed by a MTT assay, based on the mitochondrial-dependent reduction of MTT to formazan. After removing the supernatant for ELISA analysis, MTT was added to the cells, and the cells were incubated for at 37°C, 5% CO<sub>2</sub> and 90% humidity for 2 h. The supernatant was then removed, and the cells were lysed with lysis buffer (10% SDS in 0.01 N HCI). The optical density at 570 nm, corrected by the reference wavelength 690 nm, was measured using a Genios Pro microplate reader.

#### 3.6.3.4. Calculation of IL-6 secretion

The calculated concentrations of cytokines were normalized to MTT values to reduce any variation from differences in cell density. For a positive control, cells were treated with only LPS and the resulting amount of secreted cytokines was defined as 100%. The results from the experimental compounds were then calculated as a percent of this value. The entire inflammation assay, starting with cell seeding and LPS-induction, was performed in triplicate in three time independent experiment.

#### 3.7. Formulation Development

# 3.7.1. Determination of required HLB

#### 3.7.1.1. Droplet size analysis

Briefly, emulsions were prepared with surfactants blends of various HLB values. The droplet size of the emulsions was measured byphoton correlation spectroscopy (Zetasizer® version 5.00, Malvern Instruments Ltd., Malvern, UK) 24 h after preparation (Orafidiya and Oladimeji, 2002). The experiments were done in triplicate.

#### 3.7.1.2. Turbidimetric method

Briefly, emulsions were prepared with surfactants blends of various HLB values. After 7 days, emulsion was diluted with distilled water and the percentage transmittance (%T) was measured using Ultraviolet spectrophotometer (Shahin et al., 2011). Distilled water was used as a blank set at 100% transmission. The turbidity of diluted emulsions were calculated as: Turbidity = 100-%T. The experiments were done in triplicate.

# 3.7.2. Pseudoternary phase diagrams construction

Pseudoternary phase diagrams were constructed using a water titration method (Chaiyana et al., 2010). Single surfactant or surfactant mixture with the HLB value equal to the required HLB of the oils were used. Various surfactant to co-surfactant ratio were involved in the study as the factors affecting microemulsion area existed in the phase diagram.

# 3.7.2.1. Effect of surfactant type

Various surfactants such as Tween 20, Tween 60, Tween 85, Triton X-114, and Span 80 as well as surfactant mixture with the HLB value equal to the required HLB of the oils were employed as the surfactant in microemulsion system when other conditions are constant.

#### 3.7.2.2. Effect of co-surfactant type

Alkyl alcohol with various chain length including ethanol, isopropanol, and cetyl alcohol as well as propylene glycol, polyethylene glycol 400, and glycerin were employed as the cosurfactant in microemulsion system when other conditions were constant.

#### 3.7.2.3. Effect of surfactant to co-surfactant ratio

Various surfactants to co-surfactant ratios were studied when other conditions were constant.

#### 3.7.3. Characterization of selected blank microemulsion

#### 3.7.3.1. Particle size / size distribution

Particle size analysis was carried out using photon correlation spectroscopy (Zetasizer® version 5.00, Malvern Instruments Ltd., Malvern, UK). The sizing measurements were carried out at a fixed angle of 173°. The reported results were mean and S.D. of at least ten measurements on each sample.

#### 3.7.3.2. Electrical conductivity determination

Electrical conductivity of the microemulsions was measured using 100 mM NaCl solution as aqueous phase. The conductivity was measured by Cyberscan CON 11: hand-held conductivity meter (Eutech Instruments, Singapore) using conductivity/TDS electrode cell. The experiments were performed at 25±1.0°C by dipping the electrode into the test sample until equilibrium reached and reading became stable. The measurements were done in triplicate.

# 3.7.3.3. Rheology study

Viscosity of the microemulsions was measured using a Brookfield DVIII rheometer (Brookfield Engineering Laboratories, Stroughton, MA) fitted with a bob spindle. Brookfield Rheocalc operating software was used to control the measurement. A sample volume of 70 mL was used. The measurements were performed in triplicate at 25°C.

# 3.7.3.4. pH measurements

The pH of each formulation was measured at 25±1.0°C by dipping the electrode into the test sample until equilibrium reached and reading became stable. The measurements were done in triplicate.

#### 3.7.3.5. Stability study

The microemulsions were subjected to heating-cooling study of six heating-cooling cycles (24 h each at 4° C and 45° C), whereas, the controlled microemulsion was stored at room temperature under ambient atmosphere and humidity. After that, the formulations were characterized by means of external appearance, particle size, electrical conductivity, rheology, and pH measurement as previous described. The rancidity of HO in microemulsions was determined by means of peroxidation value. The evaporation of EO in microemulsions was determined by GC-MS as previous described.

#### 3.7.4. Microemulsion-based gel development

Gelling agents including sodium carboxymethyl cellulose and carbopol-940 were used for the microemulsion-based gel development. The gel base was previously prepared at the exact concentration. Then microemulsion was incorporated into the gel base.

#### 3.7.5. Characterization of microemulsion-based gel

#### 3.7.5.1. Rheology study

Viscosity of the microemulsion-based gel was measured using a Brookfield DVIII rheometer (Brookfield Engineering Laboratories, Stroughton, MA) fitted with a bob spindle. Brookfield Rheocalc operating software was used to control the measurement. A sample volume of 70 mL was used. The measurements were performed in triplicate at 25°C.

# 3.7.5.2. pH measurements

The pH of each microemulsion-based gelformulation was measured at 25±1.0°C by dipping the electrode into the test sample until equilibrium was reached and reading became stable. The measurements were done in triplicate.

#### 3.7.5.3. Stability study

The microemulsion-based gel was subjected to heating-cooling study of six heating-cooling cycles (24 h each at 4° C and 45° C), whereas, the controlled microemulsion was stored at room temperature under ambient atmosphere and humidity. After that, the formulations were characterized by means of external appearance, rheology, and pH measurement as previous described.

#### 3.8. Statistical analysis

All data were presented as a mean  $\pm$  standard deviation (SD). Individual differences were evaluated by One-Way ANOVA followed by post-hoc tests. In all cases, P < 0.05 indicated statistical significance.

# Chapter 4

# Results and discussion

#### 4.1. Characteristics of EO and HO

Two different extraction methods of *Z. cassumunar* rhizome have been described. Volatile compounds can be extracted by hydrodistillation, whereas, nonvolatile nonpolar compounds can be extracted by the hot infusion method. Each oil has its own unique characteristics as shown in **Figure 1**. EO extracted by hydrodistillation is a clear light-yellowish liquid with a characteristic odor. Our yield of EO was 0.48%v/w with a density of 0.90 g/mL, while HO extracted by hot infusion was a clear yellowish liquid with a density of 0.95 g/mL, equal to that of coconut oil, the solvent used in the hot infusion method. The colored components of *Z. cassumunar* rhizomes could be extracted efficiently by the hot infusion method; hence, in the HO extract the color was a much deeper yellow than that of the EO.



Figure 1 External appearance of EO (left) and HO (right)

The characteristic of HO as the functions of acid value, iodine value, and saponification value are shown in **Table 1**.

Table 1 Acid value, iodine value, and saponification value of HO

|              | Acid value      | lodine value                 | Saponification value |
|--------------|-----------------|------------------------------|----------------------|
|              | (mg of KOH/g)   | (g of I <sub>2</sub> /100 g) | (mg of KOH/g)        |
| НО           | 0.20 ± 0.00     | 7.4 ± 0.2                    | 265± 7               |
| Coconut oil* | $0.40 \pm 0.02$ | $6.6 \pm 0.2$                | 274 ± 2              |

<sup>\*</sup> Kardash and Tur'yan, 2005

The low acid value (lower than 2 mg KOH/g) indicated the tendency of oxidative stable of the oil (Fu et al., 2008). Acid value is theoretically twice of free fatty acid value, which determines the free fatty acid content hydrolyzed from triglyceride. Since the rancidity is the result of the oxidation of free fatty acid in oils, this low acid value and free fatty acid value would be the factors that contribute to high oxidative stability (Seneviratne and Dissanayake, 2005). The results were in good agreement with the previous study that the acid value of homemade coconut oil for HO production in this study was  $0.40 \pm 0.02$  mg of KOH/g (Seneviratne and Dissanayake, 2005). However, commercial coconut oil in the same study showed a higher acid value of  $3.5 \pm 0.9$  mg of KOH/g because of the longer storage time (Seneviratne and Dissanayake, 2005). Therefore, the life span of the oil might be a critical factor affecting the acid value.

lodine value could be used to indicate a saturated or unsaturated fat component of the oil. lodine value of oleic acid (an unsaturated fat containing 1 double bond), is 90g of I<sub>2</sub>/100 g, whereas linoleic acid (unsaturated fat containing 2 double bonds) and linolenic acid (unsaturated fat containing 3 double bonds) are 282 and 274 g of I<sub>2</sub>/100 g, respectively. The low iodine value of HO represented the low number of reactive double bonds in the molecule, place HO in the non-drying oil group which is unable to be solidified when exposed in a thin film to the air (Wicks et al., 2007). The results related to the previous study that the major components of coconut oil were saturated fats, including lauric acid (48%) and myristic acid (17%), whereas, the only small amount of unsaturated fats (7% of oleic acid and 2% of linoleic acid) were found (McNair, 1929). Therefore, oxidative cleavage of unsaturated bond decreases and the oxidation likely slows down. The iodine value in this study was in a good agreement with the previous report (Seneviratne and Dissanayake, 2005).

High saponification value represents a high number of ester content or carboxylic functional groups per unit mass of HO. The results may suggest that HO is suitable for self-emulsification process and microemulsion formation (Anderson-Foster et al., 2012). The saponification value in this study was also in a good agreement with the previous report (Seneviratne and Dissanayake, 2005).

### 4.2. Chemical compositions of EO and HO

#### 4.2.1. GC-MS analysis of EO

Relative amounts of the individual compounds were presented as peak area percentage of the total peak area of EO (**Table 2**). The GC-MS data indicated that 26 components comprising 90.5±1.3% of the total composition of EO could be identified.

Table 2 Percentage of constituents in EO identified by GC-MS analysis

| No. | RT <sup>a</sup> | Compound <sup>b</sup>   | % Area   | KI     |                  | 0                   |
|-----|-----------------|-------------------------|----------|--------|------------------|---------------------|
|     |                 |                         |          | Sample | Ref <sup>c</sup> | - Qual <sup>d</sup> |
| 1   | 3.98            | alpha-thujene           | 1.8±1.9  | 931    | 930              | 94                  |
| 2   | 4.13            | alpha-pipene            | 1.6±0.7  | 938    | 939              | 97                  |
| 3   | 4.46            | camphene                | 0.1±0.0  | 954    | 954              | 96                  |
| 4   | 5.06            | sabinene                | 17.4±1.4 | 978    | 975              | 96                  |
| 5   | 5.13            | beta-pinene             | 2.7±0.6  | 981    | 979              | 97                  |
| 6   | 5.42            | beta-myrcene            | 1.4±0.3  | 993    | 991              | 97                  |
| 7   | 5.81            | alpha-phellandrene      | 0.6±0.3  | 1008   | 1003             | 97                  |
| 8   | 6.17            | alpha-terpipene         | 6.4±4.2  | 1021   | 1017             | 98                  |
| 9   | 6.43            | para-cymene             | 2.2±3.6  | 1031   | 1025             | 95                  |
| 10  | 6.54            | beta-phellandrene       | 1.8±1.4  | 1034   | 1030             | 94                  |
| 11  | 6.60            | 1,8-cineole             | 0.3±0.1  | 1036   | 1031             | 97                  |
| 12  | 7.11            | trans-beta-ocimene      | 0.1±0.1  | 1053   | 1050             | 92                  |
| 13  | 7.50            | gamma-terpinene         | 5.8±3.0  | 1065   | 1060             | 97                  |
| 14  | 7.85            | cis-sabinene hydrate    | 0.5±1.2  | 1075   | 1070             | 98                  |
| 15  | 8.46            | terpinolene             | 2.2±2.5  | 1091   | 1089             | 98                  |
| 16  | 8.96            | trans-sabinene hydrate  | 0.5±1.0  | 1104   | 1098             | 96                  |
| 17  | 10.53           | 1-terpineol             | 1.0±0.3  | 1140   | 1134             | 96                  |
| 18  | 12.26           | terpinen-4-ol           | 40.5±6.6 | 1173   | 1177             | 98                  |
| 19  | 12.63           | gamma-terpineol         | 1.6±0.2  | 1199   | 1199             | 91                  |
| 20  | 12.75           | cis-piperitol           | 0.5±0.0  | 1202   | 1196             | 97                  |
| 21  | 13.27           | trans-piperitol         | 0.5±0.1  | 1212   | 1208             | 91                  |
| 23  | 23.29           | trans-beta-farnesene    | 0.2±0.4  | 1460   | 1457             | 90                  |
| 24  | 24.81           | zingiberene             | 0.1±0.1  | 1496   | 1494             | 94                  |
| 25  | 25.31           | beta-bisabolene         | 0.1±0.0  | 1508   | 1506             | 93                  |
| 26  | 25.92           | beta-sesquiphellandrene | 0.8±0.0  | 1521   | 1523             | 99                  |
|     |                 | Total                   | 90.5±1.3 |        |                  |                     |

RT = Retention time; a = Compounds are listed in order of their elution from a DB-5 column;
b = Peak identifications are based on MS comparisons with file spectra and relative retention time (KI); c = KI from Sparkman; d = database of WILEY275

The results from our study revealed that terpinen-4-ol (40.5±6.6%) and sabinene (17.4±1.4%) were the major constituents of EO. The results were in a good agreement with those of previous studies reporting that terpinen-4-ol was the major component (50.5%) of the essential oil from Z. cassamunar rhizomes in India (Bordoloi et al., 1999). Moreover, the essential oil from Z. cassamunar rhizomes was also reported to contain sabinene (36.71-53.50%), **V**-terpinene (5.27-7.25%)terpinen-4-ol (21.85-29.96%) and (E)-1-(3,4dimethoxyphenyl) butadiene (0.95-16.16%) (Sukatta et al., 2009). In addition, triquinacene 1,4bis (methoxy) (26.47%), (Z)-ocimene (21.97%), and terpinen-4-ol (18.45%) were the major constituents in the essential oil from Z. cassamunar rhizomes in Bangladesh (Bhuiyan et al., 2008).

#### 4.2.2. TLC analysis of HO

The chemical components of HO were analyzed by means of TLC and HPLC. TLC chromatograms of HO were developed with two different developing solvent systems as shown in **Figure 2**. Curcumin, which possesses a variety of therapeutic properties including antioxidant, analgesic, anti-inflammatory, antiseptic, and anticarcinogenic activities, was used as a marker (Nagpal and Sood, 2013). The chromatogram developed with **System I** detected under visible light exhibited a single yellow spot of curcumin and HO with the same  $R_t$  value of 0.065 (A). Additionally, HO contained absorbing compounds that diminished the uniform layer fluorescence and which were detected as dark spots on a bright green background when excited with short-wave (254 nm) UV light at the  $R_t$  values of 0.065 (A), 0.272 (C), 0.473 (F), 0.549 (G), 0.759 (I), and 0.891 (J). The dark spot at the  $R_t$  value of 0.065 of HO was consistent with curcumin. Moreover, the native fluorescence compounds of HO were visualized at the  $R_t$  values of 0.065 (A), 0.233 (B), 0.341 (D), 0.406 (E), 0.618 (H), 0.759 (I), and 0.891 (J) when excited with long-wave (366 nm) UV light.

In conclusions, a yellow spot of HO component on TLC chromatograms was detected under visible light at the same *Rf* value of a yellow spot of curcumin. Both of them were dark spots on a bright green background when excited with short-wave (254 nm) UV light. Moreover, the spot was fluorescence with the bright green color which was consistent well with that of curcumin. Therefore, we could conclude from **System I** that curcumin was the major constituent of HO.

**System II** was also used to support the conclusion concerning the HO components. Under visible light, curcumin and HO exhibited a single yellow spot at the same  $R_f$  value of 0.259 (K). Additionally, HO contained absorbing compounds that diminished the uniform layer

fluorescence and were detected as dark spots on a bright green background when excited with short-wave (254 nm) UV light at the  $R_f$  values of 0.259 (K), 0.427 (L), 0.565 (M), and 0.669 (N). The dark spot at the  $R_f$  value of 0.259 of HO was consistent with curcumin. Moreover, the native fluorescence compounds of HO were visualized at the  $R_f$  value of 0.259 (K) and 0.565 (M) when excited with long-wave (366 nm) UV light. The fluorescence spot at the  $R_f$  value of 0.065 of HO was bright green which was consistent with that of curcumin. **System II** yielded the same conclusion with **System I,** i.e. that curcumin was the major constituent of HO.

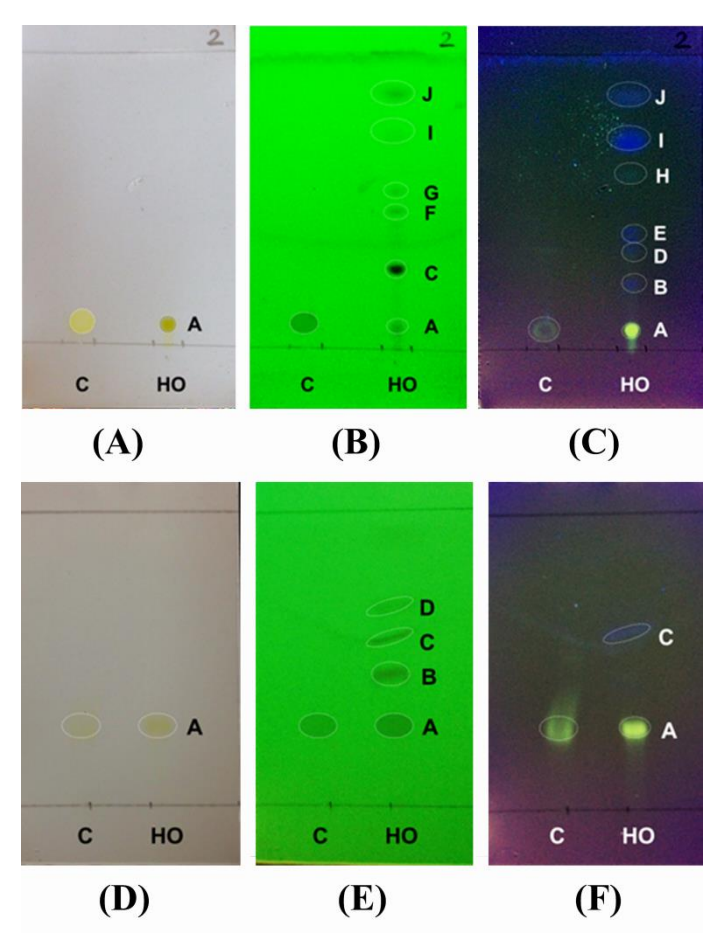


Figure 2 TLC chromatograms of curcumin (C) and HO after developing with ethanol and hexane in the ratio of 2:8 (System I) and detected under visible light (A), short-wave (254 nm) UV light (B), and long-wave (366 nm) UV light (C) and after developing with ethanol and hexane in the ratio of 4:6 (System II) and detected under visible light (D), short-wave (254 nm) UV light (E), and long-wave (366 nm) UV light (F)

## 4.2.3. HPLC analysis of HO

HO components were also analyzed by HPLC. The HPLC chromatograms (Figure 3) were detected by UV absorption at 420 nm, which is the wavelength associated with maximum

absorbance of curcumin (Kapoor and Priyadarsini, 2001; Gopinath et al., 2004). There was only one peak detected in HO at the retention time of 1.599 min, which corresponded well with that of the curcumin standard (1.599 min), leading us to conclude that the major constituent of HO was curcumin.

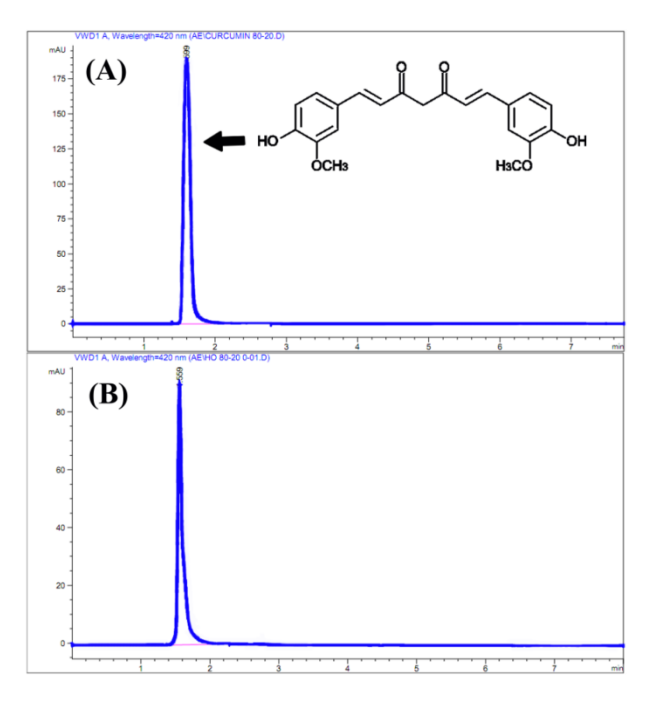


Figure 3 HPLC chromatograms of curcumin standard (A) and HO (B)

### 4.3. Cell cytotoxicity

The cell viabilities of human PBMCs after treatments with EO and HO for 48 h had no apparent toxic effects, as indicated by 100% of cell viability, even at high concentration (50%v/v) (**Figure 4**).

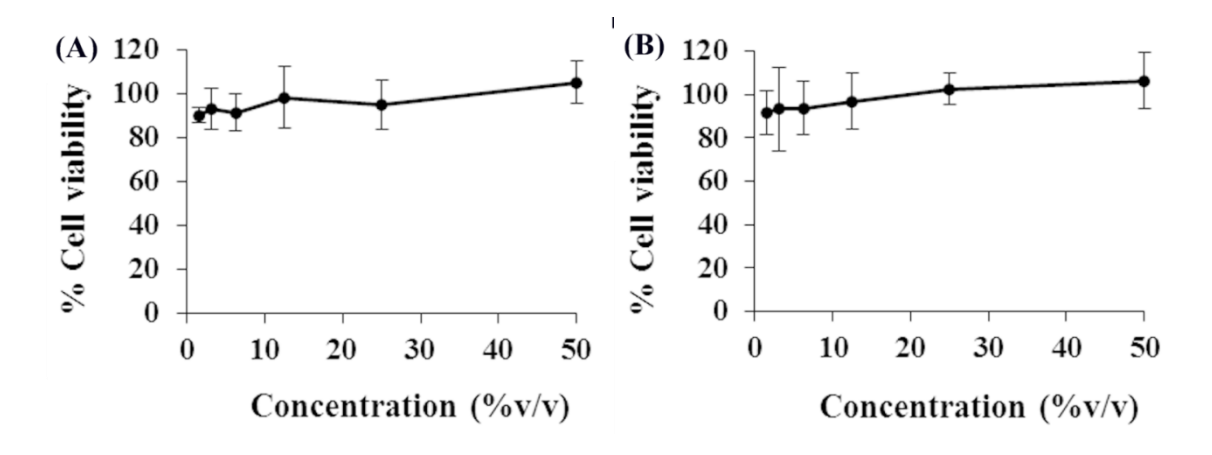


Figure 4 Dose-response curve of viability of PBMCs versus concentrations of EO (A) and HO (B) (n = 3)

# 4.4. Anti-inflammatory activity of EO and HO

#### 4.4.1. Determination of albumin denaturation inhibition

BSA denaturation inhibition of EO and HO are shown in **Figure 5** in comparison with indomethacin, a well-known anti-inflammatory agent. EO, HO, and indomethacin were able to protect BSA against heat denaturation with IC<sub>50</sub> values of 11.71±3.94  $\mu$ g/mL (R<sup>2</sup> = 0.969), 9.45±1.98  $\mu$ g/mL (R<sup>2</sup> = 0.968), and 6.20±2.58  $\mu$ g/mL (R<sup>2</sup> = 0.984), respectively. The results noted that protein denaturation inhibition of EO and HO was comparable to that of indomethacin (*P* < 0.05).

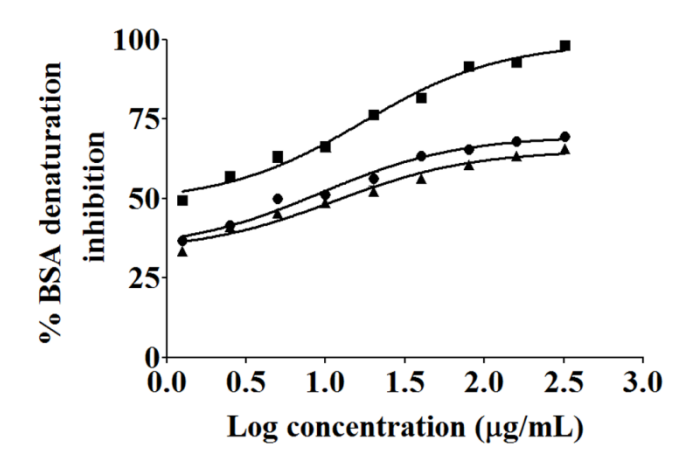


Figure 5 Effect of various concentrations of indomethacin (■), EO (▲), and HO (●) on inhibition of BSA denaturation

Denaturation of tissue protein is one of the known and documented causes of inflammation, due to the production of auto antigens (Phongpradist et al., 2015). Therefore, protein denaturation-preventing agents would be worthwhile targets for anti-inflammatory drug development. In this study, HO and EO could protect BSA against heat denaturation in the same manner as indomethacin. A previous study suggested that curcumin, was responsible for the anti-denaturation, as it interacted with the aliphatic regions around the lysine residue on the BSA (Phongpradist et al., 2015). Therefore, curcumin which is a major natural *phenolic* constituent of HO was responsible for the inhibition of BSA denaturation. Another prospective binding sites related to the anti-denaturation of BSA is aromatic tyrosine rich region (Shendkar et al., 2014). Various polyphenols have been reported for their BSA binding at this site including catechins [(-)-epigallocatechin-3-gallate, (-)-epigallocatechin, (-) -epicatechin-3-gallate], **fl**avones (kaempferol, kaempferol-3-glucoside, quercetin, naringenin), and hydroxycinnamic acids (rosmarinic acid, caffeic acid, p-coumaric acid) (Dymerski et al., 2015). In addition, several

terpenes (the major constituents of EO) were able to bind well with BSA due to their small hydrophobic molecules (Adams and Anslyn, 2009).

### 4.4.2. NF-<sub>K</sub>B inhibition

An immunoblotting assay was used to determine the levels of NF- $_{\rm K}$ B protein in U937 cells. The concentrations of EO and HO for cell treatments were based on the IC $_{20}$  values. IC $_{20}$  values of EO and HO were 7.82 $\pm$ 0.92  $\mu$ g/mL and 179.39 $\pm$ 19.20  $\mu$ g/mL, respectively. Therefore, the concentration of 7.80  $\mu$ g/mL was selected for EO and HO treatment in this experiment.

Indomethacin was used as a positive control and it was identified as a potential compound that could suppress NF-<sub>K</sub>B expression. The time-response effect of indomethacin, EO, and HO are shown in **Figure 6**. Indomethacin reduced the NF-<sub>K</sub>B expression to 88.97±2.36%, 15.00±1.92%, and 1.53±3.23% after 12, 24, and 48 h of incubation time, respectively. EO and HO showed less pronounce suppression. EO reduced the NF-<sub>K</sub>B expression to 97.97±3.53%, 82.61±1.65%, and 9.36±4.27%%, whereas, HO reduced the NF-<sub>K</sub>B expression to 94.13±5.14%, 82.73±3.25%, and 77.25±4.96% after incubated for 12, 24, and 48 h. The NF-<sub>K</sub>B suppression was most obviously observed at 48 h, the effects of major constituents of EO and HO on NF-<sub>K</sub>B protein levels were therefore investigated at that period of time.

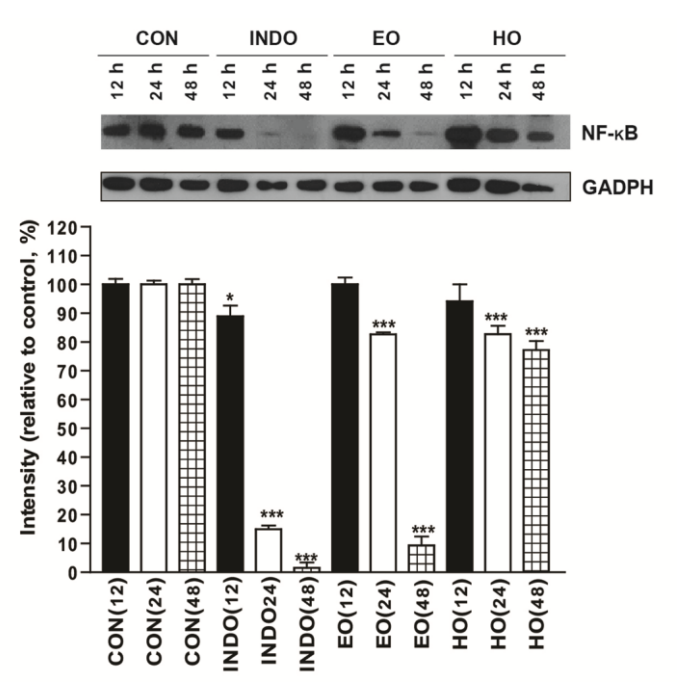


Figure 6 Western blotting of NF-<sub>K</sub>B from U937 cells treated with indomethacin (IND), control (CON), EO, and HO at 12 h (black), 24 h (white), and 48 h (grid) (n = 3, \* denote P < 0.05, \*\* denote P < 0.01, \*\*\* denote P < 0.001)

In another experiment, EO and HO at the same concentration of indomethacin (7.8  $\mu$ g/mL) were able to suppress NF- $_K$ B, as well as their major constituents (**Figure 7**). NF- $_K$ B expression was reduced to 14.37 $\pm$ 2.87%, 58.31 $\pm$ 2.74%, and 64.02 $\pm$ 3.91% after treated with indomethacin, EO, and HO, respectively. The results noted that EO showed significantly higher NF- $_K$ B suppression than HO (P < 0.05). Curcumin, the major constituent of HO significantly reduced NF- $_K$ B expression to 91.66 $\pm$ 3.89% (P < 0.05). Sabinene and terpinen-4-ol significantly reduced NF- $_K$ B expression to 53.32 $\pm$ 4.96% and 22.16 $\pm$ 7.86%, repectively (P < 0.01).

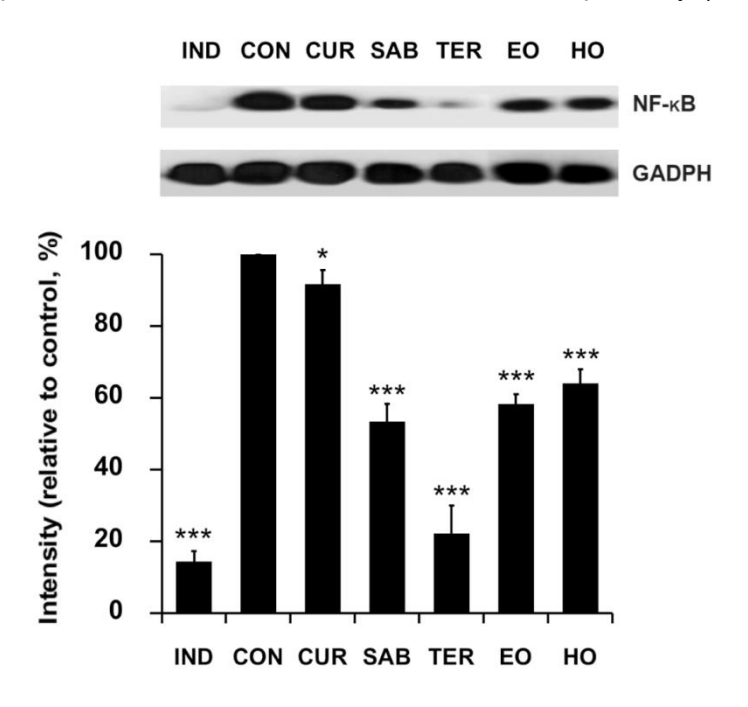


Figure 7 Western blotting of NF-<sub>K</sub>B from U937 cells treated with indomethacin (IND), control (CON), curcumin (CUR), sabinene (SAB), terpinen-4-ol (TER), EO, and HO (n = 3, \* denote P < 0.05, \*\* denote P < 0.01, \*\*\* denote P < 0.001)

NF- $_{\rm K}$ B transcription factor is a protein marker that responses to inflammations. Therefore, prevention of NF- $_{\rm K}$ B activation is directly related with reduction of the inflammatory process (Maroon et al., 2005). The duration of incubation time in Western blot analysis show a great effect on the NF- $_{\rm K}$ B suppression. At 12 h, only indomethacin could suppress the NF- $_{\rm K}$ B expression (P < 0.05). The NF- $_{\rm K}$ B suppression of EO and HO were observed after 24 h and more distinct effects were observed after 48 h.

EO, HO, and their major constituent were investigated for the capability to suppress NF- $_{\rm K}$ B expression. Both EO and HO possessed anti-inflammatory effect since they could significantly suppress the NF- $_{\rm K}$ B expression (P < 0.01). Curcumin, a major constituent of HO, also possesses good anti-inflammatory properties. Our results are in line with those of a

previous study showing that NF-<sub>K</sub>B expression is suppressed by curcumin (Surh et al., 2001). The anti-inflammatory effect of curcumin is well-known (Maheshwari et al., 2006; Menon & Sudheer, 2007). Beside NF-<sub>K</sub>B suppression, it could inhibit different molecules involved in inflammation process, including phospholipase, lipooxygenase, cyclooxygenase 2, leukotrienes, thromboxane, prostaglandins, nitric oxide, collagenase, elastase, hyaluronidase, monocyte chemoattractant protein-1, interferon-inducible protein, tumor necrosis factor, and interleukin-12 (Chainani-Wu, 2003). However, the NF-<sub>K</sub>B suppression by curcumin was less pronounced than that of HO. Therefore, the compounds responsible for anti-inflammatory effects of HO may not be due solely to curcumin. There are additional constituents of Z. cassumunar rhizome extracts that act as potent anti-inflammatory agents, such as cassumunarins, phenylbutenoids, zerumbone, (E)-4-(3',4'-dimethoxyphenyl)but-3-en-2-ol, (E)-1-(3,4-dimethoxyphenyl) butadiene, (E)-4-(30,40-dimethoxyphenyl) but-3-en-l-ol, etc. (Masuda et al., 1995; Han et al., 2005; Masuda and Jitoe, 1995; Murakami et al., 2004; Panthong et al., 1997; Chaiwongsa et al., 2013; Jeenapongsa et al., 2003; Pongprayoon et al., 1997; Suksaeree et al., 2015). Some of these compounds may be extracted by the hot infusion method and included in HO, but in only small amounts not detectable by HPLC. Due to their potent anti-inflammatory effects, only small amounts of any of the latter compounds could produce anti-inflammatory properties of HO.

Sabinene and terpinen-4-ol, major constituents of EO, showed potent anti-inflammatory effects. The NF- $_{K}$ B suppression of terpinen-4-ol was comparable to that of indomethacin. This suggests that the active constituents responsible for anti-inflammatory activity of EO were terpinen-4-ol and sabinene. In addition, terpinen-4-ol was found to suppress the production of several pro-inflammatory mediators, such as tumor necrosis factor  $\alpha$  (TNF $\alpha$ ), interleukin-1 $\beta$ , interleukin-8, interleukin-10, prostaglandin E $_2$ , and reduced superoxide production by neutrophils and monocytes stimulated with N-formyl-methionyl-leucyl-phenylalanine and lipopolysaccharide (Hart et al., 2000; Brand et al., 2001). Moreover, it significantly inhibited edema formation in the test of carrageenan-induced hind paw edema in rats (Pongprayoon et al., 1997). Thus there are different pathways of inflammation affected by terpinen-4-ol.

Similarly, sabinene has demonstrated anti-inflammatory activity through various mechanisms. It inhibited nitric oxide ion production in lipopolysaccharide plus interferon- $\gamma$  triggered macrophages (Valente et al., 2013). However, sabinene was ineffective as a topical anti-inflammatory agent in the model of carrageenan-induced hind paw edema in rats (Pongprayoon et al., 1997).

#### 4.4.3. Determination of IL-6 secretion inhibition

IL-6 secretion level of RAW 264.7 cell line after stimulated with LPS and treated with EO and HO did not show significant reduction comparing to the cell stimulated only with LPS (data not shown). Curcumin also had no effect on the inhibition of IL-6 secretion. Although EO did not show significant reduction in IL-6 secretion level, the major constituents of EO show a promising anti-inflammatory effect. The dose response effects of terpinen-4-ol and sabinene are shown in **Figure 8**. Both compounds did not show the reduction effect at the low concentration (5  $\mu$ g/mL). However, the reduction effects were distinctly presented at the concentration of 50  $\mu$ g/mL and terpinen-4-ol and sabinene significantly reduce the IL-6 secretion level to 82.42±1.90% and 79.75±6.72%, respectively (P < 0.05).

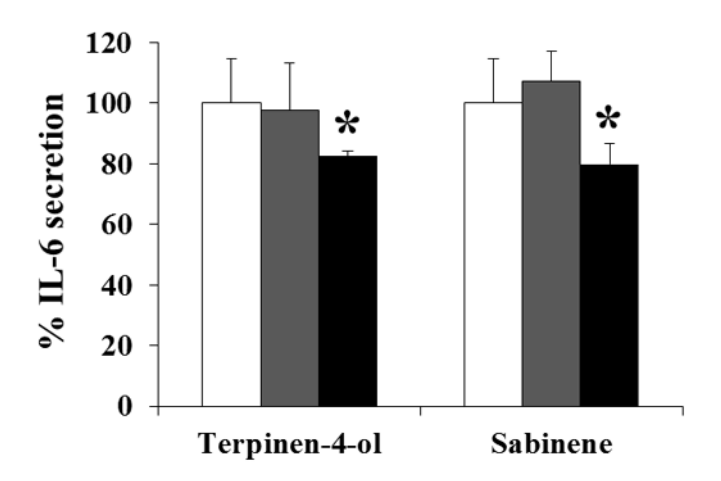


Figure 8 IL-6 secretion of RAW 264.7 cell line after treated with terpinen-4-ol and sabinene at the concentration of 5  $\mu$ g/mL (gray) and 50  $\mu$ g/mL (black) comparing to control (white) (n = 3, \* denote P < 0.05)

IL-6 was involved in the inflammation process because of its ability to regulate the transition from neutrophil to monocyte recruitment which is the hallmark of acute inflammation (Kaplanski et al., 2003). In chronic inflammation, IL-6 might increase the mononuclear-cell infiltrate and participate in disease pathogenesis (Kaplanski et al., 2003). Therefore, the compound that could reduce or inhibit the IL-6 secretion would possess anti-inflammatory effect. Our present study indicated that Terpinen-4-ol and sabinene, the major constituents of EO, significantly reduce the IL-6 secretion level which supported the conclusion concerning the anti-inflammation of EO. According to higher amount of terpinen-4-ol and sabinene in essential oil of *Z. cassumunar* comparing to other Zingiberaceous plants (Natta et al., 2008), EO

possessed high anti-inflammatory effect and hence supported the extensively used of *Z. cassumunar* in folklore remedies as anti-inflammation and antianalgesic.

## 4.5. Required HLB of EO and HO

The required HLB values of HO and EO were determined by external appearance inspection (Figure 9 and Figure 10), droplet size analysis (Figure 11), and turbidimetric method (Figure 11). All the experiments indicated that HLB values of HO and EO were 6 and 10, respectively.



Figure 9 External appearance of emulsion containing HO (A) and EO (B) using various HLB value of surfactant mixtures (Tween 20 and Span 20) ranging from 5 to 16

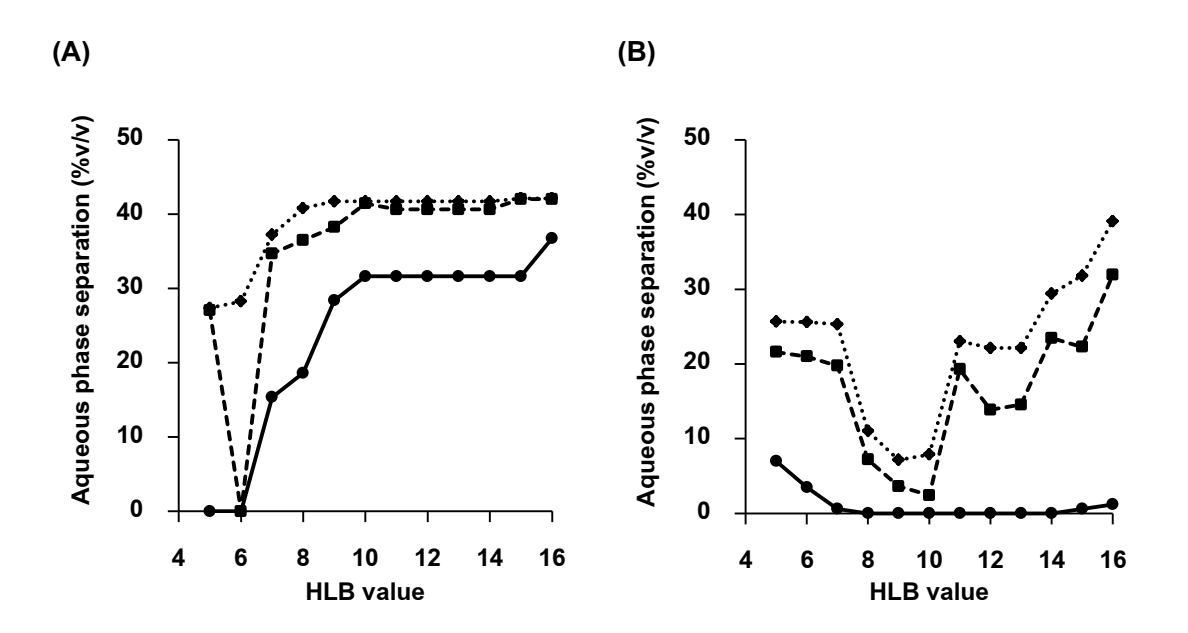
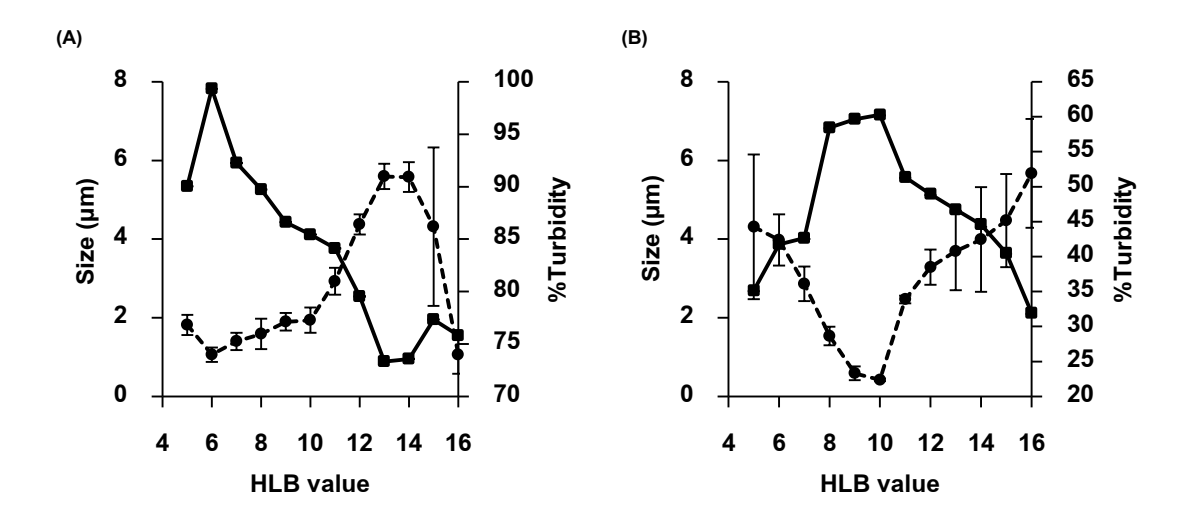


Figure 10 Aqueous phase separation of emulsion containing HO (A) and EO (B) using various HLB value of surfactant mixtures (Tween 20 and Span 20) ranging from 5 to 16 after 1 day (●), 7 days (■), and 30 days (◆)



**Figure 11** Internal droplet size (●) and Turbidity (■) of emulsion containing HO **(A)** and EO **(B)** using surfactant mixtures (Tween 20 and Span 20) with HLB ranging from 5 to 16 after 30 days

### 4.6. Microemulsion Development

#### 4.6.1. Microemulsion of EO

#### 4.6.1.1. Pseudoternary phase diagrams

#### 4.6.1.1.1. Effect of surfactant type

Various non-ionic surfactants, including individual surfactants and surfactant mixtures, were used in this study. Span 80 was mixed with Tween 20 or Triton X-114 to form the surfactant mixture having HLB value of 10 which was equal to the required HLB value of EO. The results as shown in **Figure 12** indicated that the individual surfactant gave larger microemulsion region comparing to the surfactant mixture. Therefore, Tween 20 which gave the largest microemulsion region in the phase diagram was used in the further study.

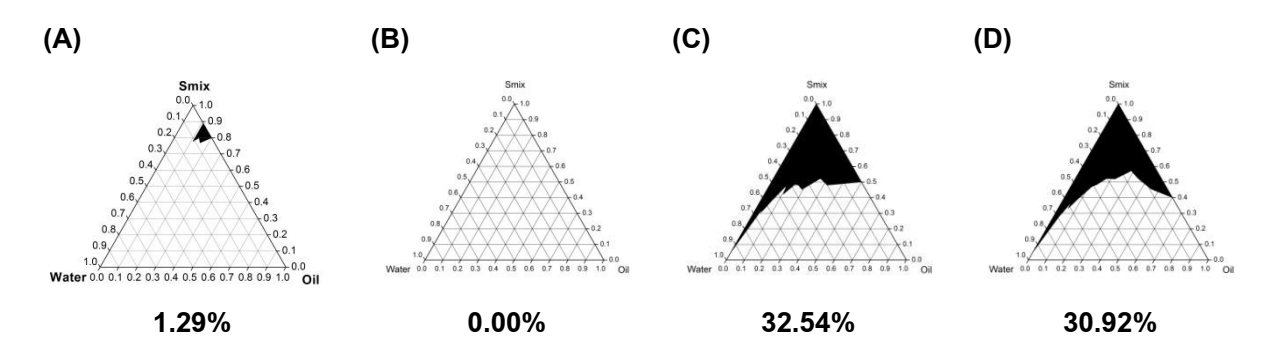
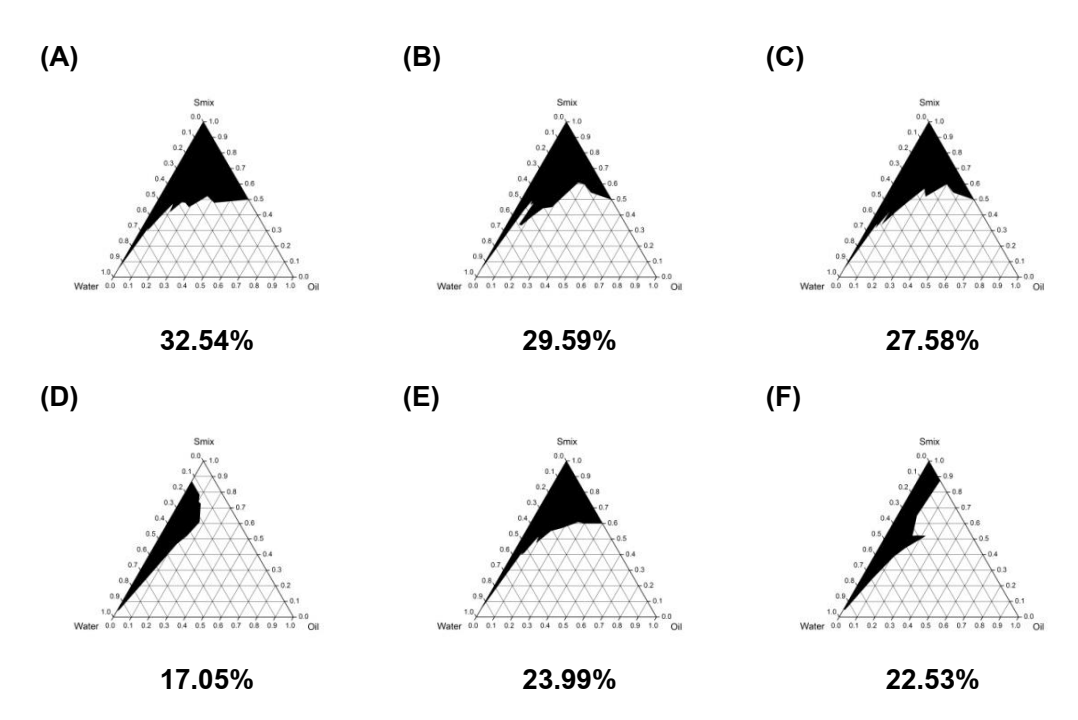


Figure 12 Pseudoternary phase diagram of EO/surfactant/ethanol/water when surfactant were Tween 20 and Span 80 (HLB = 10) (A), Triton X-114+Span 80 (HLB = 10) (B), Tween 20 (C), and Triton X-114 (D), whereas, surfactant to co-surfactant ratio was 1:1

#### 4.6.1.1.2. Effect of co-surfactant type

Various co-surfactants were used in this study. Alcohol including ethanol, propan-1-ol, and propan-2-ol gave large microemulsion region in the phase diagram as shown in **Figure 13**.



**Figure 13** Pseudoternary phase diagram of EO/Tween 20/co-surfactant /water when the co-surfactant were ethanol **(A)**, propan-1-ol **(B)**, propan-2-ol **(C)**, glycerin **(D)**, propylene glycol **(E)**, and polyethylene glycol 400 **(F)**, whereas, surfactant to co-surfactant ratio was 1:1

#### 4.6.1.1.3. Effect of surfactant to co-surfactant ratio

Surfactant to co-surfactant ratio aftected the microemulsion regions in the phase diagram. The areas were not much different in the systems using Tween 20 and ethanol (**Figure 14**), whereas, higher ratio leaded to higher microemulsion region in the systems using Tween 20 and prpylene glycol (**Figure 15**).

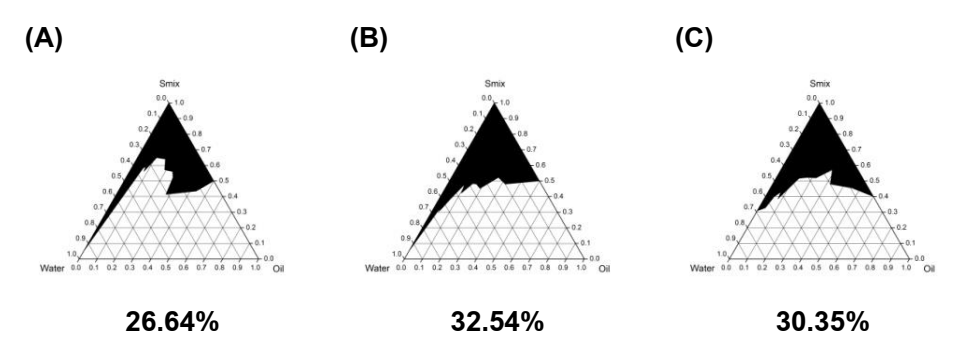


Figure 14 Pseudoternary phase diagram of EO/Tween 20/ethanol/water when the surfactant to co-surfactant ratio were 2:1 (A), 1:1 (B), and 1:2 (C)

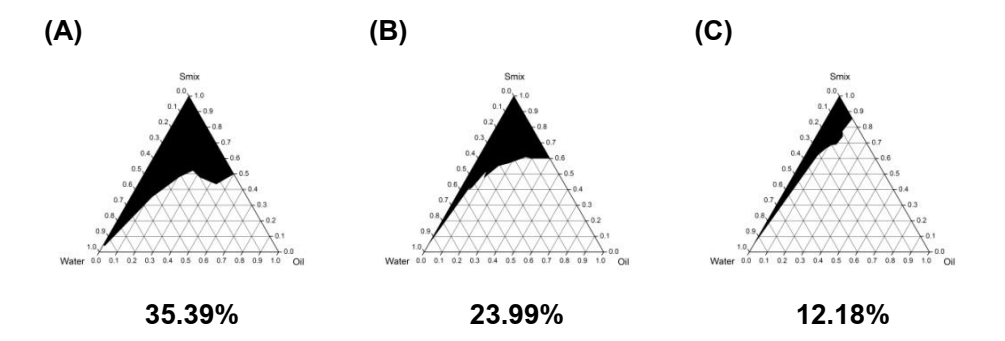
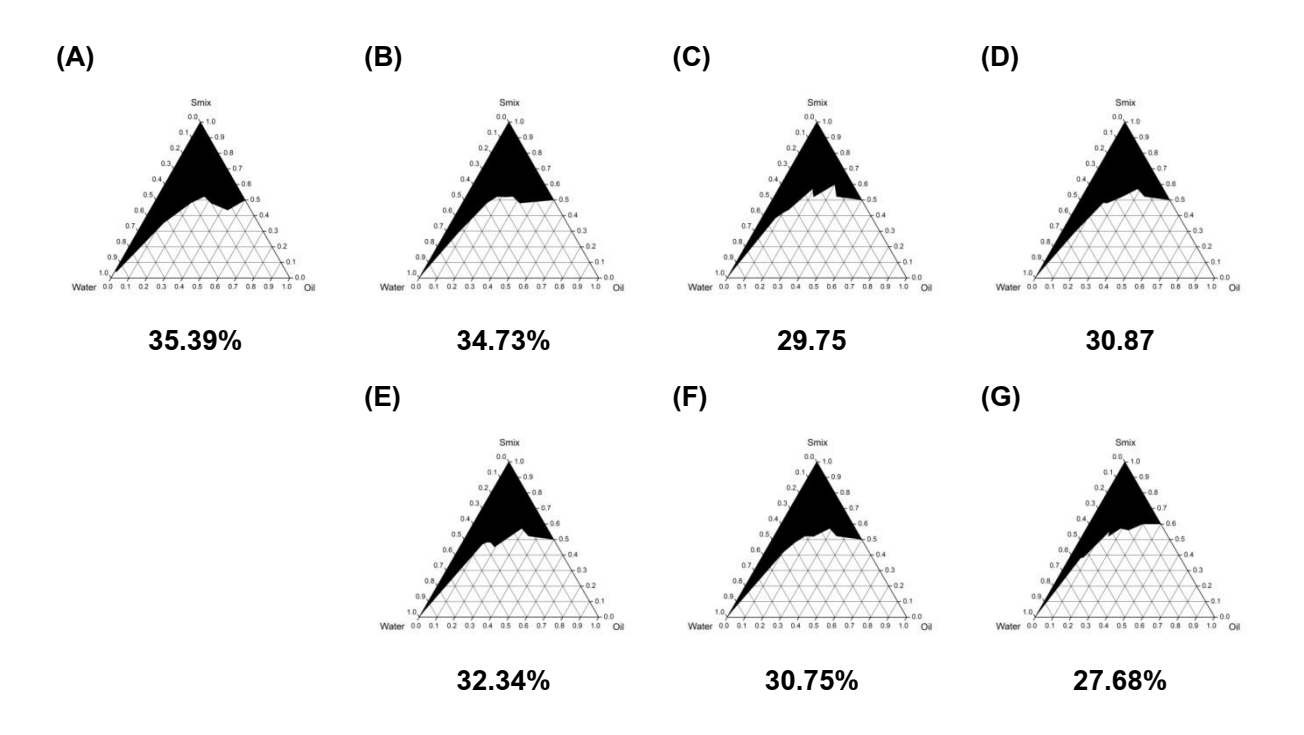


Figure 15 Pseudoternary phase diagram of EO/Tween 20/propylene glycol/water when the surfactant to co-surfactant ratio were 2:1 (A), 1:1 (B), and 1:2 (C)

# 4.6.1.1.4. Effect of ionic strength

The effects of monovalent salt (NaCl) and divalent salt (MgCl<sub>2</sub>) are shown in **Figure 16**. There was no effect from both salts except at the high concentration (1.0 M).



**Figure 16** Pseudoternary phase diagram of EO/Tween 20/propylene glycol/water phase when the surfactant to co-surfactant ratio were 2:1 and the water phase were DI water (A), 0.1 M NaCl (B), 0.5 M NaCl (C), 1.0 M NaCl (D), 0.1 M MgCl<sub>2</sub> (E), 0.5 M MgCl<sub>2</sub> (F), and 1.0 M MgCl<sub>2</sub> (G)

### 4.6.1.1.5. Effect of pH

The effects of pH are shown in **Figure 17**. There was almost no effect from pH on microemulsion region in the phase diagram.

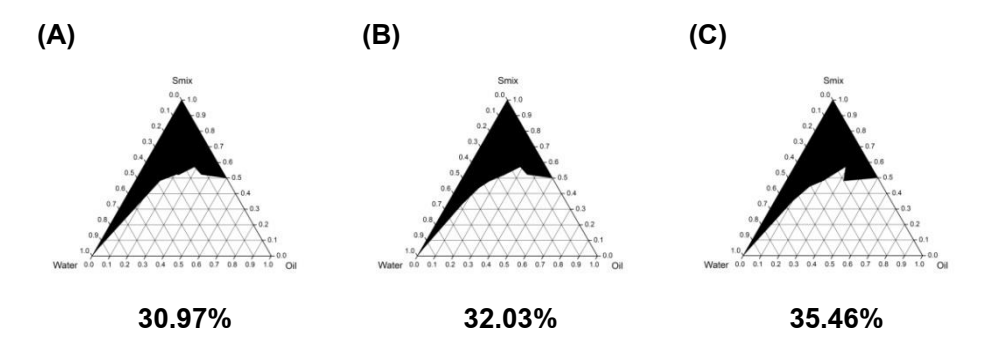


Figure 17 Pseudoternary phase diagram of EO/Tween 20/propylene glycol/water phase when the surfactant to co-surfactant ratio were 2:1 and the pH of water phase were 4.0 (A), 6.0 (B), and 8.0 (C)

#### 4.6.1.2. Characterization of selected blank microemulsion of EO

Six formulations in the pseudoternary phase diagram of EO/Tween 20/propylene glycol/water are shown in **Figure 18**. All the formulations were clear liquid with very slightly yellow color. They were then selected for the formulation characterizations including particle size, size distribution, electrical conductivity, rheology, and pH.

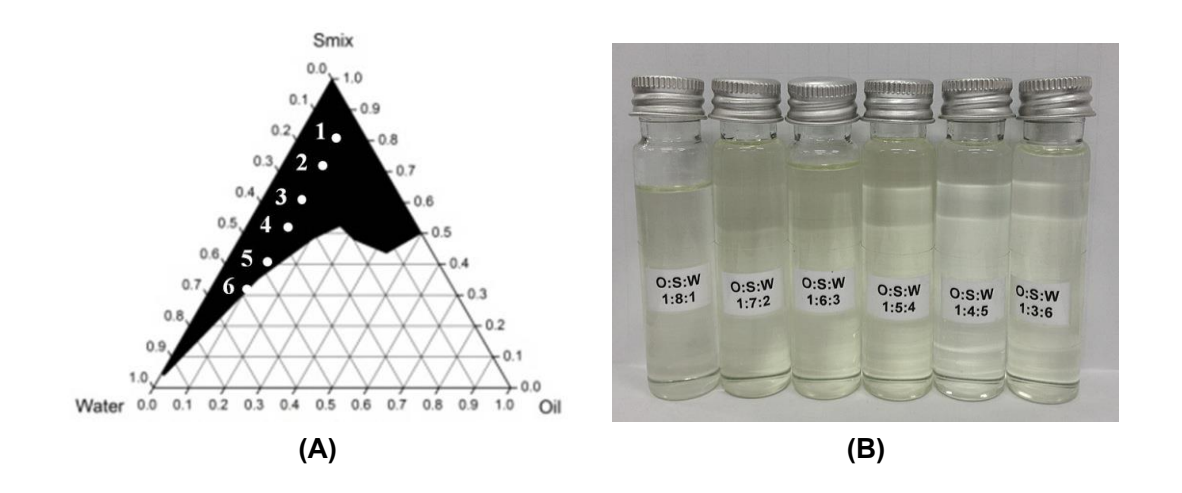


Figure 18 Pseudoternary phase diagram of EO/Tween 20/propylene glycol/water when the ratio of Tween 20 to propylene glycol was 2:1 (A), and the physical appearance of microemulsion number 1 to 6 from the left to right, respectively (B)

### 4.6.1.2.1. Particle size / size distribution

The internal droplet size and polydispersity index of each EO microemulsions are shown in **Figure 19**. The size of EO microemulsions were in the range of 211.5 to 366.7 nm with medium polydispersity index which were less than 0.38.

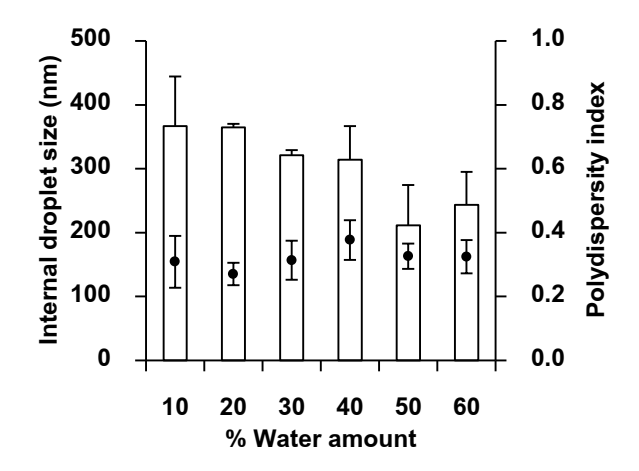
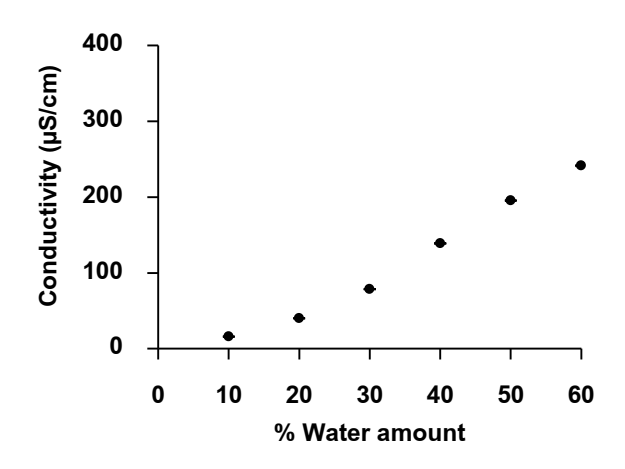


Figure 19 Internal droplet size (□) and polydispersity index (●) of microemulsions containing EO, Tween 20, propylene glycol, and water when the ratio of Tween 20 to propylene glycol was 2:1

#### 4.6.1.2.2. Electrical conductivity determination

The electrical conductivity of each microemulsions are shown in **Figure 20**. The conductivity increased as the water content in the formulations increased.



**Figure 20** Electrical conductivity of microemulsions containing EO, Tween 20, propylene glycol, and water when the ratio of Tween 20 to propylene glycol was 2:1

### 4.6.1.2.3. Rheology study

All formulation shows Newtonian's flow behaviour. The viscosity of each microemulsions as shown in **Figure 21** are in the range of 0.65 to 0.84 mPas.

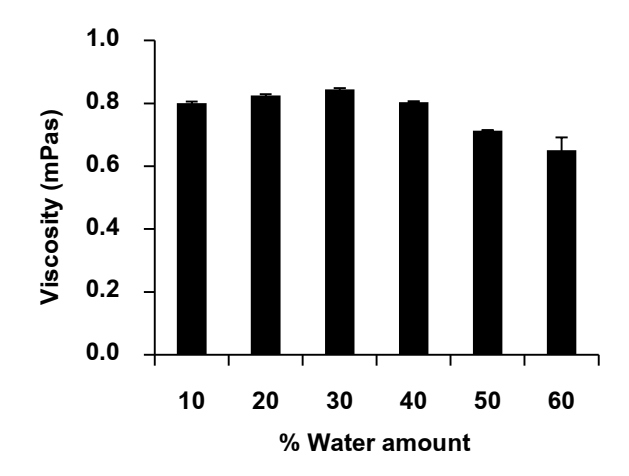


**Figure 21** Viscosity of microemulsions containing EO, Tween 20, propylene glycol, and water when the ratio of Tween 20 to propylene glycol was 2:1

#### 4.6.1.2.4. pH measurements

The pH of each EO microemulsions as shown in Figure 22 is in the range of 4.8 to 5.5.

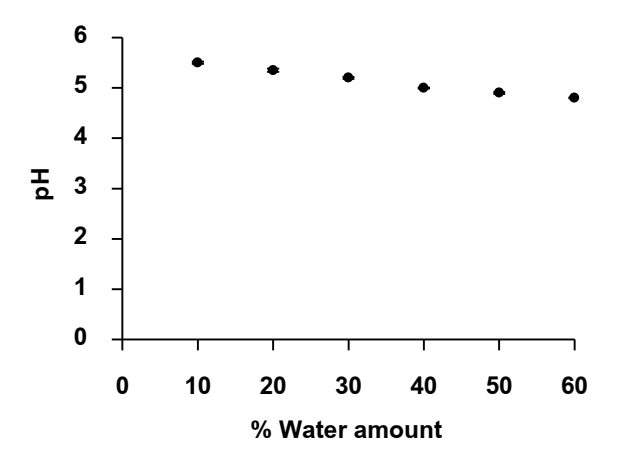


Figure 22 pH of microemulsions containing EO, Tween 20, propylene glycol, and water when the ratio of Tween 20 to propylene glycol was 2:1

#### 4.6.1.2.5. Stability study of blank microemulsion of EO

All microemulsion of EO showed a good stability after the heating-cooling stability test. There was no significantly statistical change (P < 0.05) in the physical appearance, internal droplet size, viscosity, and pH. Microemulsion number 1 (EO-1) was investigated for the EO

content after the heating-cooling stability study in a comparison with EO solution in propylene glycol. Two major constituents of EO, sabinene and terpinen-4-ol, were used as marker for the quantitative analysis by using GC-MS. The results as shown in **Figure 23** indicated that the content of sabinene in propylene glycol solution significantly decreased after the stability study (P < 0.05). In contrast, both sabinene and terpinen-4-ol content was still the same in EO-1. Therefore, it might be concluded that microemulsion tended to protect EO from the evaporation.

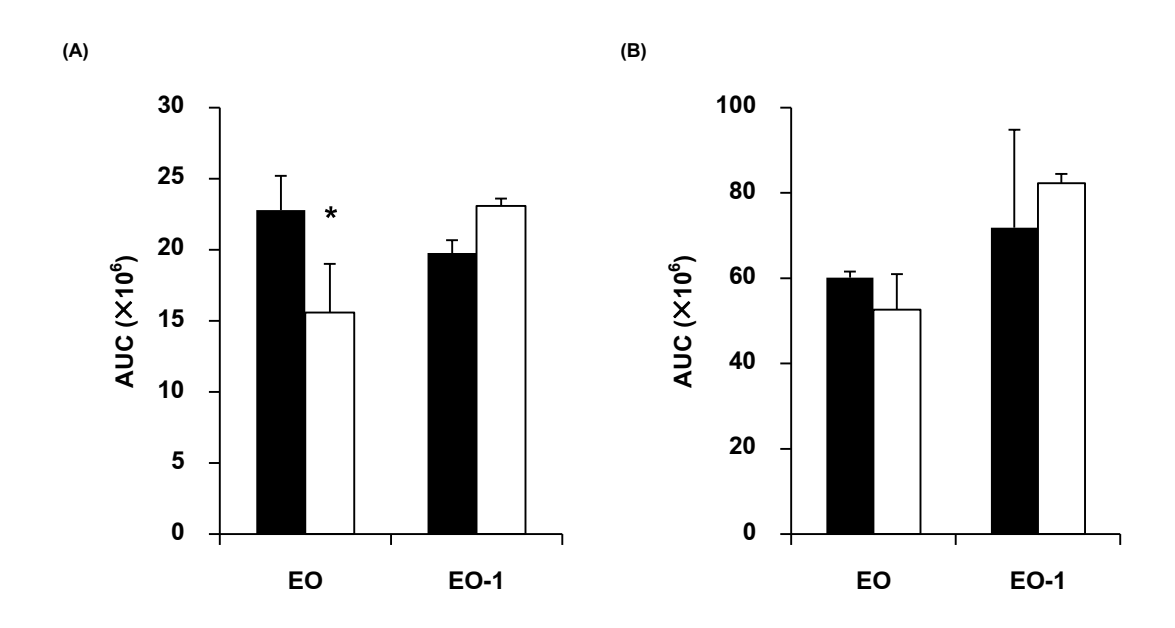


Figure 23 AUC of sabinene (A) and terpinen-4-ol (B) of EO solution in propyleneglycol (EO) and microemulsio number 1 (EO-1) before ( $\blacksquare$ ) and after ( $\square$ ) the heating-cooling stability test

#### 4.6.2. Microemulsion of HO

#### 4.6.2.1. Pseudoternary phase diagrams

# 4.6.2.1.1. Effect of surfactant type

Various non-ionic surfactants, including individual surfactants and surfactant mixtures, were used in this study. Span 80 was mixed with Tween 20 or Triton X-114 to form the surfactant mixture having HLB value of 6 which was equal to the required HLB value of HO. The results as shown in **Figure 24** indicated that the surfactant mixtures did not gave larger microemulsion region comparing to the individual surfactant. Therefore, Triton X-114 which gave the largest microemulsion region in the phase diagram were used in the further study.

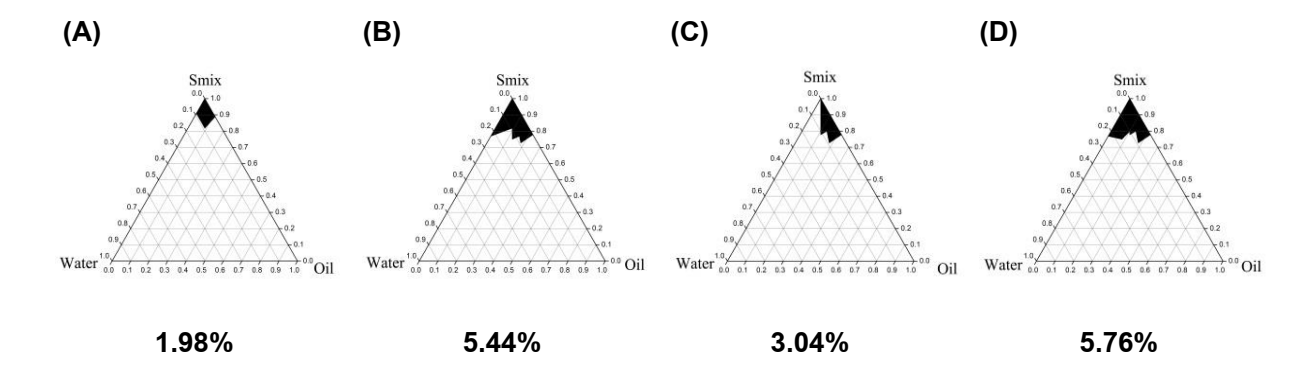


Figure 24 Pseudoternary phase diagram of HO/surfactant/propan-2-ol/water when surfactant were Tween 20 and Span 80 (HLB = 6) (A), Triton X-114+Span 80 (HLB = 6) (B),

Tween 20 (C), and Triton X-114 (D), whereas, surfactant to co-surfactant ratio was 3:2

#### 4.6.2.1.2. Effect of oil mixture

From the above results, the microemulsion regions were very small. HO were consequently diluted in castor oil or oleic acid in the ratio of 1:1. The pseudoternary phase diagrams are shown in **Figure 25**. HO and oleic acid mixture gave the largest microemulsion region of 45.25%.

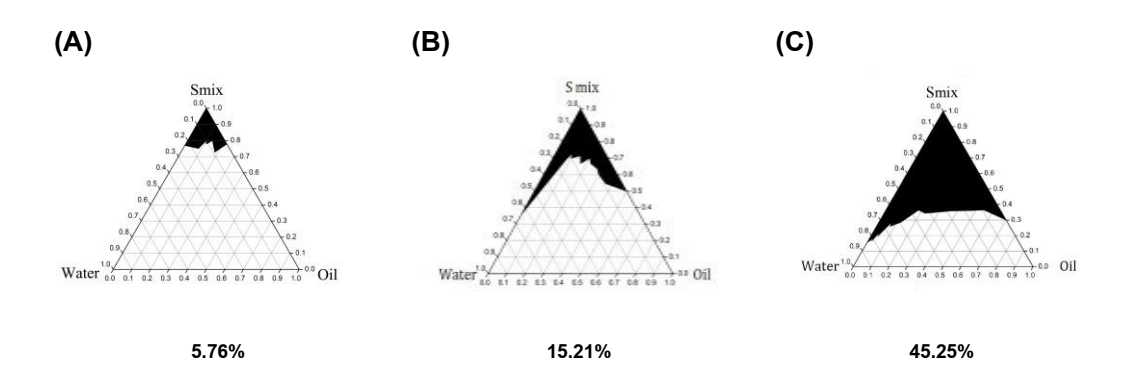


Figure 25 Pseudoternary phase diagram of oil/Triton X-114/propan-2-ol/water when the oil were HO (A), HO and castor oil (1:1) (B), and HO and oleic acid (1:1) (C), whereas, surfactant to co-surfactant ratio was 3:2

#### 4.6.2.1.3. Effect of co-surfactant type

Various co-surfactants were used in this study. Alcohols, including absolute ethanol, 95% ethanol, and propan-2-ol, gave almost the same area of microemulsion region in the phase diagram as shown in **Figure 26**.

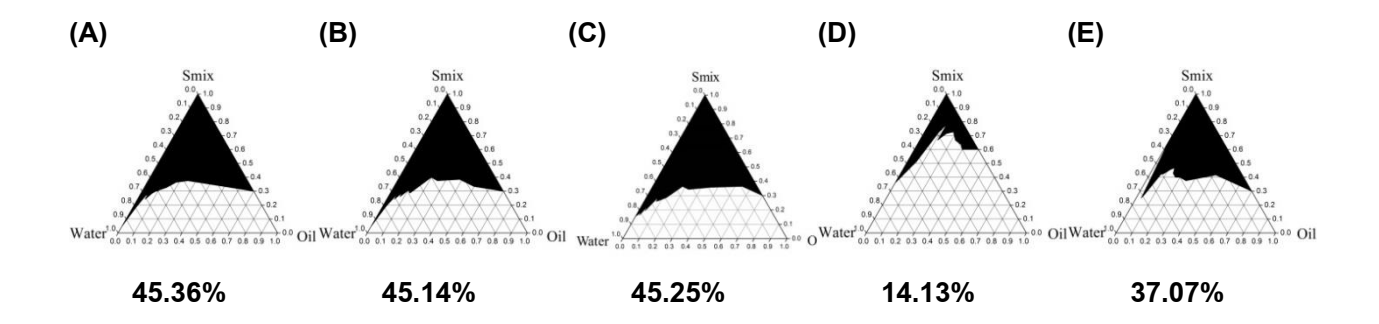


Figure 26 Pseudoternary phase diagram of HO and oleic acid (1:1)/Triton X-114/co-surfactant/
water when the co-surfactant were absolute ethanol (A), 95% ethanol (B),
propan-2-ol (C), polyethylene glycol 400 (D), and propylene glycol (E),
whereas, surfactant to co-surfactant ratio was 3:2.

#### 4.6.2.1.4. Effect of surfactant to co-surfactant ratio

Various amount of surfactant in the surfactant/co-surfactant mixture (Smix) were ranged from 20% to 80%. Higher amout of surfactant in Smix leaded to higher microemulsion region in the phase diagram (**Figure 27**).

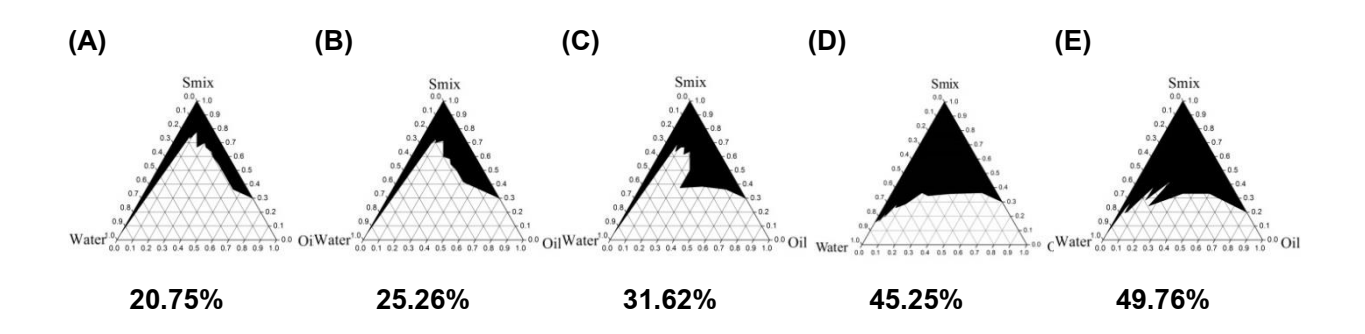


Figure 27 Pseudoternary phase diagram of HO and oleic acid (1:1)/Triton X-114/ propan-2-ol/water when the surfactant to co-surfactant ratio were 2:8 (A), 4:6 (B), 5:5 (C), 6:4 (D), and 8:2 (E)

### 4.6.2.2. Characterization of selected blank microemulsion of HO

Six formulations in the pseudoternary phase diagram of HO and oleic acid (1:1)/Triton X-114/propan-2-ol/water when the ratio of Triton X-114 to propan-2-ol was 3:2 are shown in **Figure 28**. All the formulations were clear liquid with yellow color. They were then selected for the formulation characterizations including particle size, size distribution, electrical conductivity, rheology, and pH.

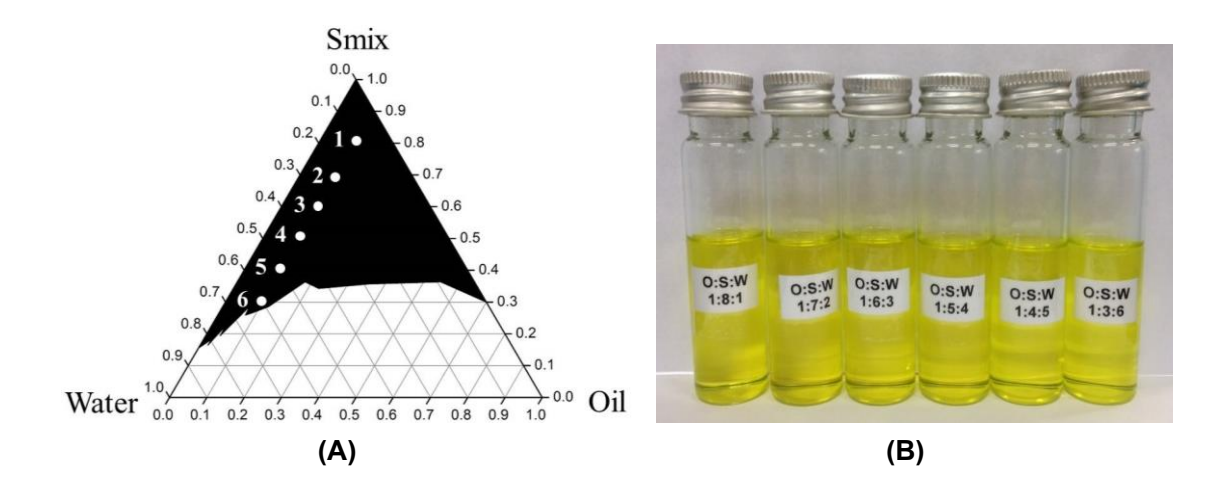


Figure 28 Pseudoternary phase diagram of HO and oleic acid (1:1)/Triton X-114/propan-2-ol/water when the ratio of Triton X-114 to propan-2-ol was 3:2 (A), and the physical appearance of microemulsion number 1 to 6 from the left to right, respectively (B)

### 4.6.2.2.1. Particle size / size distribution

The internal droplet size and polydispersity index of each HO microemulsions are shown in **Figure 29**. The size of HO microemulsions were in the range of 26.7 to 31.6 nm with small polydispersity index which was less than 0.25.

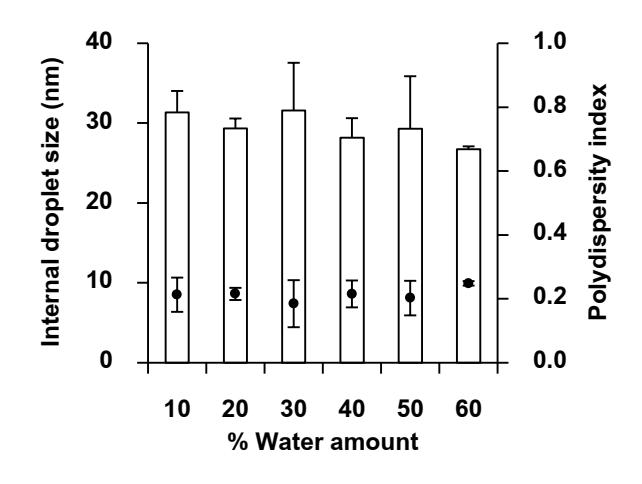
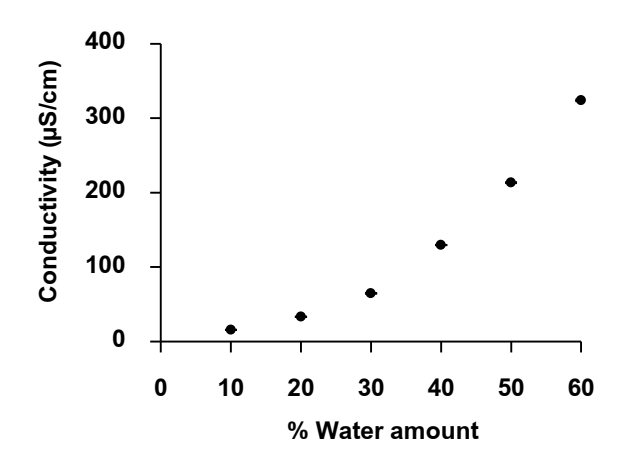


Figure 28 Internal droplet size (□) and polydispersity index (●) of microemulsions containing HO and oleic acid (1:1), Triton X-114, propan-2-ol, and water when the ratio of Triton X-114 to propan-2-ol was 3:2

### 4.6.2.2.2. Electrical conductivity determination

The electrical conductivity of each HO microemulsions are shown in **Figure 30**. The conductivity increased as the water content in the the formulations increased.



**Figure 30** Electrical conductivity of microemulsions containing HO and oleic acid (1:1), Triton X-114, propan-2-ol, and water when the ratio of Triton X-114 to propan-2-ol was 3:2

### 4.6.2.2.3. Rheology study

All formulation showed Newtonian's flow behaviour. The viscosity of each HO microemulsions as shown in **Figure 31** are in the range of 0.015 to 0.024 mPas.

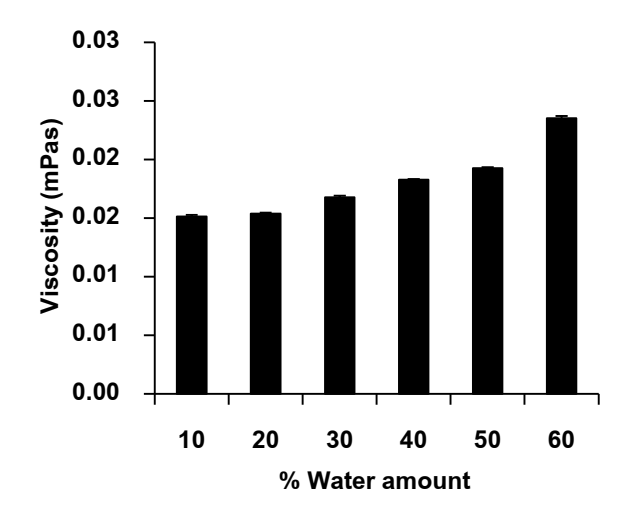


**Figure 31** Viscosity of microemulsions containing HO and oleic acid (1:1), Triton X-114, propan-2-ol, and water when the ratio of Triton X-114 to propan-2-ol was 3:2

### 4.6.2.2.4. pH measurements

The pH of each HO microemulsions as shown in **Figure 32** are in the range of 3.9 to 5.0.

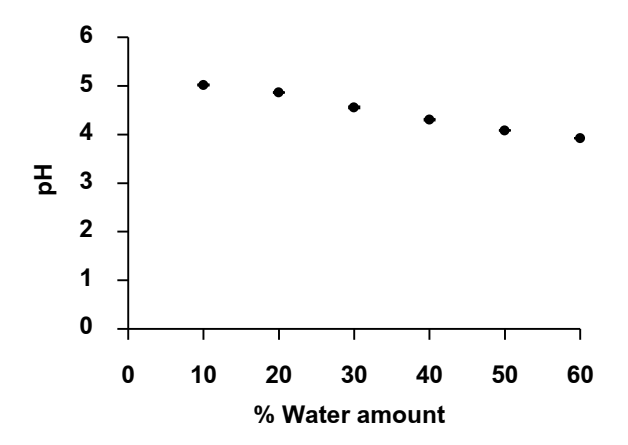


**Figure 32** pH of microemulsions containing HO and oleic acid (1:1), Triton X-114, propan-2-ol, and water when the ratio of Triton X-114 to propan-2-ol was 3:2

### 4.6.2.2.5. Stability study of blank microemulsion of HO

All microemulsion of HO showed a good stability after the heating-cooling stability test. There was no significantly statistical change (P < 0.05) in the physical appearance, internal droplet size, viscosity, and pH. Six microemulsions (HO-1 to HO-6) were investigated for peroxidation value to indicate if microemulsion could protect HO from the oxidation and rancidity. The results as shown in **Figure 33** indicated that peroxidation value of the native HO significantly increased after the heating-cooling stability study, whereas, the microemulsions showed less pronounce effect. Therefore, it might be concluded that microemulsion tended to protect HO from the oxidation and reduce the occurrence of rancidity.

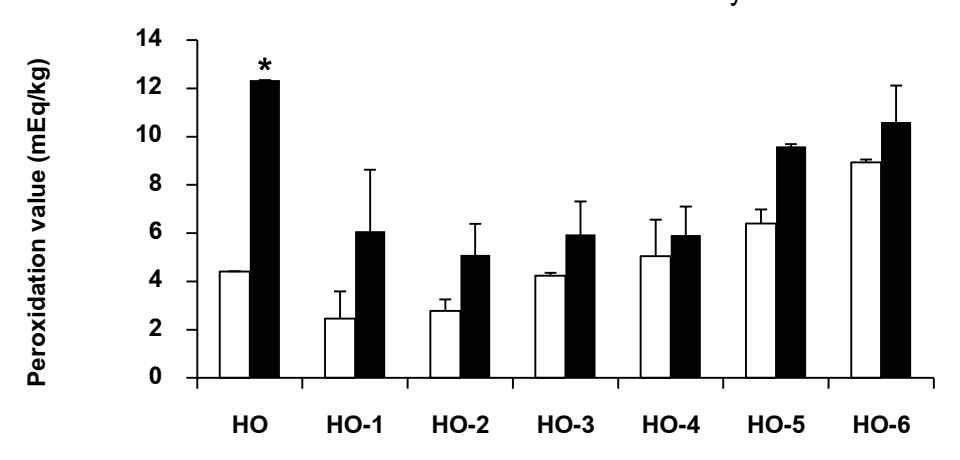


Figure 33 Peroxidation value of native HO (HO) and microemulsions of HO

before ( $\blacksquare$ ) and after ( $\square$ ) the heating-cooling stability test (P < 0.05)

#### 4.7. Cytotoxicity of microemulsions

The cell viabilities of human PBMCs after treatments with microemulsion containing EO and HO for 48 h had slightly toxic effects, as indicated around 80% of cell viability as shown in Figure 34.

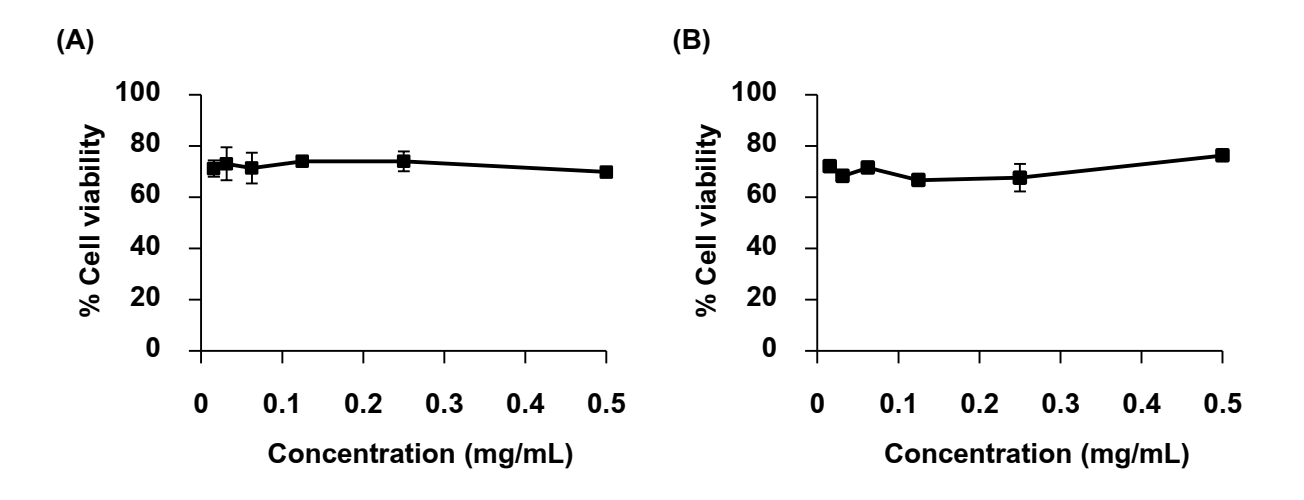


Figure 34 Dose-response curve of viability of PBMCs versus concentrations of microemulsion containing EO (A) and HO (B) (n = 3)

## 4.8. Anti-inflammatory activity of microemulsions

#### 4.8.1. Determination of albumin denaturation inhibition

BSA denaturation inhibitions of microemulsions in a comparison with the native oils are shown in **Figure 35**. The results noted that the native oil showed higher BSA denaturation inhibition than their microemulsions at low concentration (1.56%w/w) and the inhibitions seem to reach the maximum effect at higher concentrations. The likely explanation might be from the surfactant content in the microemulsion formulation. EO-2, EO-4, and EO-6 contained 70, 50 and 30%w/w of Smix, respectively. Higher amount of Smix might give a greater effect on the solubilization and led to more transparent properties of the test solution. Therefore, the inhibitions, which were calculated from the turbidity, were lower in the samples containing higher amount of Smix. Moreover, the lower inhibitory effect of microemulsion might be from the protection of the surfactant layer. Since the oils were incorporated in the internal phase of microemulsions, they need to be released from the formulation before coming across with the BSA.

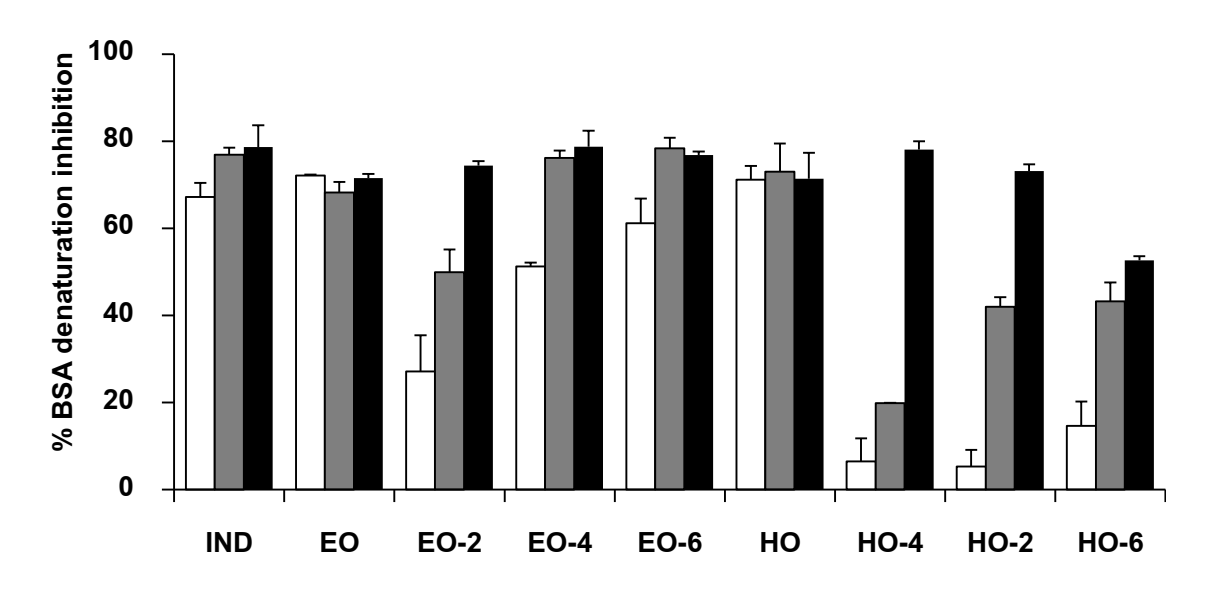


Figure 35 BSA denaturation inhibition of indomethacin (IND), EO, microemulsion containing EO (EO-2, EO-4, EO-6), HO, and microemulsion containing HO (HO-2, HO-4, HO-6) at the concentration of 1.56%w/w (□), 3.13%w/w (■), and 6.25%w/w (■)

#### 4.8.2. NF-<sub>K</sub>B inhibition

The western blottings of NF-<sub>K</sub>B from U937 cells treated with the native oils in a comparison with their microemulsion are shown in Figure 36. The results noted that microemulsion show distinctly higher NF-<sub>K</sub>B suppression effect than that of their native oils. EO reduced NF-κB expression by 26.2%, whereas, EO-2, EO-4, and EO-6 reduced NF-κB expression by 53.1%, 98.6%, and 94.9%, respectively. HO reduced NF-kB expression by 7.0%, whereas, EO-2, EO-4, and EO-6 reduced NF-<sub>K</sub>B expression by 99.7%, 99.5%, and 99.2%, respectively. The likely explanation might be from the small droplet size of the microemulsion, as well as, their higher surface area to contact with the target site. However, some effects might be from other components in the formulations. Microemulsion blanks (ME), which were the formulations contain everything except the oil, were also investigated for the NF-<sub>K</sub>B suppression effect. ME of EO microemulsion contained Tween 20, propylene glycol, and water, whereas, ME of HO microemulsion contained oleic acid, Triton X-114, propan-2-ol, and water. The results indicated that MEs had some effects on NF-KB expression. ME of EO reduced NF-<sub>κ</sub>B expression by 37.3%, whereas, ME of HO reduced NF-<sub>κ</sub>B expression by 84.3%. However, the microemulsions containing both EO and HO show distinctly higher NF-KB suppression effect than their ME. Therefore, it can be concluded that microemulsion increases the NF-<sub>K</sub>B suppression effect of the oils.

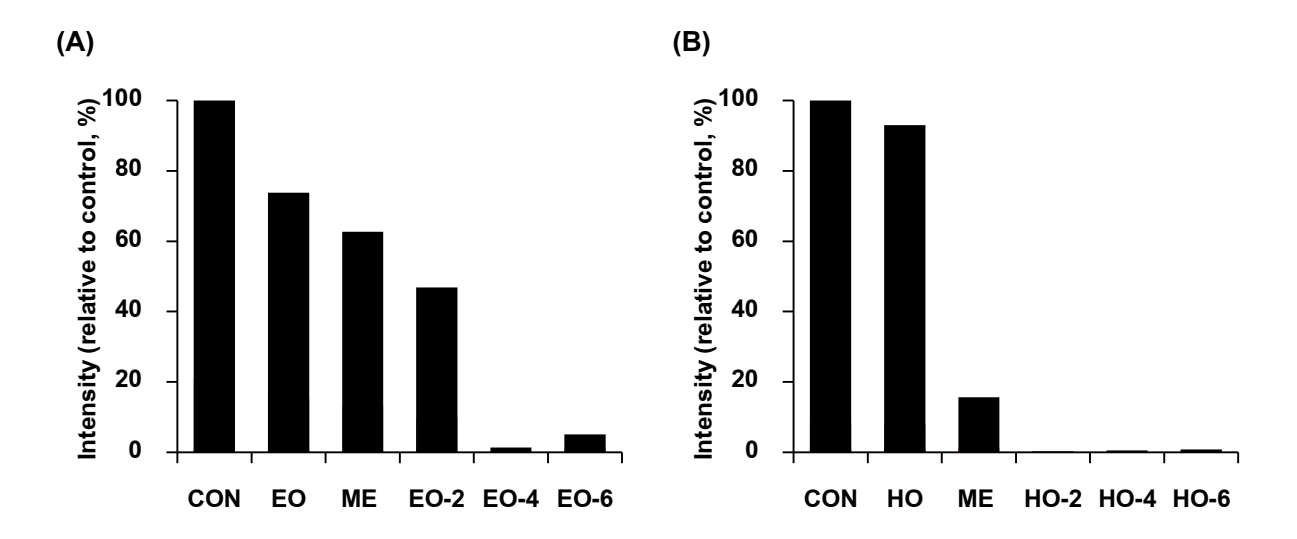


Figure 36 Western blotting of NF-<sub>K</sub>B from U937 cells treated with control (CON), microemulsion control (ME), EO, microemulsion containing EO (EO-2, EO-4, EO-6), HO, and microemulsion containing HO (HO-2, HO-4, HO-6)

### 4.9. Microemulsion-based gel development

Carbopol 940 and sodium carboxymethylcellulose (SCMC) was used as gelling agent for microemulsion-based gel development. The final concentration of carbopol 940 and SCMC in the formulation were 1, 1.5, and 2.5%w/w. Six microemulsions containing EO including EO-1 to EO-6 were incorporated to the gel base of carbopol 940 and SCMC to obtain microemulsion-based gel. The physical appearances are shown in **Figure 37**. Similarly, Six microemulsions containing HO including HO-1 to HO-6 were incorporated to the gel base and the physical appearances are shown in **Figure 38**.

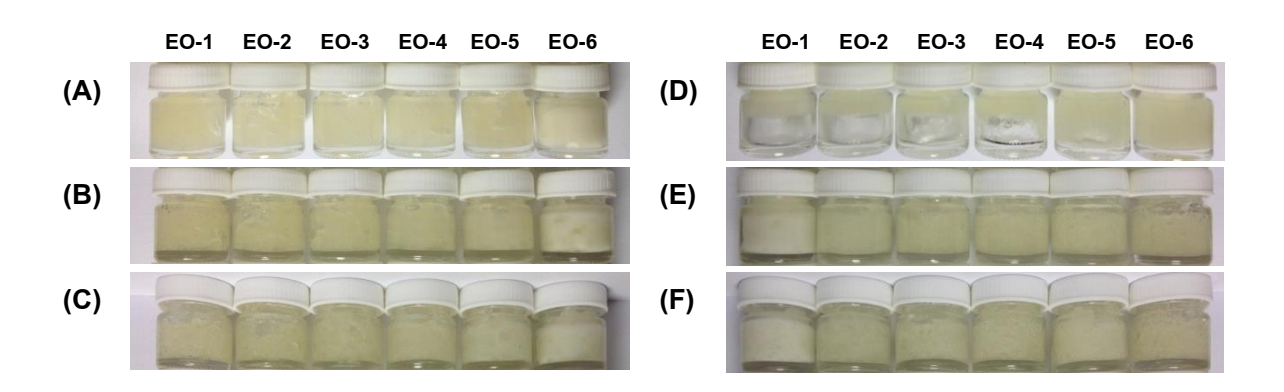
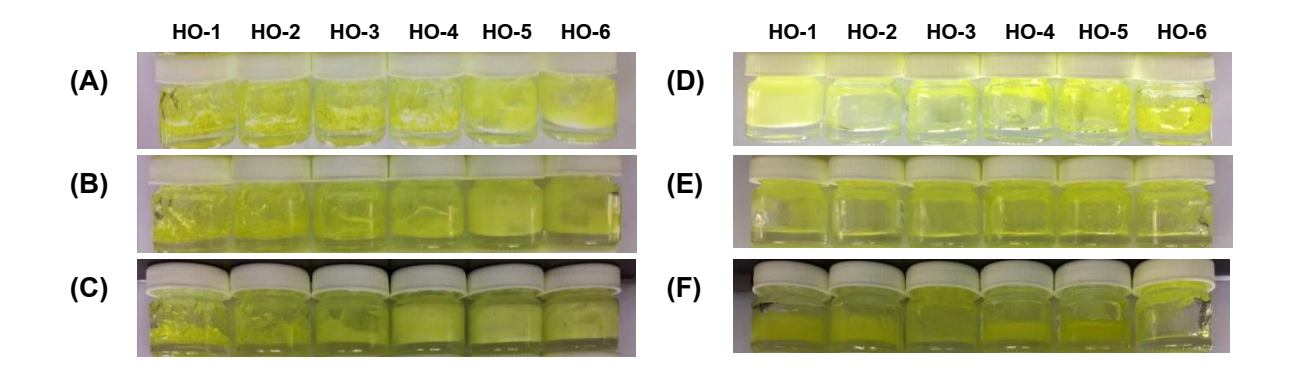


Figure 37 Microemulsion-based gel containing 1%w/w carbopol 940 (A), 1.5%w/w carbopol 940 (B), 2.5%w/w carbopol 940 (C), 1%w/w SCMC (D), 1.5%w/w SCMC (E), 2.5%w/w SCMC (F) and EO-1 to EO-6 from left to right, respectively



**Figure 38** Microemulsion-based gel containing 1%w/w carbopol 940 **(A)**, 1.5%w/w carbopol 940 **(B)**, 2.5%w/w carbopol 940 **(C)**, 1%w/w SCMC **(D)**, 1.5%w/w SCMC **(E)**, 2.5%w/w SCMC **(F)** and HO-1 to HO-6 from left to right, respectively

The appearance of microemulsion-based gel was obviously different from the gel containing the oil as shown in **Figure 39**. Incorporating the oil into microemulsion before mixing with gel base could produce the clear gel because of the transparent property of microemulsion. However, the microemulsions containing high amount of water could turn the gel base turbid due to the dilution effect.

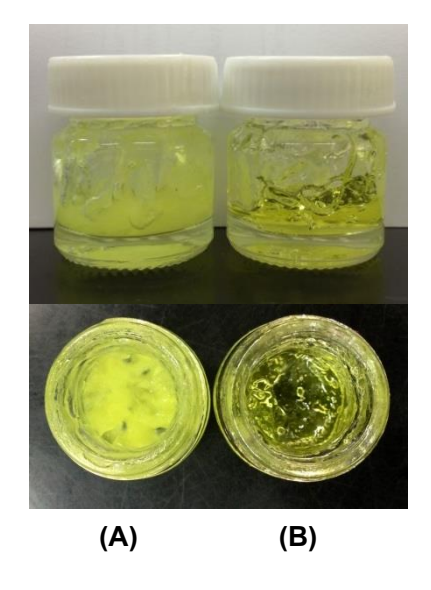


Figure 39 Gel containing HO (A) and microemulsion-based gel com containing HO (B)

### 4.9.1. Rheology study

The rheogram of microemulsion-based gel is shown in **Figure 40**. The flow behavior was pseudoplastic with thixotropy which was appropriated for the topical semisolid formulation.

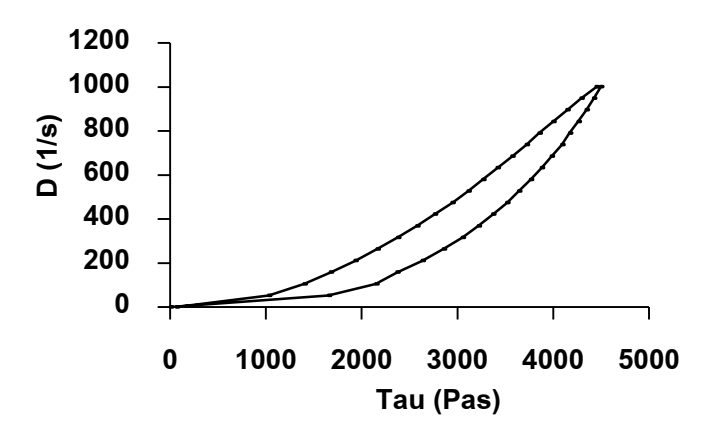


Figure 40 Rheogram of microemulsion-based gel containing 1%w/w carbopol 940 and HO-1

The viscosity of each microemulsion-based gels are shown in **Figure 41.** At the same concentration of gelling agent, carbopol 940 gave higher viscosity than SCMC. The viscosity of microemulsion-based gels increased when increased the concentration of gelling agents except in the case of EO-5 and EO-6 with carbopol 940. The likely explanation might be from the phase separation of the microemulsion-based gels.

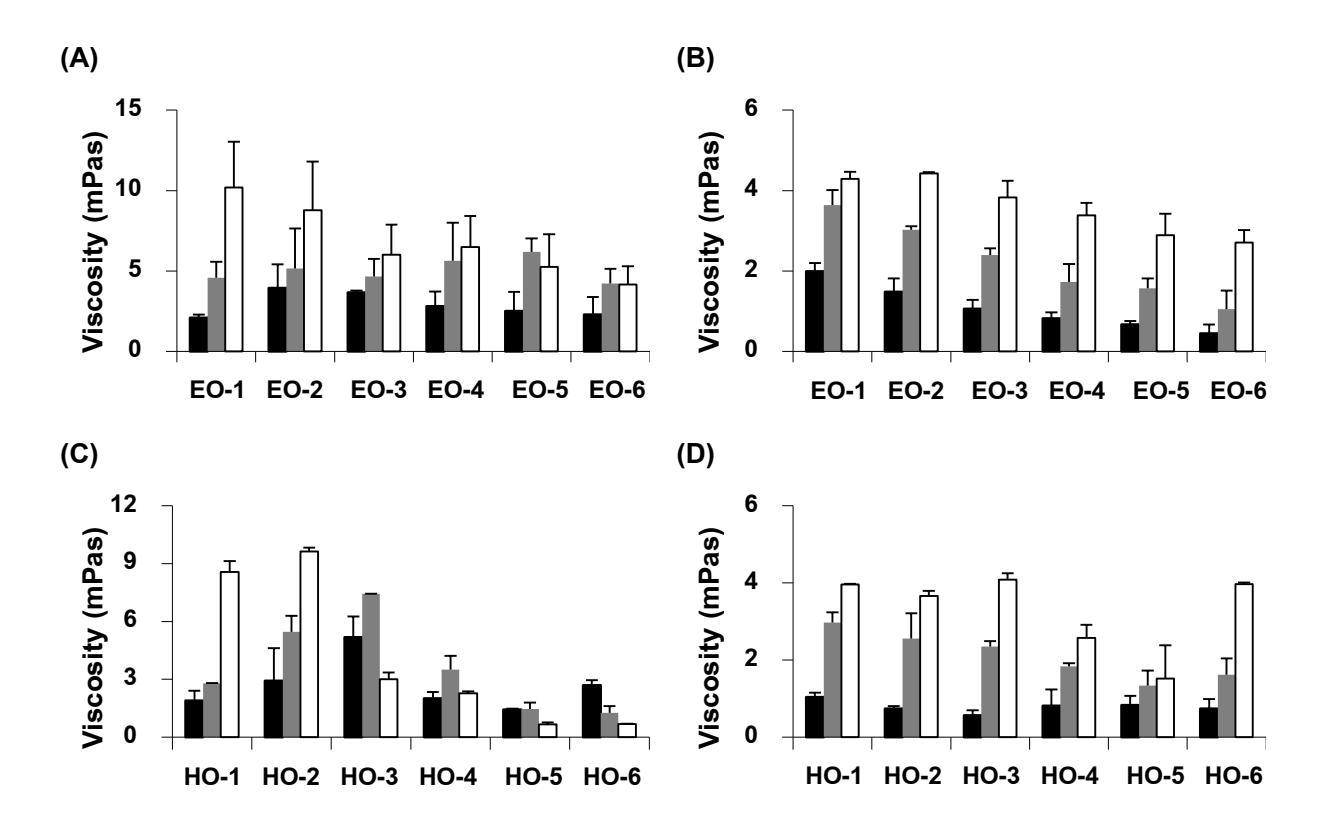


Figure 41 Viscosity of microemulsion-based gel containing 1%w/w gelling agent (■),
1.5%w/w gelling agent (■), and 2.5%w/w gelling agent (□)
when the gelling agent was carbopol 940 (A and C) or SCMC (B and D)

#### 4.9.2. pH measurements

The pH of microemulsion-based gel containing SCMC was in the range of 4.8 to 5.5, whereas, the pH of microemulsion-based gel containing carbopol 940 was in the range of 5.5 to 6.0.

#### 4.9.3. Stability study

Microemulsion-based gel of EO showed a good stability since the physical appearances were not changed as shown in **Figure 42**. The formulations using 2.5%w/w carbopol 940 and 2.5%w/w SCMC showed better characteristics comparing to the formulation using lower amount of gelling agent. The microemulsion of EO that generated the clear microemulsion-based gels were EO-1 to EO-4 for both gelling agents. The changing in pH and viscosity of the microemulsion-based gels was also observed to determine the stability of the formulation. The stability results noted that pH of microemulsion-based gel was not change from the beginning. Microemulsion-based gel containing SCMC had a pH in the range of 4.8 to 5.5, whereas, the pH of microemulsion-based gel containing carbopol 940 was in the range of 5.5 to 6.0. The viscosities of microemulsion-based gel of EO before and after the heating-cooling stability test are shown in **Figure 43**. There was no significantly change in the viscosity in the system of 2.5%w/w carbopol 940. In contrast, there were significantly decrease in viscosity in the system of 2.5%w/w SCMC. Therefore, 2.5%w/w carbopol 940 is the best choice for development of microemulsion-based gel of EO.

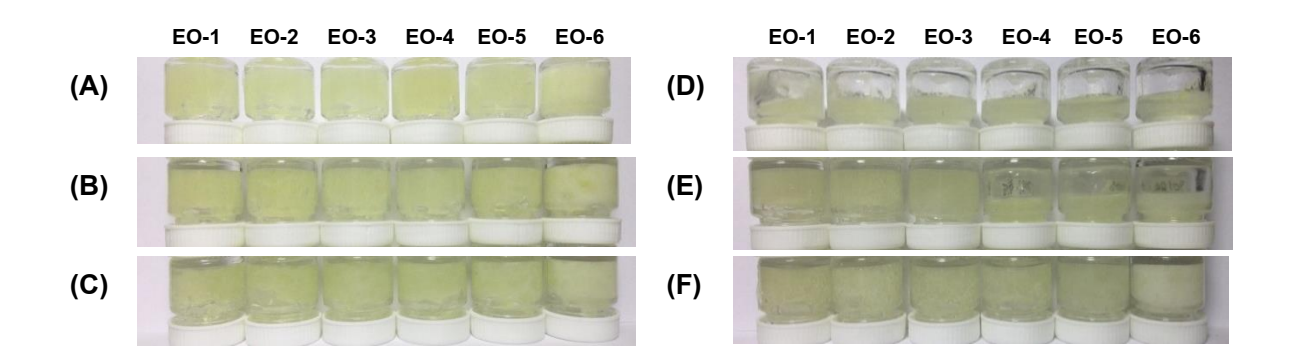


**Figure 42** Microemulsion-based gel containing 1%w/w carbopol 940 **(A)**, 1.5%w/w carbopol 940 **(B)**, 2.5%w/w carbopol 940 **(C)**, 1%w/w SCMC **(D)**, 1.5%w/w SCMC **(E)**, 2.5%w/w SCMC **(F)** and EO-1 to EO-6 from left to right, respectively after the heating-cooling stability test

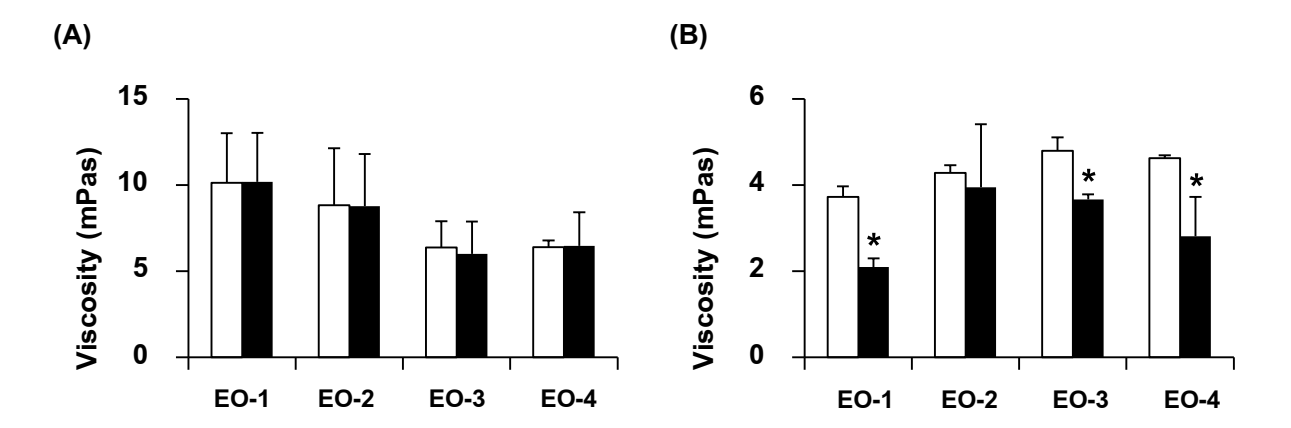


**Figure 43** Viscosity of microemulsion-based gel of EO containing 2.5%w/w carbopol 940 **(A)** and 2.5%w/w SCMC **(B)** before  $(\Box)$  and after  $(\Box)$  the heating-cooling stability test (P < 0.05)

The physical appearances of microemulsion-based gel of HO after the heating-cooling stability test are shown in **Figure 44**. The instability was observed in the formulations contained higher amount of corbopol 940 accompanied with higher content of water in the microemulsions. The formulations using 1%w/w carbopol 940 and 2%w/w SCMC showed the best characteristics. The microemulsion of HO that generated the clear microemulsion-based gels were HO-1 to HO-3 for both gelling agents. The changing in pH and viscosity of the microemulsion-based gels was also observed to determine the stability of the formulation. The stability results noted that pH of microemulsion-based gel was not change from the beginning. Microemulsion-based gel containing SCMC had a pH in the range of 4.8 to 5.5, whereas, the pH of microemulsion-based gel containing carbopol 940 was in the range of 5.5 to 6.0. The viscosities of microemulsion-based gel of HO before and after the heating-cooling stability test are shown in **Figure 45**. There was no significantly change in the viscosity in all formulation.

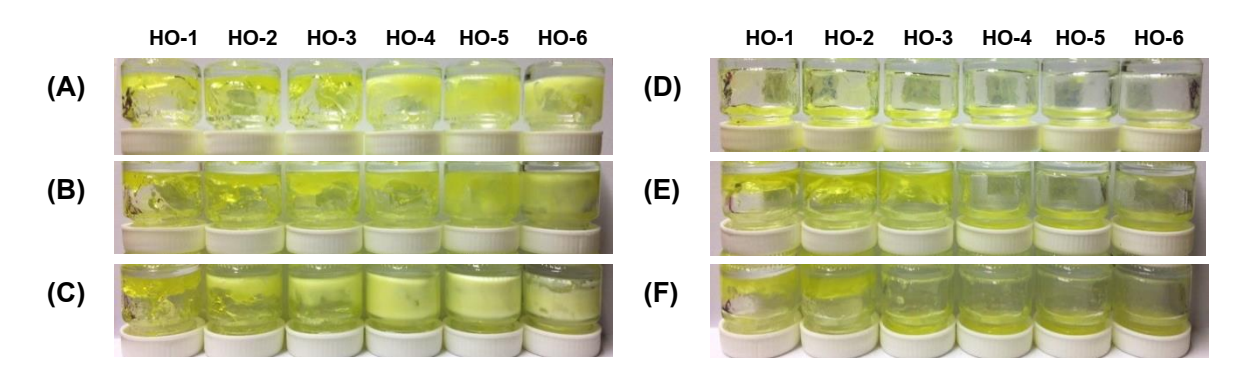


**Figure 44** Microemulsion-based gel containing 1%w/w carbopol 940 **(A)**, 1.5%w/w carbopol 940 **(B)**, 2.5%w/w carbopol 940 **(C)**, 1%w/w SCMC **(D)**, 1.5%w/w SCMC **(E)**, 2.5%w/w SCMC **(F)** and HO-1 to HO-6 from left to right, respectively after the heating-cooling stability test

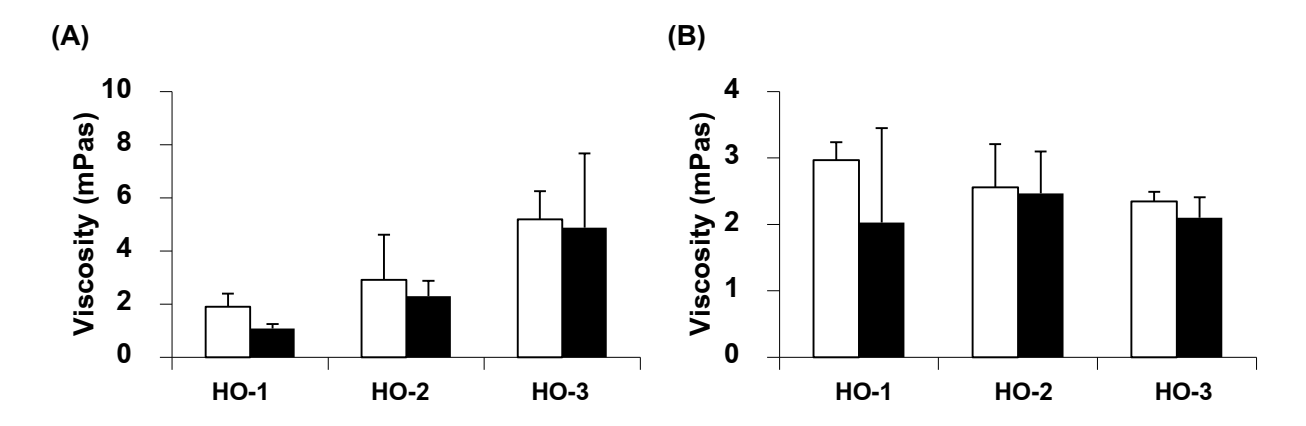


**Figure 45** Viscosity of microemulsion-based gel of HO containing 1%w/w carbopol 940 **(A)** and 2%w/w SCMC **(B)** before  $(\Box)$  and after  $(\blacksquare)$  the heating-cooling stability test (P < 0.05)

# Chapter 5

#### Conclusions

In the present study, EO was obtained by hydrodistillation of *Z. cassumunar* rhizome, whereas, HO was obtained by hot infusion of *Z. cassumunar* rhizome in coconut oil. The major constituents of EO determined by GC-MS were terpinen-4-ol (40.5±6.6%) and sabinene (17.4±1.4%). The major constituent of HO after TLC and HPLC analysis was curcumin. The characteristic of HO as the functions of acid value, iodine value, and saponification value were 0.2±0.0 mg of KOH/g, 7.4±0.2 g of I<sub>2</sub>/100 g, and 265±7 mg of KOH/g, respectively. EO and HO were considered safe as they did not affect normal cell survival in human peripheral blood mononuclear cells, as determined by MTT assay.

Several mechanisms of action were proposed to explain the anti-inflammatory activity of the native oils and their major constituents. The anti-inflammatory effect of both oils was remarkable in albumin denaturation assay since they produced the equivalent effect to indomethacin with the IC $_{50}$  values on EO, HO, and indomethacin of 12±4, 10±2, and 6±3  $\mu$ g/mL, respectively. However, NF- $_{K}$ B suppression of EO was more conspicuous than HO with the suppression of 42±3% and 36±4%, respectively. Curcumin show a good anti-inflammatory effect in BSA denaturation test and a slight effect on NF- $_{K}$ B suppression and IL-6 inhibition. Terpinen-4-ol and sabinene showed a very good anti-inflammatory effect in all assays. Therefore, the anti-inflammatory activity of EO was correlated to the presence of terpinen-4-ol and sabinene. The NF- $_{K}$ B suppression of terpinen-4-ol and sabinene were 47±5% and 78±8%, respectively. Moreover, 50  $\mu$ g/mL terpinen-4-ol and 50  $\mu$ g/mL sabinene significantly reduced IL-6 secretion level to 82±2% and 80±7%, respectively.

HLB values of HO and EO determined by external appearance inspection, droplet size analysis, and turbidimetric method were 6 and 10, respectively. Various factors affecting microemulsion development was investigated and the results indicated that surfactant type, cosurfactant type, and surfactant to co-surfactant ratio showed distinct effects on the microemulsion formation, whereas, ionic strength and pH had no effect. Two pseudoternary phase diagrams which generated the largest area of microemulsion one from EO system (EO/Tween 20/propylene glycol/water) and another one from HO system (HO and oleic acid (1:1)/Triton X-114/propan-2-ol/water) were selected for the further characterizations. The internal droplet size of EO microemulsion were in the range of 211.5 to 366.7 nm with medium polydispersity index which was less than 0.38, whereas, the internal droplet size of HO

microemulsion were in the range of 26.7 to 31.6 nm with small polydispersity index which was less than 0.25. All formulation showed Newtonian's flow behaviour. The viscosity of EO microemulsions were in the range of 0.65 to 0.84 mPas, whereas, that of HO microemulsions were in the range of 0.015 to 0.024 mPas. The pH of each microemulsions was in the range of 3.9 to 5.5. All microemulsion showed a good stability after the heating-cooling stability test. Moreover, microemulsion tended to protect EO from the evaporation and protect HO from the oxidation and reduce the occurrence of rancidity. Microemulsion of EO and HO were considered safe as the cell viabilities of human PBMCs after treatments were around 80%.

Anti-inflammatory activity of the microemulsions was investigated by means of albumin denaturation assay and western blotting. The anti-inflammatory effect was not remarkable in albumin denaturation assay since microemulsion did not show as good protein denaturation inhibition as the native oils (at low concentration of 1.56%w/w). However, the western blottings of NF-<sub>K</sub>B showed the significant greater NF-<sub>K</sub>B suppression effect of the microemulsion comparing to the native oils. Therefore, the albumin denaturation assay might not suitable for the sample contained high amount of surfactant or co-surfactant.

Carbopol 940 and SCMC were used for microemulsion-based gel development. Microemulsion-based gels had more aesthetic appearance than gels containing the native oils because of the transparent property of microemulsion. The formulations of EO showed the best characteristics with 2.5%w/w carbopol 940 and 2.5%w/w SCMC, whereas, the formulations of HO showed the best characteristics with 1%w/w carbopol 940 and 2%w/w SCMC. Microemulsion EO-1 to EO-4 and HO-1 to HO-3 could produce clear microemulsion-based gels. However, the instability was observed in some microemulsion-based gels. There were significantly decrease in viscosity in the system of 2.5%w/w SCMC of microemulsion-based gel of EO. According to microemulsion-based gel of HO, the instability was observed in the formulations contained higher amount of corbopol 940 accompanied with higher content of water in the microemulsions. In conclusions, 2.5%w/w carbopol 940 is the best choice for microemulsion-based gel development of EO and 2%w/w SCMC is the best choice for microemulsion-based gel development of HO. The microemulsion-based gels would be the aesthetic formulation for the topical treatment of various inflammatory conditions, such as muscle pains, sprains, strains, arthritis, etc.

### References

- นพมาศ สุนทรเจริญนนท์. 2555. น้ำมันไพลทอดต่างจากน้ำมันไพลกลั่นอย่างไร?. (ออนไลน์) แหล่งที่มา:http://www.pharmacy.mahidol.ac.th/thai/knowledgeinfo.php?id=109. 12 กันยายน 2556
- Adams, M. M., Anslyn, E. V. (2009). Differential sensing using proteins: exploiting the cross-reactivity of serum albumin to pattern individual terpenes and terpenes in perfume. *Journal of the American Chemical Society*, 131(47), 17068-17069.
- Adams, R. P. (2001). Quadrupole mass spectra of compounds listed in order of their retention time on DB-5. Identification of essential oils components by gas chromatography/quadrupole mass spectroscopy. *Quadruple mass spectroscopy*.
- Anderson-Foster, E. N., Adebayo, A. S., Justiz-Smith, N. (2012). Physico-chemical properties of Blighia sapida (ackee) oil extract and its potential application as emulsion base. *African Journal of pharmacy and Pharmacology*, *6*(3), 200-210.Balsinde, J., Mollinedo, F. (1988). Specific activation by concanavalin A of the superoxide anion generation capacity during U937 differentiation. *Biochemical and biophysical research communications*, *151*(2), 802-808.
- Barnes, P. J. (1997). Nuclear factor-KB. The international journal of biochemistry & cell biology, 29(6), 867-870.
- Bhuiyan, M. N. I., Chowdhury, J. U., Begum, J. (2008). Volatile constituents of essential oils isolated from leaf and rhizome of Zingiber cassumunar Roxb. *Bangladesh Journal of Pharmacology*, 3(2), 69-73.
- Boonme, P., Krauel, K., Graf, A., Rades, T., Junyaprasert, V. B. (2006). Characterization of microemulsion structures in the pseudoternary phase diagram of isopropyl palmitate/water/Brij 97: 1-butanol. *AAPS Pharmscitech*,7(2), E99-E104.
- Bordoloi, A. K., Sperkova, J., Leclercq, P. A. (1999). Essential oils of Zingiber cassumunar Roxb. from northeast India. *Journal of essential oil Research*, *11*(4), 441-445.
- Brand, C., Ferrante, A., Prager, R. H., Riley, T. V., Carson, C. F., Finlay-Jones, J. J., Hart, P. H. (2001). The water-soluble components of the essential oil of Melaleuca alternifolia (tea tree oil) suppress the production of superoxide by human monocytes, but not neutrophils, activated in vitro. *Inflammation Research*, 50(4), 213-219.
- Chainani-Wu, N. (2003). Safety and anti-inflammatory activity of curcumin: a component of tumeric (Curcuma longa). *The Journal of Alternative & Complementary Medicine*, 9(1), 161-168.

- Chaiwongsa, R., Ongchai, S., Boonsing, P., Kongtawelert, P., Panthong, A., Reutrakul, V. (2013). Active compound of Zingiber cassumunar Roxb. down-regulates the expression of genes involved in joint erosion in a human synovial fibroblast cell line. *African Journal of Traditional, Complementary and Alternative Medicines*, *10*(1), 40-48.
- Chandra, S., Chatterjee, P., Dey, P., Bhattacharya, S. (2012). Evaluation of in vitro anti-inflammatory activity of coffee against the denaturation of protein. *Asian Pacific Journal of Tropical Biomedicine*, *2*(1), S178-S180.
- Chen, H., Chang, X., Du, D., Li, J., Xu, H., Yang, X. (2006). Microemulsion-based hydrogel formulation of ibuprofen for topical delivery. *International Journal of Pharmaceutics*, 315(1), 52-58.
- Dymerski, T., NamieŚnik, J., Vearasilp, K., Arancibia-Avila, P., Toledo, F., Weisz, M., Katrich, E., Gorinstein, S. (2015). Comprehensive two-dimensional gas chromatography and three-dimensional fluorometry for detection of volatile and bioactive substances in some berries. *Talanta*, *134*, 460-467.
- Ferrero-Miliani, L., Nielsen, O. H., Andersen, P. S., Girardin, S. E. (2007). Chronic inflammation: importance of NOD2 and NALP3 in interleukin-1 $\beta$  generation. *Clinical & Experimental Immunology*, 147(2), 227-235.
- Fu, H., Yang, L., Yuan, H., Xiao, F., Lo, Y. M. (2008). Production of low acid value edible oil with reduced TFAs by electrochemical hydrogenation in a diaphragm reactor. *Journal of the American Oil Chemists' Society*, *85*(11), 1087-1096.
- Gallarate, M., Carlotti, M. E., Trotta, M., Bovo, S. (1999). On the stability of ascorbic acid in emulsified systems for topical and cosmetic use. *International journal of pharmaceutics*, 188(2), 233-241.
- Gasco, M. R., Trotta, M. (1986). Nanoparticles from microemulsions. *International journal of pharmaceutics*, 29(2), 267-268.
- García-Román, R., Pérez-Carreón, J. I., Márquez-Quiñones, A., Salcido-Neyoy, M. E., Villa-Treviño, S. (2007). Persistent activation of NF-kappaB related to IkappaB's degradation profiles during early chemical hepatocarcinogenesis. *Journal of carcinogenesis*, 6(1), 5.
- Ghosh, S., May, M. J., Kopp, E. B. (1998). NF-**K**B and Rel proteins: evolutionarily conserved mediators of immune responses. *Annual review of immunology*, *16*(1), 225-260.
- Gilroy, D. W., Colville-Nash, P. R., Willis, D., Chivers, J., Paul-Clark, M. J., Willoughby, D. A. (1999). Inducible cyclooxygenase may have anti-inflammatory properties. *Nature medicine*, *5*(6), 698-701.

- Gopinath, D., Ahmed, M. R., Gomathi, K., Chitra, K., Sehgal, P. K., Jayakumar, R. (2004).

  Dermal wound healing processes with curcumin incorporated collagen films. *Biomaterials*, 25(10), 1911-1917.
- Gupta, R. R., Jain, S. K., Varshney, M. (2005). AOT water-in-oil microemulsions as a penetration enhancer in transdermal drug delivery of 5-fluorouracil. *Colloids and Surfaces B: Biointerfaces*, *41*(1), 25-32.
- Habsah, M., Amran, M., Mackeen, M. M., Lajis, N. H., Kikuzaki, H., Nakatani, N., Rahman, A.A., Ali, A. M. (2000). Screening of Zingiberaceae extracts for antimicrobial and antioxidant activities. *Journal of ethnopharmacology*, 72(3), 403-410.
- Han, A. R., Kim, M. S., Jeong, Y. H., Lee, S. K., Seo, E. K. (2005). Cyclooxygenase-2 inhibitory phenylbutenoids from the rhizomes of Zingiber cassumunar. *Chemical and pharmaceutical bulletin*, *53*(11), 1466-1468.
- Hart, P. H., Brand, C., Carson, C. F., Riley, T. V., Prager, R. H., Finlay-Jones, J. J. (2000). Terpinen-4-ol, the main component of the essential oil of Melaleuca alternifolia (tea tree oil), suppresses inflammatory mediator production by activated human monocytes. *Inflammation Research*, 49(11), 619-626.
- Jeenapongsa, R., Yoovathaworn, K., Sriwatanakul, K. M., Pongprayoon, U., Sriwatanakul, K. (2003). Anti-inflammatory activity of (E)-1-(3, 4-dimethoxyphenyl) butadiene from Zingiber cassumunar Roxb. *Journal of ethnopharmacology*, *87*(2), 143-148.
- Kankkunen, T., Sulkava, R., Vuorio, M., Kontturi, K., Hirvonen, J. (2002). Transdermal iontophoresis of tacrine in vivo. *Pharmaceutical research*, *19*(5), 705-708.
- Kaplanski, G., Marin, V., Montero-Julian, F., Mantovani, A., Farnarier, C. (2003). IL-6: a regulator of the transition from neutrophil to monocyte recruitment during inflammation. *Trends in immunology*, *24*(1), 25-29.
- Kapoor, S., & Priyadarsini, K. I. (2001). Protection of radiation-induced protein damage by curcumin. *Biophysical Chemistry*, *92*(1), 119-126.
- Kardash, E., Tur'yan, Y. I. (2005). Acid value determination in vegetable oils by indirect titration in aqueous-alcohol media. *Croat Chem Acta*, *78*(1), 99-103.
- Kogan, A., Garti, N. (2006). Microemulsions as transdermal drug delivery vehicles. *Advances in colloid and interface science*, *123*, 369-385.
- Krauel, K., Girvan, L., Hook, S., Rades, T. (2007). Characterisation of colloidal drug delivery systems from the naked eye to Cryo-FESEM. *Micron*, *38*(8), 796-803.
- Kreilgaard, M. (2002). Influence of microemulsions on cutaneous drug delivery. *Advanced Drug Delivery Reviews*, *54*, S77-S98.

- Kreilgaard, M., Pedersen, E. J., Jaroszewski, J. W. (2000). NMR characterisation and transdermal drug delivery potential of microemulsion systems. *Journal of controlled release*, 69(3), 421-433.
- Lawrence, T. (2009). The nuclear factor NF-KB pathway in inflammation. *Cold Spring Harbor perspectives in biology*, *1*(6), a001651.
- Lee, K. M., Kang, B. S., Lee, H. L., Son, S. J., Hwang, S. H., Kim, D. S., Park J. S., Cho, H. J. (2004). Spinal NF-kB activation induces COX-2 upregulation and contributes to inflammatory pain hypersensitivity. *European Journal of Neuroscience*, *19*(12), 3375-3381.
- Maheshwari, R. K., Singh, A. K., Gaddipati, J., Srimal, R. C. (2006). Multiple biological activities of curcumin: a short review. *Life sciences*, 78(18), 2081-2087.
- Masuda, T., Jitoe, A. (1994). Antioxidative and antiinflammatory compounds from tropical gingers: isolation, structure determination, and activities of cassumunins A, B, and C, new complex curcuminoids from Zingiber cassumunar. *Journal of Agricultural and Food Chemistry*, 42(9), 1850-1856.
- Masuda, T., Jitoe, A. (1995). Phenylbutenoid monomers from the rhizomes of Zingiber cassumunar. *Phytochemistry*, *39*(2), 459-461.
- Masuda, T., Jitoe, A., Mabry, T. J. (1995). Isolation and structure determination of cassumunarins A, B, and C: new anti-inflammatory antioxidants from a tropical ginger, Zingiber cassumunar. *Journal of the American Oil Chemists' Society*, 72(9), 1053-1057.
- Maroon, J. C., Bost, J. W., Borden, M. K., Lorenz, K. M., Ross, N. A. (2006). Natural antiinflammatory agents for pain relief in athletes. *Neurosurgical focus*, 21(4), 1-13.
- McNair, J. B. (1929). The taxonomic and climatic distribution of oils, fats, and waxes in plants. *American Journal of Botany*, 832-841.
- Menon, V. P., Sudheer, A. R. (2007). Antioxidant and anti-inflammatory properties of curcumin.

  In *The molecular targets and therapeutic uses of curcumin in health and disease* (pp. 105-125). Springer US.
- Mense, S. (2003). The pathogenesis of muscle pain. *Current pain and headache reports*, 7(6), 419-425.
- Mizushima, Y., Kobayashi, M. (1968). Interaction of anti-inflammatory drugs with serum proteins, especially with some biologically active proteins. *Journal of Pharmacy and Pharmacology*, 20(3), 169-173.
- Murakami, A., Miyamoto, M., Ohigashi, H. (2004). Zerumbone, an anti-inflammatory phytochemical, induces expression of proinflammatory cytokine genes in human colon adenocarcinoma cell lines. *Biofactors*, *21*(1-4), 95-101.

- Anderson-Foster, E. N., Adebayo, A. S., Justiz-Smith, N. (2012). Physico-chemical properties of Blighia sapida (ackee) oil extract and its potential application as emulsion base. *African Journal of pharmacy and Pharmacology*, 6(3), 200-210.
- Nagpal, M., Sood, S. (2013). Role of curcumin in systemic and oral health: An overview. *Journal of Natural Science, Biology and Medicine*, *4*(1), 3-7.
- Nandhasri, P., Pawa, K. K. (2003, February). Quality control of luk prakop, a Thai herbal combination. In *III WOCMAP Congress on Medicinal and Aromatic Plants-Volume 5:*Quality, Efficacy, Safety, Processing and Trade in Medicinal 679 (pp. 131-136).
- Natta, L., Orapin, K., Krittika, N., Pantip, B. (2008). Essential oil from five Zingiberaceae for anti food-borne bacteria. *International Food Research Journal*, *15*, 337-346.
- Official and Tentative Methods of the American Oil Chemists' Society. (1984). edited by David Firestone. 14th ed. American Oil Chemists' Society, Champaign, Cd 1-25, 28, 023.
- Orafidiya, L. O., Oladimeji, F. A. (2002). Determination of the required HLB values of some essential oils. *International journal of pharmaceutics*, *237*(1), 241-249.
- Ozaki, Y., Kawahara, N., Harada, M. (1991). Anti-inflammatory effect of Zingiber cassumunar Roxb. and its active principles. *Chemical and pharmaceutical bulletin*, 39(9), 2353-2356.
- Padmanabhan, P., Jangle, S. N. (2012). Evaluation of in-vitro anti-inflammatory activity of herbal preparation, a combination of four medicinal plants. *International Journal of Applied and Basic Medical Research*, 2, 109-116.
- Panthong, A., Kanjanapothi, D., Niwatananant, W., Tuntiwachwuttikul, P., Reutrakul, V. (1997).

  Anti-inflammatory activity of compound D {(E)-4-(3', 4'-dimethoxyphenyl) but-3-en-2-ol} isolated from Zingiber cassumunar Roxb. *Phytomedicine*, 4(3), 207-212.
- Phongpradist, R., Chaiyana, W., Anuchapreeda, S. (2015). Curcumin-loaded multi-valent ligands conjugated-nanoparticles for anti-inflammatory activity. *International Journal of Pharmacy and Pharmaceutical Sciences*, 7(4), 203-208.
- Phongpradist, R., Chittasupho, C., Okonogi, S., Siahaan, T., Anuchapreeda, S., Ampasavate, C., Berkland, C. (2010). LFA-1 on leukemic cells as a target for therapy or drug delivery. *Current pharmaceutical design*, *16*(21), 2321-2330.
- Pithayanukul, P., Tubprasert, J., Wuthi-Udomlert, M. (2007). In vitro antimicrobial activity of Zingiber cassumunar (Plai) oil and a 5% Plai oil gel. *Phytotherapy research*, 21(2), 164-169.
- Pongprayoon, U., Soontornsaratune, P., Jarikasem, S., Sematong, T., Wasuwat, S., Claeson, P. (1997). Topical antiinflammatory activity of the major lipophilic constituents of the rhizome of *Zingiber cassumunar*. Part I: The essential oil. *Phytomedicine*, *3*(4), 319-322.

- Prajapati, B., Singhal, M., Yashwant, S. G., Gupta, V. (2010). Role of NFkB in various immunological & inflammatory disorders. *International Journal of Pharmacological Research*, 2, 35-39.
- Rahman, H., Eswaraiah, M. C., Dutta, A. M. (2015). In-vitro Anti-inflammatory and Anti-arthritic Activity of Oryza sativa Var. Joha Rice (An Aromatic Indigenous Rice of Assam). 15(1), 115-121.
- Rogerio, A. P., Dora, C. L., Andrade, E. L., Chaves, J. S., Silva, L. F., Lemos-Senna, E., Calixto, J. B. (2010). Anti-inflammatory effect of quercetin-loaded microemulsion in the airways allergic inflammatory model in mice. *Pharmacological Research*, *61*(4), 288-297.
- Ryan, G. B., Majno, G. (1977). Acute inflammation. A review. *The American journal of pathology*, 86(1), 183.
- Sakat, S., Juvekar, A. R., Gambhire, M. N. (2010). In vitro antioxidant and anti-inflammatory activity of methanol extract of Oxalis corniculata Linn. *International Journal of Pharmacy and Pharmaceutical Sciences*, *2*(1), 146-155.
- Schmidts, T., Nocker, P., Lavi, G., Kuhlmann, J., Czermak, P., Runkel, F. (2009). Development of an alternative, time and cost saving method of creating pseudoternary diagrams using the example of a microemulsion. *Colloids and Surfaces A: Physicochemical and Engineering Aspects*, 340(1), 187-192.
- Seneviratne, K., Dissanayake, D. M. S. (2011). Effect of method of extraction on the quality of coconut oil. *Journal of Science of the University of Kelaniya Sri Lanka*, 2, 63-72.
- Shahin, M., Hady, S. A., Hammad, M., Mortada, N. (2011). Development of stable O/W emulsions of three different oils. *International Journal of Pharmaceutical Sciences and Research*, 2, 45-51.
- Shendkar, A. K., Chaudhari, S. G., Shendkar, Y. K. (2014). *In vitro* antiartthritic activity of *Withania coagulans* Dunal fruits. *Indo American Journal of Pharmaceutical Research*, 4(2), 915-924.
- Shishodia, S., Amin, H. M., Lai, R., Aggarwal, B. B. (2005). Curcumin (diferuloylmethane) inhibits constitutive NF-KB activation, induces G1/S arrest, suppresses proliferation, and induces apoptosis in mantle cell lymphoma. *Biochemical pharmacology*, 70(5), 700-713.
- Sintov, A. C., Botner, S. (2006). Transdermal drug delivery using microemulsion and aqueous systems: influence of skin storage conditions on the in vitro permeability of diclofenac from aqueous vehicle systems. *International Journal of Pharmaceutics*, 311(1), 55-62.

- Sintov, A. C., Shapiro, L. (2004). New microemulsion vehicle facilitates percutaneous penetration in vitro and cutaneous drug bioavailability in vivo. *Journal of Controlled Release*, 95(2), 173-183.
- Sukatta, U., Rugthaworn, P., Punjee, P., Chidchenchey, S., Keeratinijakal, V. (2009). Chemical composition and physical properties of oil from Plai (Zingiber cassumunar Roxb.) obtained by hydro distillation and hexane extraction. *Kasetsart Journal (Natural Science)*, 43, 212-217.
- Suksaeree, J., Charoenchai, L., Madaka, F., Monton, C., Sakunpak, A., Charoonratana, T., Pichayakorn, W. (2015). Zingiber cassumunar blended patches for skin application: Formulation, physicochemical properties, and in vitro studies. *Asian journal of pharmaceutical sciences*, *10*(4), 341-349.
- Surh, Y. J., Chun, K. S., Cha, H. H., Han, S. S., Keum, Y. S., Park, K. K., Lee, S. S. (2001). Molecular mechanisms underlying chemopreventive activities of anti-inflammatory phytochemicals: down-regulation of COX-2 and iNOS through suppression of NF-KB activation. *Mutation Research/Fundamental and Molecular Mechanisms of Mutagenesis*, 480, 243-268.
- Tak, P. P., Firestein, G. S. (2001). NF-KB: a key role in inflammatory diseases. *The Journal of clinical investigation*, 107(1), 7-11.
- Tripathi, P., Dubey, N. K., Shukla, A. K. (2008). Use of some essential oils as post-harvest botanical fungicides in the management of grey mould of grapes caused by Botrytis cinerea. *World Journal of Microbiology and Biotechnology*, *24*(1), 39-46.
- Tuntiwachwuttikul, P., Pancharoen, O., Jaipetch, T., Reutrakul, V. (1981). Phenylbutanoids from Zingiber cassumunar. *Phytochemistry*, *20*(5), 1164-1165.
- Vane, J. O. H. N., Botting, R. (1987). Inflammation and the mechanism of action of anti-inflammatory drugs. *The FASEB journal*, 1(2), 89-96.
- Vane, J. R., Botting, R. M. (1995). New insights into the mode of action of anti-inflammatory drugs. *Inflammation Research*, *44*(1), 1-10.
- Watnasirichaikul, S., Davies, N. M., Rades, T., Tucker, I. G. (2000). Preparation of biodegradable insulin nanocapsules from biocompatible microemulsions. *Pharmaceutical research*, *17*(6), 684-689.
- Wicks Jr, Z. W., Jones, F. N., Pappas, S. P., Wicks, D. A. (2007). *Organic coatings: science and technology*. John Wiley & Sons.

# **Appendix**

# Output จากโครงการวิจัยที่ได้รับทุนจาก สกว.

# 1. ผลงานตีพิมพ์ในวารสารวิชาการนานาชาติ

# 1.1 ผลงานที่ตีพิมพ์แล้ว

Chaiyana W., Phongpradist R., Leelapornpisid P., Anuchapreeda S. Microemulsion-based hydrogel for topical delivery of indomethacin. *International Journal of Pharmacy and Pharmaceutical Sciences*, 2015; 7(2): 213-219.

# 1.2 ผลงานตามที่คาดไว้ในสัญญาโครงการ

**Chaiyana W.**, Anuchapreeda S., Phongpradist R., Leelapornpisid P., Mueller M., Viernstein H. Anti-inflammatory effects of essential oil and hot infused oil from *Zingiber cassumunar* Roxb. rhizome. *Bangladesh Journal of Pharmacology*.

# 2. การนำผลงานวิจัยไปใช้ประโยชน์

- เชิงพาณิชย์

-ไม่มี-

- เชิงนโยบาย

-ไม่มี-

- เชิงสาธารณะ

-ไม่มี-

# - เชิงวิชาการ

จากผลการดำเนินงานโครงการ "การพัฒนาตำรับไมโครอิมัลชันเจล จากสารสกัดไพลที่มีฤทธิ์ต้านการอักเสบ" ซึ่งสามารถพัฒนาตำรับไมโคร อิมัลชันเจลที่มีคุณลักษณะสวยงามน่าใช้และมีความคงตัวที่ดี สามารถสร้างองค์ ความรู้ โดยมีการตีพิมพ์ผลงานในวารสารระดับนานาชาติ และนำเสนอผลงาน ในที่ประชุมระดับชาติ นอกจากนี้ยังมีการนำผลงานวิจัยไปใช้ในการพัฒนาการ เรียนการสอนระดับมหาวิทยาลัยในสาขาวิชาต่างๆ ได้แก่ กระบวนวิชาประมวล วิชาการพัฒนาผลิตภัณฑ์ยา (461566) ปัญหาพิเศษทางวิทยาศาสตร์เภสัช กรรม 2 (461592) ปัญหาพิเศษทางวิทยาศาสตร์เครื่องสำอาง (463795) สัมมนาวิทยาศาสตร์เครื่องสำอาง 1 (463791) วัตถุดิบในเครื่องสำอาง (461471) การพัฒนาผลิตภัณฑ์เครื่องสำอางและเวชสำอาง (463701) ของคณะ เภสัชศาสตร์มหาวิทยาลัยเชียงใหม่ และกระบวนวิชา Cosmetic Science for Skin Care (1701353) ของสำนักวิทยาศาสตร์เครื่องสำอาง มหาวิทยาลัยแม่ฟ้า หลวง

# 3. อื่นๆ

# - การเสนอผลงานในที่ประชุมวิชาการ

Witchayanrat J., Sukdechosawang C., **Chaiyana W.** Development of Indomethacin Microemulsion Development of Indomethacin Microemulsion- -Based Gel from Hot Extract of Plai Based Gel from Hot Extract of Plai. Faculty of Pharmacy, Chiang Mai University, Thailand, 27 April 2015. (Poster)

Chaiyana W., Phongpradist R., Anuchapreeda S. (2016) Antiinflammatory activity of essential oil and hot infusion oil from Plai rhizome. The 15th TRF-OHEC Annual Congress (TOAC 2016) Strengthen a Powerful Collaborative Reserve Community, Phetchaburi, Thailand, 6-8 January 2016. (Poster)

**Original Article** 

#### MICROEMULSION-BASED HYDROGEL FOR TOPICAL DELIVERY OF INDOMETHACIN

# WANTIDA CHAIYANA<sup>1,\*</sup>, RUNGSINEE PHONGPRADIST<sup>1</sup>, PIMPORN LEELAPORNPISID<sup>1</sup>, SONGYOT ANUCHAPREEDA<sup>2</sup>

<sup>1</sup>Department of Pharmaceutical Science, Faculty of Pharmacy, Chiang Mai University, Chiang Mai 50200, Thailand, <sup>2</sup>Division of Clinical Microscopy, Department of Medical Technology, Faculty of Associated Medical Sciences, Chiang Mai University, Chiang Mai, 50200, Thailand.

Email: wantida.chaiyana@gmail.com

Received: 06 Nov 2014 Revised and Accepted: 29 Nov 2014

#### ABSTRACT

**Objective:** The present study aims to develop and characterize microemulsion from herbal infused oil of *Zingiber cassumunar* (HO) and microemulsion-based hydrogel (MBH) containing indomethacin. The release patterns of indomethacin from MBH were also investigated.

**Methods:** HO was produced by hot extraction of *Z. cassumunar* rhizome in coconut oil, and characterized for acid value, iodine value, and saponification value. The cytotoxicity of HO on human peripheral blood mononucleared cells (PBMCs) was also investigated. Pseudoternary phase diagram was constructed to study suitable compositions of microemulsion containing HO, oleic acid, Triton X-114, propan-2-ol, and water. Indomethacin was then incorporated into the microemulsion and finally blended with gel base (2% Carbopol 940 or 3% sodium carboxymethylcellulose) to produce MBH. The indomethacin MBH was characterized for appearance, pH, viscosity, and *in vitro* release characteristics.

Results: H0 exhibited an acid value of  $0.203 \pm 0.004$  mg of K0H/g, iodine value of  $7.39 \pm 0.15$  g of  $I_2/100$  g, and saponification value of  $265.4 \pm 7.3$  mg of K0H/g with no cytotoxic effect on human PBMCs. The microemulsion region in the pseudoternary phase diagram of H0, oleic acid, Triton X-114, propan-2-ol, and water was 45.25%. Six microemulsions (ME1– ME6) containing 10% of H0 and oleic acid mixture (1:1) as the oil phase and Triton X-114 and propan-2-ol (3:2) as surfactant mixture were formulated and characterized. The droplet size was in the range of 26 to 32 nm with polydispersity index less than 0.3. They showed a Newtonian flow behavior with the viscosity ranging from  $15.12 \pm 0.15$  to  $16.78 \pm 0.12$  Pas. The microemulsion was incorporated into hydrogel using 3% sodium carboxymethylcellulose or 2% Carbopol 940. Only ME1 – ME3 gave clear MBH; therefore, they were studied in the *in vitro* release of indomethacin, and the results indicated the sustained-release characteristic fitted the Higuchi model.

**Conclusion:** The topical MBH, containing microemulsion of HO, oleic acid, Triton X-114, propan-2-ol and water, might be a promising approach for sustained transdermal delivery of poor water-soluble compounds, including indomethacin.

Keywords: Sustained release, Microemulsion, Hydrogel, Indomethacin, Zingiber cassumunar, Herbal infusion oil, Coconut oil, Oleic acid.

#### INTRODUCTION

Indomethacin is a non-steroidal anti-inflammatory drug and also used for analgesic, and antipyretic [1]. The therapeutic action of indomethacin is believed to inhibit cyclooxygenase (COX) activity and thereby block the production of prostaglandins [2]. There are many isozymes of COXs including COX-1 and COX-2, which are different in physiological functions because of the disparate in their tissue expression and regulation [3]. COX-1 is constitutively expressed in almost all tissues, whereas COX-2 expression is highly restricted. Therefore, inhibition of COX-1 leads to many adverse events, especially serious gastrointestinal side effects such as bleeding, ulceration, and perforation of the esophagus, stomach, small intestine, or large intestine, which can be fatal [4-5]. Since indomethacin is a nonselective inhibitor of COXs [6], oral administration of indomethacin might cause such serious adverse events. The incidence of these adverse events might depend on the degree of enzyme inhibition and the daily fluctuations in enzyme activity, especially at the gastrointestinal tract. Transdermal application might be used to improve overall tolerability and offer many advantages over conventional oral medications, including smooth and continuous drug delivery, reduced C<sub>max</sub> and steadier systemic drug levels [7].

Transdermal drug delivery offers many advantages over other traditional routes; however, the barrier nature of the skin made it difficult for most drugs to be delivered through it [8]. Therefore, effective formulations which are able to deliver the therapeutic agents through this barrier would be essential. Practical water insolubility of indomethacin due to its low polarity [2], is a problem in the formulation development. There are many studies on

solubility enhancing techniques of indomethacin such as using nanospheres, complexation, and microemulsion [9-11].

Microemulsion, belonging to a group of colloidal drug delivery systems, is an optically transparent, low viscosity, and thermodynamically stable dispersions of oil, water, and surfactant, frequently in combination with co-surfactants [12-14]. The systems can be differentiated from a coarse emulsion by visual inspection, when microemulsion is clear, whereas, coarse emulsion is opaque [14]. Depending on their microstructure, microemulsions can be categorized into the droplet and bicontinuous type. In a droplet type, the dispersed oil or water is surrounded by surfactant molecules forming micelles or reverse micelles in the continuous component, whereas, bicontinuous microemulsions are characterized by a sponge-like microstructure, with comparatively large oil and water domains intertwining, separated by a surfactant layer [15]. Microemulsion provides a promising alternative for transdermal delivery of both hydrophilic and lipophilic drugs [16]. Cosolubilization of components with different solubility would attain a synergistic effect for a specific therapeutic goal [13]. The use of microemulsions in pharmaceuticals is advantageous not only due to the low-cost and ease of preparation (zero interfacial tension and almost spontaneous formation), but also because of the improved bioavailability, stability (long shelf-life), high surface area (high solubilization capacity), very small droplet size (5-200 nm), and good appearance [13,16]. Small droplets of microemulsion have better chance to transport bioactive molecules in a more controlled fashion [13]. Microemulsions were also used as a protecting medium for entrapment of drugs from degradation, hydrolysis and oxidation [13]. Moreover, microemulsion can be used as a template for developing many formulations, including hydrogel and organogel.

Zingiber cassumunar Roxb. is an aromatic plant which is widely distributed in various parts of Thailand. It was used in folklore remedies, especially rheumatism and muscular pain [17-18]. The rhizome of Z. cassumunar has been used as a component in herbal compress balls and massage oil for muscular pain relief since the ancient time [19]. Recently, there were many studies of Z. cassumunar that related to the anti-inflammatory property, such as muscular pain and rheumatism [20]. Z. cassumunar was extracted using solvent extraction or hydrodistillation to obtain essential oil [18,21-22]. However, the herbal oil infusion from Z. cassumunar in folklore remedies has not been investigated.

Therefore, the aims of this study were to develop microemulsion from herbal infused oil of *Z. cassumunar* (HO) and microemulsion-based hydrogel (MBH) containing indomethacin as a topical delivery system.

#### **MATERIALS AND METHODS**

#### **Materials**

Indomethacin, oleic acid, 3-(4,5-dimethylthiazolyl-2)-2,5-diphenyl tetrazolium bromide (MTT), phenolphthalein TS, triethanolamine, Carbopol 940, sodium carboxymethylcellulose (SCMC), and Triton X-114 were purchased from Sigma-Aldrich (St. Louis, MO, USA). Fetal bovine serum (FBS) was purchased from Biochrom AG (Berlin, Germany). Ficoll-paque plus was purchased from Lymphoprep™ Axis-Shield PoC AS, (Oslo, Norway). Disodium hydrogen phosphate, dipotassium hydrogen phosphate, sodium hydroxide, potassium hydroxide, potassium iodide, iodobromide, hydrochloric acid, and sodium thiosulfate were purchased from Fisher Chemicals (Loughborough, UK). RPMI 1640, Penicillin, Streptomycin, and Trypan blue were purchased from GIBCO™ Invitrogen (Grand Island, NY, USA). Hydrochloric acid was AR grade and purchased from Merck (Darmstadt, Germany). Ethanol, methanol, propan-2-ol, dimethyl sulfoxide (DMSO), hexane, ethyl acetate, and ether were AR grade and purchased from Labscan (Dublin, Ireland). Herbal infused oil was prepared from rhizome parts of Zingiber cassumunar and coconut oil were purchased from a local market in Chiang Mai province, Thailand.

#### Herbal infused oil preparation

The rhizomes of *Z. cassumunar* were sliced into small pieces and extracted by heated coconut oil for 3-4 h, then filtered to obtain HO and stored in a well-closed container protecting from light until further use.

#### Thin layer chromatography of HO

Samples of HO were spotted on the TLC plate. The plate was subsequently developed in two developing solvent systems, including System 1 (methanol, hexane, and ethyl acetate in the ratio of 1.5:2.5:1) and System 2 (methanol, hexane, and ethyl acetate in the ratio of 1.5:2.5:1). After the solvents evaporated, the plate was observed in daylight, UV light at 254 nm and UV light at 366 nm.

#### Characterization of HO

#### Acid value determination

Acid value was determined by indirect titration method [23]. Briefly, 10 g of HO was mixed with 50 mL of ethanol/ether mixture (1:1). The mixture was subsequently shaken until homogeneous. Phenolphthalein TS was added as an indicator in the titration with 0.1 N NaOH. End point of the titration was indicated at the first permanent pink color which was persisted for at least 10 s. The acid value which was expressed as the amount of NaOH (in milligrams) necessary to neutralize free fatty acid contained in 1 g of oil was then calculated. The experiments were done in triplicate.

#### **Iodine value determination**

Determination of iodine value was carried out according to the AOCS official method with slight modification [24]. Briefly, 0.2 g of oil was dissolved in 10 mL of chloroform. The mixture was shaken until homogenous. Then 25 mL of iodobromide was added, and the reaction was carried out in the dark for 30 min. Potassium iodide solution (30 mL of KI in 100 mL of water) was then added to stop

the reaction. The remaining iodine was titrated using 0.1 N sodium thiosulfate ( $Na_2S_2O_3$ ) solution. The iodine value which is expressed as grams of halogen (calculated as iodine) absorbed by 100 g of substance was then calculated. The experiments were done in triplicate.

#### Saponification value determination

Saponification value was determined according to the AOCS official method with slight modification [24]. Briefly, 2 g of oil was dissolved in 25 mL of alcoholic KOH. After 30 min of reflux with the assistance of heating from water bath, 1 mL of phenolphthalein TS was added as an indicator for the titration. The sample was then titrated with 0.5 N HCl and the end point was indicated at the appearance of amber yellow color. The saponification value which was expressed as the milligrams of KOH necessary to neutralize the free acids and to saponify the esters present in 1 g of substance was then calculated. The experiments were done in triplicate.

#### Cell cytotoxicity of HO

The effect of HO on cell viability of peripheral blood mononuclear cells (PBMCs) was determined by a colorimetric technique using 3-(4,5-dimethylthiazol-2-yl)-2,5-diphenyl tetrazolium bromide (MTT) assay [25].

#### PBMCs isolation

Whole blood (20-25 mL) was obtained from the same donor throughout the research. The whole blood sample was diluted with equal volume of phosphate buffer saline (PBS). After that, the diluted blood sample was carefully layered on Ficoll-Paque Plus and then centrifuged at 5000×g for 30 min at 18-20°C. The mononuclear cell layer was carefully collected. The cells were washed three times by PBS and resuspended in RPMI-1640 media with 100 IU/mL penicillin, 100  $\mu g/mL$  streptomycin, and 10% v/v fetal bovine serum (FBS). The viable PBMCs number was counted with equal volume of trypan blue solution.

#### Cell viability assay

The effect of HO on cell viability of PBMCs was determined by MTT assay. Briefly, 100  $\mu L$  of PBMCs with the cell concentration of  $1\times10^5$  cells/mL was added to the 96-well plate and incubated at  $37^{\circ}\text{C}$ , 5% CO $_2$  and 90% humidity incubator for 24 h. Then 100  $\mu L$  of various concentrations of HO was added to the cells compared to untreated cells and incubated again in the same condition for 48 h. After that, 100  $\mu L$  of media was removed from each well and 15  $\mu L$  of MTT dye solution (5 mg/mL) was added into each well and further incubation for 4 h. Then all media were removed from the 96-well plate. Dimethylsulfoxide (DMSO) (200  $\mu L$ ) was added to each well to solubilize the formazan crystal. Finally, the plate was read at 540 nm using a microplate-reader. All the experiment was done in three times independent experiment.

#### Optimization of microemulsion form HO

### Pseudoternary phase diagram construction

Pseudoternary phase diagrams of the oil mixture of HO and oleic acid with a weight ratio of 1:1 (Omix) was constructed using a slightly modified water titration method [26]. Triton X-114 was combined with propan-2-ol with a weight ratio 3:2 to obtain surfactant mixture (Smix). Omix and Smix were then mixed with various weight ratios (0:1, 1:9, 2:8, 3:7, 4:6, 5:5, 6:4, 7:3, 8:2, 9:1, and 1:0) and the resulting mixtures were subsequently titrated with water under moderate agitation at room temperature. The samples were classified as microemulsion when they appeared visually as clear liquids. The different formulations were made in triplicate. The pseudoternary phase diagrams were drawn by OriginPro 8 program. The ME regions were measured by ImageJ 1.47v program.

### Particle size/size distribution of microemulsion

Particle size analysis was carried out using photon correlation spectroscopy (Zetasizer® version 5.00, Malvern Instruments Ltd., Malvern, UK). The sizing measurements were carried out at a fixed angle of  $173^\circ$ . The reported results are the mean and S.D. of at least ten measurements on the sample.

#### Formulation of indomethacin MBH

#### **Indomethacin MBH preparation**

Indomethacin was dissolved in the selected micro emulsions and then incorporated into gel base of 2% Carbopol 940 or 3% sodium carboxymethyl cellulose (SCMC) to form MBH. The final concentration of indomethacin in MBH was 1%.

#### Rheology study

Viscosity of the microemulsions and MBH were measured using a Brookfield DVIII rheometer (Brookfield Engineering Laboratories, Stroughton, MA) fitted with a bob spindle and plate spindle, respectively. Brookfield Rheocalc operating software was used to control the measurement. A sample volume of microemulsion was 70 mL, whereas that of MBH was only 1-3 g. The measurements were performed in triplicate at 25°C.

#### pH measurements

The pH of microemulsions and MBH were measured at  $25\pm1.0^{\circ}C$  by dipping the electrode into the test sample until reached the equilibrium, and reading became stable. The measurements were done in triplicate.

#### In vitro release studies

The *in vitro* release studies of indomethacin were investigated using a slightly modified method of Shin, *et al.* [27]. Briefly, 1 mL of various MBH or gel base containing indomethacin was placed into  $2.5 \times 2.5$  cm dialysis bag (Cellu Sep T2, Membrane Filtration Products, USA). Each dialysis bag was then introduced into a 50 mL of PBS pH 7.4 at  $32^{\circ}$ C. The medium was removed at definite time intervals. Once the medium was removed, the same amount of a fresh medium was immediately replaced. The investigation was carried out for 24 h. The amount of the released indomethacin was determined by UV spectrophotometry (Shimadzu, Japan) at 320 nm.

#### Statistical analysis

All data were demonstrated as a mean ± standard deviation (S.D.). Individual differences were evaluated by One-Way ANOVA: post-hoc test. In all cases, *p*< 0.05 indicates significance.

#### RESULTS AND DISCUSSION

#### TLC fingerprint of HO

HO was clear yellowish liquid with a characteristic odor. On the TLC plate that was developed with solvent **System 1**, there were two yellow spots detected under visible light with  $R_{\rm f}$  value of 0.66 and 0.75. Absorbing compounds at the  $R_{\rm f}$  value of 0.66, 0.75, and 0.83 diminished the uniform layer fluorescence and were detected as dark spots on a bright green background when excited with shortwave (254 nm) UV light and the native fluorescence compounds were visualized at the  $R_{\rm f}$  value of 0.66, 0.75, and 0.83 when excited with long-wave (366 nm) UV light. Using the developing solvent **System 2**, there was only one yellow spot detected under visible light with  $R_{\rm f}$  value of 0.64. However, two spots were detected at the  $R_{\rm f}$  value of 0.64 and 0.77 when excited with short-wave and longwave UV light.

#### Chemical characterization of HO

The characteristic of HO as the functions of acid value, iodine value, and saponification value are shown in table 1. The low acid value (lower than 2 mg KOH/g) indicated the tendency of oxidative stable of the oil [28]. Acid value is theoretically twice of free fatty acid value, which determines the free fatty acid content hydrolyzed from triglyceride. Since the rancidity is the result of the oxidation of free fatty acid in oils, this low acid value and free fatty acid value would be the factors that contribute to high oxidative stability [29]. The results were in good agreement with the previous study that the acid value of homemade coconut oil for HO production in this study was 0.40  $\pm$  0.02 mg of KOH/g [29]. However, commercial coconut oil in the same study showed a higher acid value of 3.5 $\pm$  0.9 mg of KOH/g because of the longer storage time [29]. Therefore, the life span of the oil might be a critical factor affecting the acid value.

Table 1: Acid value, iodine value, and saponification value of HO

|                 | Acid value<br>(mg of<br>KOH/g) | Iodine value<br>(g of I <sub>2</sub> /100 g) | Saponification<br>value<br>(mg of KOH/g) |
|-----------------|--------------------------------|--|--|
| НО              | $0.20 \pm 0.00$                | $7.4 \pm 0.2$                                | 265± 7                                   |
| Coconut oil[23] | $0.40 \pm 0.02$                | $6.6 \pm 0.2$                                | 274 ± 2                                  |

lodine value could be used to indicate a saturated or unsaturated fat component of the oil. Iodine value of oleic acid (an unsaturated fat containing 1 double bond), is 90g of  $\rm I_2/100$  g, whereas linoleic acid (unsaturated fat containing 2 double bonds) and linolenic acid (unsaturated fat containing 3 double bonds) are 282 and 274 g of  $\rm I_2/100$  g, respectively. The low iodine value of HO represented the low number of reactive double bonds in the molecule, place HO in the non-drying oil group which is unable to be solidified when exposed in a thin film to the air [30].

The results related to the previous study that the major components of coconut oil were saturated fats, including lauric acid (48%) and myristic acid (17%), whereas, the only small amount of unsaturated fats (7% of oleic acid and 2% of linoleic acid) were found [31]. Therefore, oxidative cleavage of unsaturated bond decreases and the oxidation likely slows down. The iodine value in this study was in a good agreement with the previous report [29].

High saponification value represents a high number of ester content or carboxylic functional groups per unit mass of HO. The results may suggest that HO is suitable for self-emulsification process and microemulsion formation [32]. The saponification value in this study was also in a good agreement with the previous report [29].

#### Cytotoxicity of HO

The cell viability of human PBMCs after exposure to H0 for 48 h is shown in fig. 1. The H0 was very safe since it had no toxic effect on human PBMCs with a 100% of cell viability were observed even at high concentration ( $50 \, \text{Wv/v}$ ) were used.

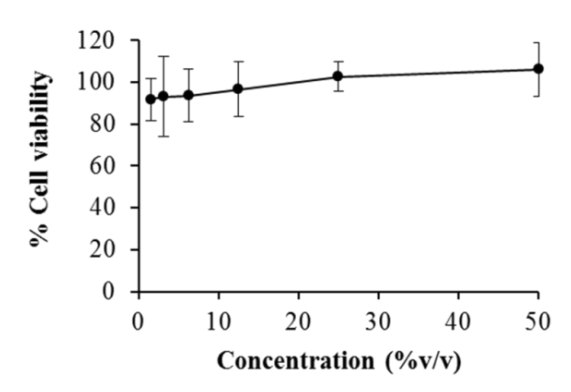


Fig. 1: Dose-response curve of viability of PBMCs versus concentrations of HO

#### **Indomethacin MBH**

Since one of the unique factors associated with microemulsions is the presence of different structures formed by altering the curvature of interface, construction of the phase diagrams enables determination of aqueous dilutability and range of compositions that form a microemulsion region [33]. Pseudoternary phase diagram of HO and oleic acid (1:1)/Triton X-114 and propan-2-ol (2:1)/water is shown in fig. 2. The microemulsion region in the phase diagram was 45.25%. Oleic acid was mixed with HO and used as an oil phase in the system since oleic acid has been reported to act as a penetration enhancer by lipid fluidization and phase separation [34-35]. Six formulations in the microemulsion region (ME1 - ME6) were formulated and characterized for their particle size and size distribution as the results shown in fig. 3. The particle size was in the range of 26 to 32 nm which were in the microemulsion range [36].

The particle size distributions were intermediate (PDI<0.3). All formulations were optically isotropic and transparent since their particle sizes were less than the wavelength of light [37].

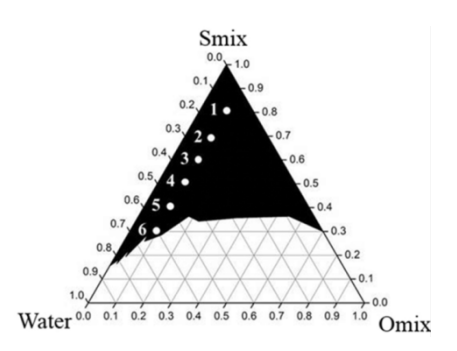


Fig. 2: Pseudoternary phase diagram of HO and oleic acid (1:1)/Triton X-114 and propan-2-ol (3:2)/water. The dark area represents the microemulsion region. Formulation ME1 - ME6 are composed of 10% HO and oleic acid with various ratios of Smix and water

The low viscosity of microemulsion is inappropriate for the topical use. Therefore, the viscosity was increased after adding thickening agents. Thickening agents not only changed the appearance of the system but also influenced the release of drugs [38]. Recently, various gelling agents, including Carbopols, xanthum gum,

carrageenan, sodium alginate, ethyl cellulose, and hydroxypropyl methylcellulose have been used to prepare the MBH in order to improve the viscosity of microemulsions [39].

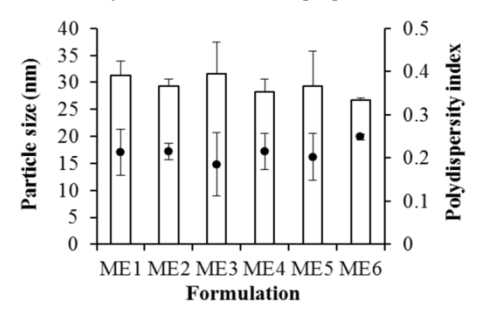


Fig. 3: Particle size and size distribution of microemulsions ME1 – ME6

In this study, each microemulsion formulation was incorporated into gel base of 3% SCMC or 2% Carbopol 940. ME1, ME2, and ME3 gave the clear appearance with both gel bases. Higher content of water in microemulsions resulting in the insufficient amount of Smix made the MBH translucent or turbid. Therefore, ME1, ME2, and ME3 were selected for incorporation of indomethacin since the clear appearance was still observed after the addition of gel bases. Indomethacin could be dissolved well in each microemulsion and produced clear gel after incorporated with gel bases of 3% SCMC producing S-ME1, S-ME2, S-ME3, and 2% Carbopol 940 producing C-ME1, C-ME2, and C-ME3, respectively.

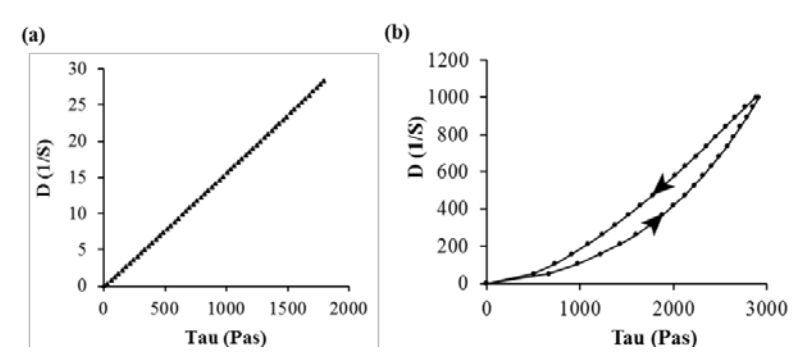


Fig. 4: Rheogram of microemulsion, ME1 (a) and MBH using gel base of 2% Carbopol 940 which contained 1% indomethacin, C-ME1 (b)

The rheograms of microemulsion as shown in fig. 4a revealed the Newtonian's flowed behavior, which stress versus strain rate curve is linear and passes through the origin. The viscosity was calculated from the well-known Newtonian equation;  $\tau = \mu(du/dy)$ , when  $\tau$  is the shear stress (Pa),  $\mu$  is the viscosity and du/dy is the velocity gradient perpendicular to the direction of shear or strain rate (s-1). The viscosity of microemulsions as shown in table 2 was very low leading to the confirmation of microemulsion formation [40-41]. The rheogram of MBH containing 1% indomethacin as shown in fig. 4b exhibiting pseudoplastic flow with thixotropic property indicating a good characteristic of the gel for external use [42]. The viscosities of MBH were calculated using the following equation,  $\eta'_a = \eta'_{\infty} +$  $[(\eta'_{\theta} - \eta'_{\infty})/(1+(kF)^n)]$ , where  $\eta'_{a}$  is the apparent dynamic viscosity,  $\eta'_{\infty}$  is the infinite dynamic viscosity,  $\eta'_{\theta}$  is the zero frequency dynamic viscosity, k is the frequency at which formulation first displays frequency dependent viscosity, n is the slope of the frequency-dependent region, and F is the oscillatory frequency [43-44]. The viscosities of MBH, using 2% Carbopol 940 or 3% SCMC are shown in table 2. The results were in line with the previous study showing that Carbopol 940 gave clearer gel with higher viscosity comparing to SCMC [45-46]. There was no statistical difference in viscosities of MBH using the same gel base incorporated with various microemulsions since the viscosity of the gel base was much more prominent. However, increasing in water content from ME-1 (10% water) to ME-3 (30% water) led to lower trend in viscosity of S-ME3 compared to S-ME2 and S-ME1, respectively. The pH of MBH was in the range of 5.0 to 5.5, which is extremely matched with human cutaneous pH and appropriate for using as a topical formulation. Acidity of cutaneous has many important roles such as select and maintain the normal cutaneous microbiota, protect the skin against infection and activate pH-dependent enzymes involved in the process of keratinization [47].

Table 2: Viscosity of microemulsion and MBH

| Formulation | Viscosity        |                |                |
|-------------|------------------|----------------|----------------|
|             | Microemulsion    | MBH (Pas)      |                |
|             | (Pas)            | Carbopol 940   | SCMC           |
| 1           | $15.12 \pm 0.15$ | $4300 \pm 521$ | $2192 \pm 539$ |
| 2           | $15.37\pm0.10$   | $4695\pm1646$  | $2132\pm183$   |
| 3           | $16.78\pm0.12$   | $5128\pm243$   | $1249 \pm 47$  |

#### In vitro release studies

The *in vitro* of indomethacin MBH release profiles of indomethacin are shown in fig. 5. To determine the release patterns of indomethacin from each formulation, cumulative release was plotted versus time or square root of time to show the zero order or Higuchi released pattern, respectively. The equation responsible for zero

order is  $Q = K_0 t$ , where Q is the cumulative release of indomethacin.  $K_{\theta}$  is the zero-order rate constant expressed in units of concentration/time, and t is the time. On the other hands, the equation responsible for Higuchi's release is  $Q = K_H t^{1/2}$ , where  $K_H$  is the Higuchi dissolution constant.  $K_H$ ,  $K_\theta$  and square of correlation coefficients (R2) of each plot are shown in table 3. The release of indomethacin from all formulations was clearly described by the Higuchi model since the linear plots with resultant R<sup>2</sup> over 0.97 were found when accumulative release of indomethacin was plotted versus the square root of time, besides the formulation of 3% SCMC, which shows low R<sup>2</sup> value (0.726). Higuchi describes a drug release as a diffusion process based on the Fick's first law which the rate controlling step is the diffusion through the topical gel base [48-49]. According to the Fick's first law; diffusion coefficient of each formulation could be defined using the following equation, I = -1 $D(d\rho/dx)$ , where J is the flux of a drug which is simply defined as the mass or number of molecules moving through a given crosssectional area (12.5 cm²) during a given period of time, D is the diffusion coefficient, and  $d\rho/dx$  is the concentration gradient. The velocity of diffusion is related to the diffusion coefficient, which is dependent on the size of the solute molecule and the viscosity of the formulations as described by the Stokes-Einstein's equation, D =  $RT/(6\pi\eta N_0 r_A)$ , where R is the gas constant, T is absolute temperature,  $r_A$  is the radius of spherical solute,  $N_\theta$  is Avogadro's number, and  $\eta$  is the viscosity of the formulations. Therefore, viscosity is one of the major factors affecting the release of compound from the formulations. The results were in a good agreement since among 6 formulations of MBH, S-ME3 which was the formulation with the lowest viscosity had the highest release rate ( $K_H$ ). In contrast, C-ME1 which exhibited the highest viscosity had the lowest release rate. Comparing to the traditional gel formulation, MBH showed the sustained-release pattern. The results were in a good agreement with many previous studies. Fouad  $et\ al.$  developed poloxamer MBH containing microemulsion of Capryol®, Labrasol®, Transcutol®, and water for sustained transdermal delivery of diclofenac epolamine [50]. Josef  $et\ al.$  developed the sustained delivery of hydrophobic drugs using composite hydrogels, prepared by embedding oil-in-water microemulsions in hydrophilic hydrogels of alginate solution crosslinking with calcium ions [51].

Baboota *et al.* developed MBH of betamethasone dipropionate and salicylic acid containing the microemulsion prepared by oleic acid: sefsol (1.5:1), Tween 20, isopropyl alcohol, and distilled water [38]. Moreover, many anti-inflammatory drugs have been formulated into MBH such as betamethasone dipropionate, diclofenac epolamine, triptolide, etc. to provide sustained transdermal delivery [38,50]. In this study, MBH containing HO, oleic acid, Triton X-114, propan-2-ol, water, and hydrogel base showed a sustained-release manner. Therefore, it may prolong the effective duration. The MBH would be another promising approach for transdermal delivery of indomethacin and maybe applied to other poor water-soluble compounds. The transdermal delivery of the optimized MBH and evaluation in animal skin or animal model are needed to be further investigated.

Table 3: Higuchi release rate constant  $(K_H)$ , zero-order rate constant  $(K_0)$  and square of correlation coefficient  $(R^2)$  of indomethacin release from each gel formulations

| Formulation | Higuchi's model |                | Zero order model |                |
|-------------|-----------------|----------------|------------------|----------------|
|             | $K_H$           | R <sup>2</sup> | $K_{0}$          | R <sup>2</sup> |
| Carbopol    | 1.250           | 0.990          | 0.218            | 0.971          |
| C-ME1       | 0.812           | 0.983          | 0.143            | 0.991          |
| C-ME2       | 0.698           | 0.991          | 0.118            | 0.920          |
| C-ME3       | 0.626           | 0.998          | 0.107            | 0.941          |
| SCMC        | 1.553           | 0.726          | 0.231            | 0.519          |
| S-ME1       | 0.720           | 0.974          | 0.122            | 0.906          |
| S-ME2       | 0.821           | 0.993          | 0.140            | 0.928          |
| S-ME3       | 1.057           | 0.991          | 0.179            | 0.920          |

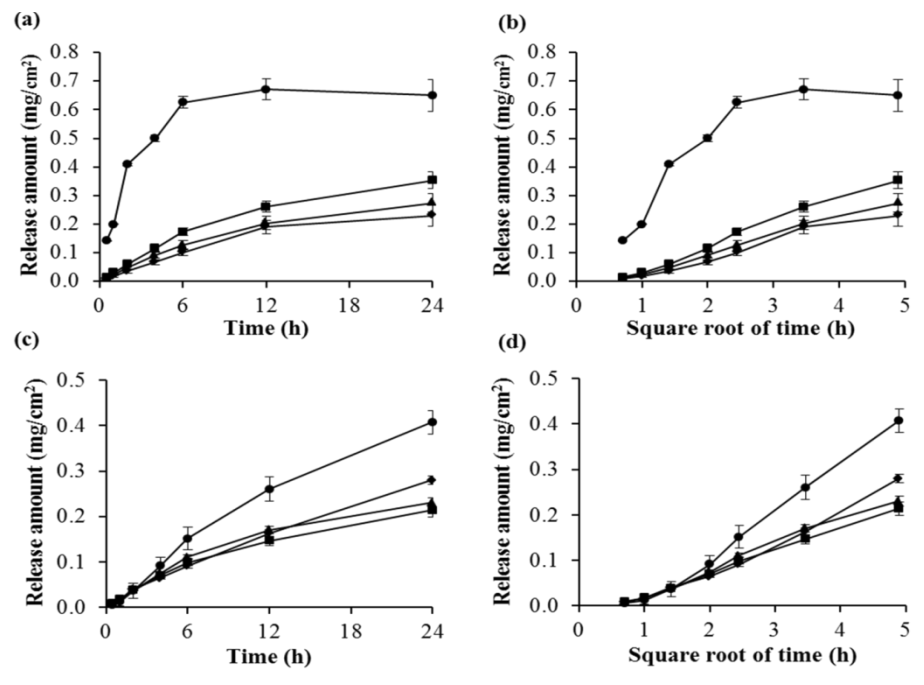


Fig. 5: Drug release profiles plotting the cumulative release of indomethacin from the formulations using 3% SCMC versus time (a) and square root of time (b), as well as, cumulative release of indomethacin from the formulations using 2% Carbopol 940 versus time (c) and square of time (d) which incorporated with indomethacin (●) or indomethacin in ME1 (♠), ME2 (♠), and ME3 (■)

#### CONCLUSION

HO, obtained by hot oil extraction of Zingiber cassumunar in coconut oil, showed safety profile on human PBMCs. HO was mixed with oleic acid (Omix) and used in the construction of pseudoternary phase diagrams. Triton X-114 and propan-2-ol were used as a surfactant and a co-surfactant, respectively. The microemulsion region in the phase diagram was 45.25%. Microemulsion (ME1 - ME6) containing 10% Omix exhibited the droplet size in the range of 26 to 32 nm with intermediate polydispersity index (PDI < 0.3). The viscosity ranged from 15.12  $\pm$  0.15 to 16.78  $\pm$  0.12 Pas and the flow behavior were in line with Newtonian's flow. ME1 - ME3 gave clear MBH using 3% SCMC or 2% Carbopol 940 as gelling agents. In vitro release study indicated the sustained-release characteristics with Higuchi's pattern of indomethacin from each MBHs. The topical MBH, containing microemulsion of HO, oleic acid, Triton X-114, propan-2-ol and water, might be a promising approach for sustained transdermal delivery of poor water-soluble compounds, especially indomethacin.

#### ACKNOWLEDGEMENT

The authors are grateful for financial support received from the Thailand Research Fund through the TRF grant for new researcher (No. TRG 5780029) and Chiang Mai University Grant for New Researcher

#### CONFLICT OF INTERESTS

The authors report no conflicts of interest.

#### REFERENCES

- Remington JP. Remington: The science and practice of pharmacy. Troy DB, Beringer P, editors. Indomethacin. 21st ed. Lippincott Williams and Wilkins; 2006.
- Ruidiaz MA, Delgado DR, Mora CP, Yurquina A, Martínez F. Estimation of the indomethacin solubility in ethanol+ water mixtures by the extended Hildebrand solubility approach. Rev Colomb Cienc Quím Farm 2010;39(1):79-95.
- 3. Crofford LJ. COX-1 and COX-2 tissue expression: implications and predictions. J Rheumatol 1997;49:S15-9.
- Allison MC, Howatson AG, Torrance CJ, Lee FD, Russell RI. Gastrointestinal damage associated with the use of nonsteroidal antiinflammatory drugs. N Engl J Med 1992;327(11):749-54.
- Ng SC, Chan FK. NSAID-induced gastrointestinal and cardiovascular injury. Curr Opin Gastroenterol 2010;26(6):611-7.
- Blobaum AL, Uddin MJ, Felts AS, Crews BC, Rouzer CA, Marnett LJ. The 2'-trifluoromethyl analogue of indomethacin is a potent and selective COX-2 inhibitor. ACS Med Chem Lett 2013;4(5):486-90.
- Lefevre G, Pommier F, Sedek G, Allison M, Huang HL, Kiese B, et al. Pharmacokinetics and bioavailability of the novel rivastigmine transdermal patch versus rivastigmine oral solution in healthy elderly subjects. J Clin Pharmacol 2008;48(2):246-52.
- El Maghraby GM. Transdermal delivery of hydrocortisone from eucalyptus oil microemulsion: Effects of cosurfactants. Int J Pharm 2008;355(1):285-92.
- Jambhekar S, Casella R, Maher T. The physicochemical characteristics and bioavailability of indomethacin from βcyclodextrin, hydroxyethyl-β-cyclodextrin, and hydroxypropylβ-cyclodextrin complexes. Int J Pharm 2004;270(1):149-66.
- Nandi I, Bari M, Joshi H. Study of isopropyl myristate microemulsion systems containing cyclodextrins to improve the solubility of 2 model hydrophobic drugs. AAPS Pharm Sci Tech 2003;4(1):71-9.
- Niwa T, Takeuchi H, Hino T, Kunou N, Kawashima Y. Preparations of biodegradable nanospheres of water-soluble and insoluble drugs with D, L-lactide/glycolide copolymer by a novel spontaneous emulsification solvent diffusion method, and the drug release behavior. J Control Release1993;25(1):89-98.
- Kankkunen T, Sulkava R, Vuorio M, Kontturi K, Hirvonen J. Transdermal iontophoresis of tacrine *in vivo*. Pharm Res 2002;19(5):705-8.
- 13. Kogan A, Garti N. Microemulsions as transdermal drug delivery vehicles. Adv Colloid Interface Sci 2006;123:369-85.

- Krauel K, Girvan L, Hook S, Rades T. Characterisation of colloidal drug delivery systems from the naked eye to Cryo-FESEM. Micron 2007;38(8):796-803.
- Kreilgaard M, Pedersen EJ, Jaroszewski JW. NMR characterisation and transdermal drug delivery potential of microemulsion systems. J Control Release 2000;69(3):421-33.
- 16. Boonme P, Krauel K, Graf A, Rades T, Junyaprasert VB. Characterization of microemulsion structures in the pseudoternary phase diagram of isopropyl palmitate/water/Brij 97:1-butanol. AAPS Pharm Sci Tech 2006;7(2):E99-104.
- 17. Pithayanukul P, Tubprasert J, Wuthi-Udomlert M. *In vitro* antimicrobial activity of *Zingiber cassumunar* (Plai) oil and a 5% Plai oil gel. Phytother Res 2007;21(2):164-9.
- Sukatta U, Rugthaworn P, Punjee P, Chidchenchey S, Keeratinijakal V. Chemical composition and physical properties of oil from Plai (*Zingiber cassumunar* Roxb.) obtained by hydrodistillation and hexane extraction. Kasetsart J (Nat Sci) 2009;43:212-7.
- Nandhasri P, Pawa KK. Quality control of luk prakop, a Thai herbal combination. In III WOCMAP congress on medicinal and aromatic plants-volume 5: Quality, Efficacy, Safety. Proc Trade Med 2003;679:131-6.
- 20. Mense S. The pathogenesis of muscle pain. Curr pain headache rep 2003;7(6):419-25.
- Jeenapongsa R, Yoovathaworn K, Sriwatanakul KM, Pongprayoon U, Sriwatanakul K. Anti-inflammatory activity of (E)-1-(3, 4dimethoxyphenyl) butadiene from *Zingiber cassumunar* Roxb. J Ethnopharmacol 2003;87(2):143-8.
- 22. Ozaki Y, Kawahara N, Harada M. Anti-inflammatory effect of *Zingiber cassumunar* Roxb. and its active principles. Chem Pharm Bull 1991;39(9):2353.
- 23. Kardash E, Tur'yan YI. Acid value determination in vegetable oils by indirect titration in aqueous-alcohol media. Croat Chem Acta 2005;78(1):99-103.
- American Oil Chemists' Society. Official methods and recommended practices of the American Oil Chemists' Society. Firestone D, editors. Vol 5. Champaign, IL, US: AOCS; 1989.
- 25. Phongpradist R, Chittasupho C, Okonogi S, Siahaan T, Anuchapreeda S, Ampasavate C, et al. LFA-1 on leukemic cells as a target for therapy or drug delivery. Curr Pharm Des 2010;16(21):2321-30.
- Chaiyana W, Saeio K, Hennink WE, Okonogi S. Characterization of potent anticholinesterase plant oil based microemulsion. Int J Pharm 2010;401(1):32-40.
- 27. Shin HS, Kim SY, Lee YM. Indomethacin release behaviors from pH and thermoresponsive poly (vinyl alcohol) and poly (acrylic acid) IPN hydrogels for site-specific drug delivery. J Appl Polym Sci 1997;65(4):685-93.
- 28. Fu H, Yang L, Yuan H, Xiao F, Lo YM. Production of low acid value edible oil with reduced TFAs by electrochemical hydrogenation in a diaphragm reactor. J Am Soc 2008;85(11):1087-96.
- Seneviratne KN, Dissanayake DMS. Effect of method of extraction on the quality of coconut oil. J Sci University Kelaniya Sri Lanka 2005;2:63-72.
- 30. Wicks JrZW, Jones FN, Pappas SP, Wicks DA. Organic coatings: science and technology. Wiley-Interscience; 2007.
- 31. McNair JB. The taxonomic and climatic distribution of oils, fats, and waxes in plants. Am J Bot 1929;16(10):832-41.
- 32. Naomi E, Adebayo AS, Justiz-Smith N. Physico-chemical properties of *Blighia sapida* (ackee) oil extract and its potential application as emulsion base. Afri J Pharm Pharmacol 2012;6(3):200-10.
- 33. Mehta SK, Kaur G. Microemulsions: thermodynamic and dynamic properties. Thermodyn 2011:381-406.
- Naik A, Pechtold LA, Potts RO, Guy RH. Mechanism of oleic acidinduced skin penetration enhancement in vivo in humans. J Control Release 1995;37(3):299-306.
- 35. Touitou E, Godin B, Karl Y, Bujanover S, Becker Y. Oleic acid, a skin penetration enhancer, affects Langerhans cells and corneocytes. J Control Release 2002;80(1):1-7.
- 36. Garcí a Sánchez F, Eliosa-Jiménez G, Salas-Padrón A Hernández-Garduza O, Ápam-Martí nez D. Modeling o

- microemulsion phase diagrams from excess Gibbs energy models. Chem Eng J 2001;84(3):257-74.
- 37. Benedek GB. Theory of transparency of the eye. Appl Opt 1971;10(3):459-73.
- 38. Baboota S, Alam MS, Sharma S, Sahni JK, Kumar A, Ali J. Nanocarrier-based hydrogel of betamethasone dipropionate and salicylic acid for treatment of psoriasis. Int J Pharm Investig 2011;1(3):139-47.
- 39. Xu L, Pan J, Chen Q, Yu Q, Chen H, Xu H, Qiu Y, *et al. In vivo* evaluation of the safety of triptolide-loaded hydrogel-thickened microemulsion. Food Chem Toxicol 2008;46(12):3792-9.
- Paul BK, Moulik SP. Microemulsions: an overview. J Disper Sci Technol 1997;18(4):301-67.
- 41. Burghardt WR, Krishnan K, Bates FS, Lodge TP. Linear viscoelasticity of a polymeric bicontinuous microemulsion. Macromolecules 2002;35(10):4210-5.
- Islam MT, Rodríguez-Hornedo N, Ciotti S, Ackermann C. Rheological characterization of topical carbomer gels neutralized to different pH. Pharm Res 2004;21(7):1192-9.
- 43. Cross MM. Rheology of non-Newtonian fluids: a new flow equation for pseudoplastic systems. J Colloid Sci 1965;20(5):417-37.
- 44. Andrews GP, Gorman SP, Jones DS. Rheological characterisation of primary and binary interactive bioadhesive gels composed of

- cellulose derivatives designed as ophthalmic viscosurgical devices. Biomaterials 2005;26(5):571-80.
- Sabri LA, Sulayman HT, Khalil YI. An investigation release and Rheological properties of Miconazole nitrate from Emulgel. Iraqi J Pharm Sci 2009;18(2):26-31.
- 46. Kittipongpatana OS, Burapadaja S, Kittipongpatana N. Carboxymethyl mungbean starch as a new pharmaceutical gelling agent for topical preparation. Drug Dev Ind Pharm 2009;35(1):34-42.
- 47. Matousek JL, Campbell KL. A comparative review of cutaneous pH. Vetdermatol 2002;13(6):293-300.
- 48. Costa P, Sousa Lobo JM. Modeling and comparison of dissolution profiles. Eur J Pharm Sci 2001;13(2):123-33.
- Nallagundla S, Patnala S, Kanfer I. Comparison of *in vitro* release rates of acyclovir from cream formulations using vertical diffusion cells. AAPS Pharm Sci Tech 2014;15(4):1-6.
- Fouad SA, Basalious EB, El-Nabarawi MA, Tayel SA. Microemulsion and poloxamer microemulsion-based gel for sustained transdermal delivery of diclofenac epolamine using in-skin drug depot: *in vitro/in vivo* evaluation. Int J Pharm 2013;453(2):569-78.
- 51. Josef E, Zilberman M, Bianco-Peled H. Composite alginate hydrogels: an innovative approach for the controlled release of hydrophobic drugs. Actabiomater 2010;6(12):4642-9.



# Wantida Chayana <wantida.chaiyana@gmail.com>

# [BJP] Submission Acknowledgement

1 ข้อความ

**Prof. Mir Misbahuddin** <dgdabd@gmail.com> ถึง: Wantida Chaiyana <wantida.chaiyana@gmail.com>

24 เมษายน 2559 01:35

Dear Dr. Wantida Chaiyana:

Thank you for submitting the manuscript, "Anti-inflammatory properties of essential oil and hot infused oil from Zingiber cassumunar Roxb. Rhizome" to Bangladesh Journal of Pharmacology. With the online journal management system that we are using, you will be able to track its progress through the editorial process by logging in to the journal web site:

Manuscript URL:

http://www.banglajol.info/index.php/BJP/author/submission/27469

Username: wantida\_chaiyana

There is no need to reply this e-mail. It is an automated generate reply to the author(s).

Always mention the manuscript ID during any correspondence with the editor.

Please visit our journal website on Twitter https://twitter.com/BJP\_Bangladesh

If you have any questions, please contact me. Thank you for considering this journal as a venue for your work.

Prof. Mir Misbahuddin Bangladesh Journal of Pharmacology

Prof. Mir Misbahuddin, Editor, Bangladesh Journal of Pharmacology http://www.banglajol.info/index.php/BJP Anti-inflammatory properties of essential oil and hot infused oil

from Zingiber cassumunar Roxb. Rhizome

Wantida Chaiyana<sup>1</sup>, Songyot Anuchapreeda<sup>2</sup>, Rungsinee Phongpradist<sup>1</sup>,

Pimporn Leelapornpisid<sup>1</sup>, Monika Mueller<sup>3</sup> and Helmut Viernstein<sup>3</sup>

<sup>1</sup>Department of Pharmaceutical Science, Faculty of Pharmacy, Chiang Mai University,

Chiang Mai 50200, Thailand; <sup>2</sup>Division of Clinical Microscopy, Department of Medical

Technology, Faculty of Associated Medical Sciences, Chiang Mai University, Chiang Mai,

50200, Thailand; <sup>3</sup>Department of Pharmaceutical Technology and Biopharmaceutics,

University of Vienna, Althanstrasse 14, Vienna, Austria

Corresponding author: Wantida Chaiyana

Department of Pharmaceutical Science, Faculty of Pharmacy, Chiang Mai University,

Chiang Mai 50200, Thailand

Tel +66-53-944-309

Fax +66-53-222-741

E-mail address: wantida.chaiyana@gmail.com

1

Abstract

Essential oil (EO) and hot infused oil (HO) from Zingiber cassumunar rhizome were

analyzed for their chemical composition. The anti-inflammatory activities of the oils

examined included the inhibition of albumin denaturation, nuclear factor-kappa B (NF-κB)

expression, and interleukin-6 (IL-6) secretion. The major constituents of EO as determined by

gas chromatography-mass spectrometry were terpinen-4-ol and sabinene. HO was obtained

by hot infusion in coconut oil and the major constituent after thin layer chromatography and

high performance liquid chromatography analysis was curcumin. Both EO and HO possessed

significant anti-inflammatory activities in the albumin denaturation assay and suppressed NF-

κB expression. Sabinene possessed potent NF-κB suppression by 77.8 ± 7.9%. Moreover,

terpinen-4-ol and sabinene significantly reduced IL-6 secretion levels by  $82.4 \pm 1.9\%$  and

 $79.8 \pm 6.7\%$ , respectively. Therefore, the anti-inflammatory activity of Z. cassumunar oil is

mainly attributable to the volatile compounds and it is hence attractive for practical

application.

Keywords: Zingiber cassumunar, inflammation, nuclear factor-kappa B, interleukin-6,

sabinene, terpinen-4-ol

2

### Introduction

Zingiber cassumunar Roxb. (Zingiberaceae) is widely distributed throughout Southeast Asia. Plant species of this family are easily recognized by the characteristic aromatic leaves and fleshy rhizomes (Habsah et al., 2000). Plants from this genus contain essential oils (EO) within the oil glands that are commonly found in most plant parts. The rhizomes of Z. cassumunar are used in folk remedies for the treatment of many conditions, especially rheumatism and muscular pain (Pithayanukul et al., 2007; Sukatta et al., 2004). The plant has been used as a component in herbal compress balls and massage oils for pain relief (Nandhasri and Pawa, 2003). Massage oil from Z. cassumunar is widely used by local people in Thailand. During the past decade, a number of pure compounds isolated from Z. cassumunar have been reported for their various biological activities, especially antiinflammatory activity related to the relief of muscular pain (Tuntiwachwuttikul et al., 1981; Masuda and Jitoe, 1994; Pongprayoon et al., 1997; Panthong et al., 1997). However, the antiinflammatory activity of Z. cassumunar extract made by local Thai people using the hot infusion method has not been investigated. This study is thus the first report concerning the anti-inflammatory effects of hot infused oil (HO) from Z. cassumunar. The comparison of anti-inflammatory effects of HO and EO would also be firstly reported in the present study.

Inflammation is an aspect of the non-specific immune response that occurs in reaction to bodily injury. The cardinal signs of inflammation are increased blood flow, elevated cellular metabolism, vasodilatation, release of soluble mediators, extravasation of fluids, and cellular influx due to a complex array of enzyme activation, mediator release, fluid extravasations, cell migration, tissue breakdown, and tissue repair (Ryan and Majno, 1977; Ferrero-Miliani et al., 2007; Vane and Botting, 1995). Several complex pathways associated with persistent or chronic inflammation have been detailed. Denaturation of tissue protein is frequently associated with inflammation (Padmanabhan and Jangle, 2012). Therefore, protein

denaturation inhibition has been widely used as an *in vitro* screening model for antiinflammatory activity (Mizushima & Kobayashi, 1968).

Nuclear factor-kappa B (NF-κB) is a protein that acts as a switch to turn inflammation on and off in the human body (Maroon et al., 2005). After the detection of noxious stimuli, including infectious agents, free radicals, and other causes of cellular injury, NF-κB activates the genes that lead to the production of inflammatory cytokines (Gilroy et al., 1999). Normally, NF-κB is localized in the cytoplasm of the cell and is bound with IκB, which is an inhibitory protein blocking the nuclear localization signal (Ghosh et al., 1998). A variety of cytokine stimuli can degrade the IκB resulting in the nuclear translocation of NF-κB (Maroon et al., 2005). Therefore, NF-κB is regarded as an important transcription factor for understanding the inflammation process (Lee et al., 2004).

Interleukin-6 (IL-6) is a pleiotropic cytokine involved in the regulation of immune responses. The cytokine is produced by a variety of cell stimulations, such as infection, trauma, or immunological challenge (Tilg et al., 1994). Investigation of IL-6 secretion levels in macrophage cells after stimulation by lipopolysaccharide (LPS) can be used to assay the anti-inflammatory effect of studied compounds (Mueller et al., 2010).

In the present study, the chemical constituents responsible for the anti-inflammatory effects of EO and HO from *Z. cassumunar* rhizomes were identified by evaluating albumin denaturation inhibition, NF-κB suppression using Western blot analysis, and IL-6 secretion level using enzyme-linked immunosorbent assay (ELISA).

#### **Materials and Methods**

#### Plant materials

Zingiber cassumunar Roxb. or Zingiber montanum (J.Koenig) Link ex A.Dietr. is variously known as 'Cassumunar ginger'or locally as 'Plai' in central Thailand. However, different names are used in different regions; e.g. 'Wan-Fai' by Northeastern people and 'Bpu-lai' by Northern people. The rhizomes of *Z. cassumunar* were collected from Chiang Mai, Thailand. The plant material used in this study was identified by Dr. Wantida Chiyana. Specimens were authenticated and a voucher specimen (number 22126) was deposited in the official Herbarium of the Faculty of Pharmacy, Chiang Mai University, Thailand.

# Chemical materials

Indomethacin, bovine serum albumin (BSA), 3-(4,5-dimethylthiazolyl-2)-2,5diphenyl tetrazolium bromide (MTT), phenolphthalein TS, sodium deoxycholate, and Tween 20 were purchased from Sigma-Aldrich (St. Louis, MO, USA). Fetal calf serum and fetal bovine serum (FBS) were obtained from Biochrom AG (Berlin, Germany). Ficoll-paque plus was purchased from Lymphoprep<sup>™</sup> Axis-Shield PoC AS, (Oslo, Norway). Anhydrous sodium sulphate, disodium hydrogen phosphate, dipotassium hydrogen phosphate, sodium hydroxide, potassium hydroxide, sodium chloride, and sodium thiosulfate were purchased from Fisher Chemicals (Loughborough, UK). Tris base was purchased from Fisher Chem Alert (Fair Lawn. USA). RPMI-1640, Dulbecco modified eagle medium (DMEM), Penicillin/Streptomycin, L-glutamine, and trypan blue were purchased from Invitrogen<sup>™</sup> (Grand Island, NY, USA). Hydrochloric acid was AR grade obtained from Merck (Darmstadt, Germany). Ethanol, methanol, dimethyl sulfoxide (DMSO), chloroform, ethyl acetate, and hexane were AR grade and were purchased from Labscan (Dublin, Ireland). Acetone and acetronitrile were HPLC grade purchased from Merck (Darmstadt, Germany).

Horseradish peroxidase (HRP)-conjugated sheep anti-rabbit IgG antibody was obtained from Promega (Madison, WI, USA). Sodium dodecyl sulfate (SDS) was purchased from EMD Millipore Corporation (Billerica, MA, USA). Polyvinylidine fluoride transfer membrane was purchased from Pall Corporation (Pensacola, FL, USA). Rabbit polyclonal anti-GAPDH IgG and lipopolysaccharide (LPS) were purchased from Cell Signaling Technology<sup>®</sup> (Boston, MA). Rabbit polyclonal anti-NF-kB IgG, p105/p50 (Phospho-Ser337) was purchased from OriGene Inc. (Rockville, MD, USA). SuperSignal<sup>®</sup> West Pico Chemiluminescent was purchased from Pierce (Rockford, IL, USA). Coconut oil was purchased from a local market in Chiang Mai province, Thailand. Protease inhibitors were obtained from Amresco (Solon, OH, USA).

### Oil extraction

### Essential oil distillation

The rhizomes of *Z. cassumunar* were subjected to hydrodistillation for 3 h using a clevenger type apparatus. The obtained EO was dried over anhydrous sodium sulfate and stored in a refrigerator and protected from light until further use. The yield of EO was recorded and the density was measured using a pycnometer.

# Hot infused oil preparation

HO was prepared by the method of Chaiyana et al. (Chaiyana et al., 2014). Briefly, 1 kg of *Z. cassumunar* rhizomes were sliced into small pieces and extracted with 1 L of heated coconut oil for 3-4 h. The oil was then filtered to obtain HO and stored in a tightly closed light-protected container until further use.

# Chemical composition analysis

# Gas chromatography–mass spectrometry (GC-MS) of EO

EO was analyzed for its chemical composition by GC-MS. The GC-MS analysis was performed on an Agilent 6890 gas chromatograph (Agilent Technologies, CA, USA) coupled to an electron impact (EI, 70 eV) with HP 5973 mass selective detector (Hewlett Packard, CA, USA) fitted with a fused silica capillary column (HP-5MS) supplied by Hewlett Packard, USA (30.0 m × 250 mm, i.d. 0.25 mm film thickness). The analytical conditions were as follows: carrier gas: helium (ca. 1.0 mL/min), injector temperature: 260°C, oven temperature: 3 min isothermal at 100°C (No peaks before 100°C after first injection), then at 3°C/min to 188°C and then at 20°C/min to 280°C (3 min isothermal), and the detector temperature was 280°C. The identification of individual compounds was based on their retention times relative to those of authentic samples and matching spectral peaks available from Wiley, NIST and NBS mass spectral libraries. The Kováts retention indices (KI) were obtained by GC-MS analysis of an aliquot of the volatile oil spiked with an n-alkanes mixture containing each homologue from n-C8 to n-C20. Identification of the compounds was based on a comparison of their mass spectra with known compounds in the database (WILEY&NIST) and spectroscopic data (Adams, 2001). The experiments were done in triplicate.

# Thin layer chromatography (TLC) of HO

HO was diluted in a mixture of chloroform and acetone (50:50) before spotting on the TLC plate. The plate was then developed in two developing solvent systems, ethanol and hexane in the ratios of 2:8 (System I) and 4:6 (System II). Curcumin standard was used as a marker in this study. The developed plate was then observed in daylight, UV light at 254 nm, and UV light at 366 nm. Retardation factors ( $R_f$ ) were then calculated using the following equation:  $R_f = D_s/D_f$ , whereas,  $D_s$  is the distance that the sample traveled before dropping out

of the solution and  $D_f$  is the distance that the solvent traveled. The experiments were done in duplicate.

# High performance liquid chromatography (HPLC) of HO

Briefly, HPLC analyses were performed using an HP1100 system with a thermostatically controlled column oven and a UV detector set at 420 nm (Hewlett-Packard, Palo Alto, CA). A reversed phase column Eclipse XDB-C18 (4.6 × 150 mm, 5-micron, Agilent, USA) was connected with an Eclipse XDB-C18 guard column (4.6 × 12.5 mm mm, 5-micron, Algilent, USA). A mixture of acetonitrile and acetone in the ratio of 80:20 was used to elute samples at ambient temperature at a flow rate of 1 mL/min and 20 μL of sample were injected. Curcumin standard was used as a marker. Samples and mobile phases were filtered through a 0.45 mm Millipore filter, type GV (Millipore, Bedford, MA) prior to HPLC injection. The experiments were done in duplicate.

# Cell culture and condition

U937 (human leukemic monocyte lymphoma) cells were grown in RPMI-1640 culture medium supplemented with 100 IU/mL penicillin, 100  $\mu$ g/mL streptomycin, 10% FBS, and 2 mM L-glutamine. The cells were incubated at 37°C in a humidified atmosphere of 5% CO<sub>2</sub> (Balsinde and Mollinedo, 1988).

RAW 264.7 cells (American Type Culture Collection, ATCC-TIB-71) were grown in DMEM culture medium supplemented with 10% FBS. The cells were incubated at 37°C in a humidified atmosphere of 5% CO<sub>2</sub> (Mueller et al., 2010).

Peripheral blood mononuclear cells (PBMCs) were isolated from whole blood that was collected from the same healthy donor throughout the research. The whole blood sample was diluted with the same volume of phosphate buffer saline (PBS), pH 7.4. After that, the

diluted blood sample was carefully layered onto a Ficoll-Paque Plus. The mixture was centrifuged at  $5{,}000 \times g$  for 30 min at room temperature. The undisturbed mononuclear cell layer was then carefully transferred out. The cells were washed and pelleted down with three volumes of PBS two times each and resuspended in RPMI-1640 media with 100 IU/mL penicillin, 100  $\mu$ g/mL streptomycin, and 10% FBS. The viable PBMC number was counted with an equal volume of trypan blue solution.

# Cell cytotoxicity

The effects of EO and HO on the viability of peripheral blood mononuclear cells (PBMCs) were determined by a colorimetric technique using the MTT assay (Phongpradist et al., 2010). Briefly, 100  $\mu$ L PBMCs at a cell concentration of  $1.0 \times 10^5$  cells/mL were added into each well of a 96-well plate and incubated at 37°C, 5% CO<sub>2</sub> and 90% humidity for 24 h. Then 100  $\mu$ L of various concentrations of samples were added to the cells compared with untreated cells and incubated again under the same conditions for 48 h. After the corresponding period, 100  $\mu$ L of media were removed and 15  $\mu$ L of MTT (5 mg/mL) were added into each well and incubated for 4 h. All media were then removed by turning the 96-well plate upside down. Then 200  $\mu$ L of DMSO were added into each well to solubilize the formazan crystals. The plate was then read at 540 nm using a microplate reader (Bio-Rad Laboratories Ltd., Japan). All experiments were done in triplicate.

# Anti-inflammatory activity

Determination of albumin denaturation inhibition

Determination of albumin denaturation inhibition was used to evaluate the antiinflammation activity (Rahman et al., 2015). Briefly, BSA aqueous solution (0.5% w/v) was mixed with various concentrations of test solution and incubated at 37°C for 20 min. Then the temperature was increased to 57°C and kept at that level for 3 min. After cooling, PBS (pH 6.3) was added and the absorbance was measured using a UV-Visible spectrophotometer (Shimadzu, japan) at 255 nm. The percentage inhibition was calculated using the following equation: % Inhibition = 1 - [(S-C)/S], where S is the turbidity in the presence of a certain concentration of the test sample and C is the turbidity in absence of the test sample. Indomethacin was used as a positive control. All of the experiments were done in triplicate.

# Determination of NF-κB level by Western blot analysis

The immunoblotting assay was used to determine the level of NF-κB. The U937 cells were incubated with indomethacin, EO, and HO for 12, 24, and 48 h to determine the timedependent effects. The cells were also incubated with curcumin (the major constituent of HO) as well as terpinen-4-ol, and sabinene (the major constituents of EO) for 48 h to measure the levels of NF-κB suppression. The cells were lysed in RIPA buffer (25 mM Tris•HCl, pH 7.6, 150 mM NaCl, 1% NP-40, 1% sodium deoxycholate, 0.1% SDS) containing protease inhibitors. Cell lysates were collected by centrifugation at 7,826 × g for 15 min, at room temperature. The protein concentrations were measured by the Folin-Lowry method and standardized with BSA. Whole protein lysate (50 µg) was separated by SDS-PAGE and transferred to a polyvinylidene fluoride (PVDF) membrane. The membrane was blocked for nonspecific binding by 5% non-fat dry milk in PBS containing 0.1% Tween 20 for 2 h and probed by anti-NF-κB for 2 h. GAPDH was used as an internal control. The secondary antibody conjugated with horse radish peroxidase (HRP) was added. Peroxidase activity was detected using chemiluminescence reagents (Shishodia et al., 2005). The protein band levels were quantified by a scan densitometer and Quantity One software, version 4.6.3 (Bio-Rad laboratories, Hercules, CA, USA). The density value of each band was normalized to that of the GAPDH band.

# Determination of IL-6 secretion inhibition by ELISA

LPS stimulated RAW 264.7 cells were used to examine the effects of EO and HO on inflammation. The cell culture was performed following the method of Mueller et al. with slight modifications (Mueller et al., 2010). Briefly, RAW 264.7 cells were seeded at a density of  $2 \times 10^6$  cells per well in 24 well plates, and incubated at 37°C, 5% CO<sub>2</sub> and 90% humidity for 24 h. On the following day, test compounds in ethanolic solution in DMEM were added, and further incubated in the same condition for 2 h. After that LPS was added to set the final concentration at 1  $\mu$ g/mL and further incubated in the same conditions for 24 h. On the third day, the media was removed and centrifuged at  $13,500 \times g$  for 10 min to remove cells. The supernatant was divided into aliquots and analyzed by ELISA. Cells that were not treated with LPS served as a negative control and cells incubated with ethanol and LPS served as a positive control. The IL-6 in cell supernatant (100  $\mu$ L) was determined by ELISA according to the manufacturer's protocol (R&D Systems). All incubation steps were performed at room temperature. The optical density at 450 nm, corrected by the reference wavelength 570 nm, was measured with a Genios Pro microplate reader (Tecan, Crailsheim, Germany).

# Determination of cell viability via the MTT assay

Simultaneously with the ELISA, the viability of LPS-stimulated cells was assessed by the MTT assay, based on the mitochondrial-dependent reduction of MTT to formazan. After removing the supernatant for ELISA analysis, MTT was added to the cells, and the cells were incubated for at 37°C, 5% CO<sub>2</sub> and 90% humidity for 2 h. The supernatant was then removed, and the cells were lysed with lysis buffer (10% SDS in 0.01 N HCl). The optical density at 570 nm, corrected by the reference wavelength 690 nm, was measured using a Genios Pro microplate reader.

# Calculation of IL-6 secretion

The calculated concentrations of cytokines were normalized to MTT values to reduce any variation from differences in cell density. For a positive control, cells were treated with only LPS and the resulting amount of secreted cytokines was defined as 100%. The results from the experimental compounds were then calculated as a percent of this value. The entire inflammation assay, starting with cell seeding and LPS-induction, was performed in triplicate in three time independent experiments.

# Statistical analysis

All data were presented as a mean  $\pm$  standard deviation (SD). Individual differences were evaluated by One-Way ANOVA followed by post-hoc tests. In all cases, P < 0.05 indicated statistical significance.

#### **Results**

# Characteristics of EO and HO

Two different extraction methods of *Z. cassumunar* rhizome have been described. Volatile compounds can be extracted by hydrodistillation, whereas, nonvolatile nonpolar compounds can be extracted by the hot infusion method. Each oil extract has its own unique characteristics. EO extracted by hydrodistillation is a clear light-yellowish liquid with a characteristic odor. Our yield of EO was 0.48% (v/w) with a density of 0.90 g/mL, while HO extracted by hot infusion was a clear yellowish liquid with a density of 0.95 g/mL, equal to that of coconut oil, the solvent used in the hot infusion method. The colored components of *Z. cassumunar* rhizomes could be extracted efficiently by the hot infusion method; hence, in the HO extract the color was a much deeper yellow than that of the EO.

# GC-MS analysis of EO

Relative amounts of the individual compounds were presented as peak area percentage of the total peak area of EO (**Table I**). The GC-MS data indicated that 26 components comprising 90.5±1.3% of the total composition of EO could be identified.

# TLC analysis of HO

TLC chromatograms of HO were developed with two different developing solvent systems (**Figure 1**). Curcumin, which possesses a variety of therapeutic properties including antioxidant, analgesic, anti-inflammatory, antiseptic, and anticarcinogenic activities, was used as a marker (Nagpal and Sood, 2013). The chromatogram developed with **System I** detected under visible light exhibited a single yellow spot of curcumin and HO with the same  $R_f$  value of 0.065 (A). Additionally, HO contained absorbing compounds that diminished the uniform layer fluorescence and which were detected as dark spots on a bright green background when excited with short-wave (254 nm) UV light at the  $R_f$  values of 0.065 (A), 0.272 (C), 0.473 (F), 0.549 (G), 0.759 (I), and 0.891 (J). The dark spot at the  $R_f$  value of 0.065 of HO was consistent with curcumin. Moreover, the native fluorescence compounds of HO were visualized at the  $R_f$  values of 0.065 (A), 0.233 (B), 0.341 (D), 0.406 (E), 0.618 (H), 0.759 (I), and 0.891 (J) when excited with long-wave (366 nm) UV light. The fluorescence spot at the  $R_f$  value of 0.065 of HO was bright green, which was consistent with that of curcumin.

**System II** was also used to support the conclusions from the HO component. Under visible light, curcumin and HO exhibited a single yellow spot at the same  $R_f$  value of 0.259 (K). Additionally, HO contained absorbing compounds that diminished the uniform layer fluorescence and were detected as dark spots on a bright green background when excited with

short-wave (254 nm) UV light at the  $R_f$  values of 0.259 (K), 0.427 (L), 0.565 (M), and 0.669 (N). The dark spot at the  $R_f$  value of 0.259 of HO was consistent with curcumin. Moreover, the native fluorescent compounds of HO were visualized at the  $R_f$  value of 0.259 (K) and 0.565 (M) when excited with long-wave (366 nm) UV light. The fluorescence spot at the  $R_f$  value of 0.065 of HO was bright green, which was consistent with that of curcumin.

# HPLC analysis of HO

HO components were also analyzed by HPLC. The HPLC chromatograms (**Figure 2**) were detected by UV absorption at 420 nm, which is the wavelength associated with maximum absorbance of curcumin (Kapoor and Priyadarsini, 2001; Gopinath et al., 2004). There was only one peak detected in HO at the retention time of 1.599 min that corresponded well with that of the standard curcumin (1.599 min), leading to conclude that the major constituent of HO was curcumin.

# Cytotoxic effects of EO and HO on human PBMCs

The cell viabilities of human PBMCs after treatments with EO and HO for 48 h had no apparent toxic effects, as indicated by 100% of cell viability, even at high concentration (50% v/v) (**Figure 3**).

# Effect of EO and HO on protein denaturation by albumin denaturation inhibition method

BSA denaturation inhibition of EO and HO are shown in **Figure 4** in comparison with indomethacin, a well-known anti-inflammatory agent. EO, HO, and indomethacin were able to protect BSA against heat denaturation with IC<sub>50</sub> values of 11.7  $\pm$  3.9  $\mu$ g/mL (R<sup>2</sup> = 0.969), 9.5  $\pm$  2.0  $\mu$ g/mL (R<sup>2</sup> = 0.968), and 6.2  $\pm$  2.6  $\mu$ g/mL (R<sup>2</sup> = 0.984), respectively. The protein denaturation inhibition of EO and HO was comparable to that of indomethacin (*P* < 0.05).

# Effects of EO and HO on NF-kB protein levels in U937 cells by Western blot analysis

An immunoblotting assay was used to determine the levels of NF- $\kappa$ B protein in U937 cells. The concentrations of EO and HO for cell treatments were based on the IC<sub>20</sub> values (non-cytotoxic doses). IC<sub>20</sub> values of EO and HO were  $7.8\pm0.9~\mu g/mL$  and  $179.4\pm19.2~\mu g/mL$ , respectively. Therefore, the concentration of  $7.8~\mu g/mL$  was selected for EO and HO treatment in this experiment.

Indomethacin was used as a positive control and was identified as a potential compound that could suppress NF- $\kappa$ B expression. The time-response effects of indomethacin, EO, and HO are shown in **Figure 5**. The suppression of NF- $\kappa$ B protein levels after indomethacin treatment for 12, 24, and 48 h were  $11.0 \pm 2.4\%$ ,  $85.0 \pm 1.9\%$ , and  $98.5 \pm 3.2\%$ , respectively. EO and HO showed less pronounced suppression. The NF- $\kappa$ B protein levels after EO treatment were  $2.0 \pm 3.5\%$ ,  $17.4 \pm 1.7\%$ , and  $90.6 \pm 4.3\%$ , while HO treatment were  $5.9 \pm 5.1\%$ ,  $17.3 \pm 3.3\%$ , and  $22.8 \pm 5.0\%$ , respectively with increased treatment time. The NF- $\kappa$ B suppression was most obviously observed at 48 h; the effects of the major constituents of EO and HO on NF- $\kappa$ B protein levels were therefore investigated at that period of time.

In another experiment, EO and HO at the same concentration of indomethacin (7.8 μg/mL) were able to suppress NF-κB, as well as their major constituents (**Figure 6**). After indomethacin, EO, and HO treatments, NF-κB protein levels were  $85.3 \pm 2.9\%$ ,  $41.7 \pm 2.7\%$ , and  $36.0 \pm 3.9\%$ , respectively. EO showed significantly greater suppression of NF-κB protein level than HO (P < 0.05). Sabinene and terpinen-4-ol (the major constituents of EO) significantly reduced NF-κB expression by  $46.7 \pm 5.0\%$  and  $77.8 \pm 7.8\%$ , respectively (P < 0.01). Curcumin, the major constituent of HO, also significantly reduced NF-κB expression by  $8.3 \pm 3.9\%$  (P < 0.05).

# Effects of EO and HO on IL-6 protein levels in RAW 264.7 cells by ELISA

The IL-6 secretion levels of RAW 264.7 cell line after being stimulated with LPS and treated with EO and HO were not significantly reduced compared to the cells stimulated with LPS alone (data not shown). Curcumin had a slight effect on the inhibition of IL-6 secretion. Although EO did not significantly reduce IL-6 secretion, the major constituents of EO show a promising anti-inflammatory effect. The dose response effects of terpinen-4-ol and sabinene are shown in **Figure 7**. Neither compound had an effect at the low concentration (5  $\mu$ g/mL). However, the reduction effects were distinctly presented at the concentration of 50  $\mu$ g/mL and terpinen-4-ol and sabinene significantly reduced the IL-6 secretion levels to 82.4  $\pm$  1.9% and 79.8  $\pm$  6.7%, respectively (P < 0.05).

# **Discussion**

Our study revealed that terpinen-4-ol ( $40.5 \pm 6.6\%$ ) and sabinene ( $17.4 \pm 1.4\%$ ) were the major constituents of EO. The results were in a good agreement with those of previous studies reporting that terpinen-4-ol was the major component (50.5%) of the essential oil from *Z. cassamunar* rhizomes in India (Bordoloi et al., 1999). Moreover, the essential oil from *Z. cassamunar* rhizomes also contains sabinene (36.71-53.50%),  $\gamma$ -terpinene (5.27-7.25%), terpinen-4-ol (21.85-29.96%) and (E)-1-(3,4-dimethoxyphenyl) butadiene (0.95-16.16%) (Sukatta et al., 2009). In addition, triquinacene 1,4-bis (methoxy) (26.47%), (Z)-ocimene (21.97%), and terpinen-4-ol (18.45%) were the major constituents in the essential oil from *Z. cassamunar* rhizomes in Bangladesh (Bhuiyan et al., 2008).

The chemical components of HO were analyzed by means of TLC and HPLC. A spot of HO component was detected at the same *Rf* value of curcumin and presented the same character after the detection under various conditions, including day light, short-wave (254)

nm) UV light, and long-wave (366 nm) UV light. Two developing solvent systems yielded the same conclusion that curcumin was the major constituent of HO. The results from HPLC analysis also supported this conclusion since HO and curcumin were detected at the same  $R_f$  value of 1.599 min.

Denaturation of tissue protein is one of the known and documented causes of inflammation, and is due to the production of auto antigens (Phongpradist et al., 2015). Therefore, protein denaturation-preventing agents would be worthwhile targets for antiinflammatory drug development. In this study, HO and EO could protect BSA against heat denaturation in the same manner as indomethacin. A previous study suggested that curcumin was responsible for the anti-denaturation since it interacted with the aliphatic regions around the lysine residue on the BSA (Phongpradist et al., 2015). Another prospective binding site related to the anti-denaturation of BSA is the aromatic tyrosine rich region (Shendkar et al., 2014). Various polyphenols have been reported to bind BSA at this site, including catechins [(-)-epigallocatechin-3-gallate, (-)-epigallocatechin, (-)-epicatechin-3-gallate], (kaempferol, kaempferol-3-glucoside, quercetin, naringenin), and hydroxycinnamic acids (rosmarinic acid, caffeic acid, p-coumaric acid) (Dymerski et al., 2015). Curcumin is a polyphenolic compound, therefore, binding to the aromatic tyrosine rich region might be another pathway to inhibit BSA denaturation. On the other hand, several terpenes were able to bind well with BSA due to their being small hydrophobic molecules (Adams and Anslyn, 2009), therefore, the BSA denaturation inhibition of EO could be due to the major constituents of terpenes.

NF-κB transcription factor is a protein marker that responds to inflammations. Therefore, prevention of NF-κB activation is directly related with reduction of the inflammatory process (Maroon et al., 2005). The duration of incubation time had a large effect on NF-κB suppression. At 12 h, only indomethacin could suppress the NF-κB

expression (P < 0.05). The NF- $\kappa$ B suppression of EO and HO were observed after 24 h and more distinct effects were observed after 48 h.

EO, HO, and their major constituents were investigated for their capability to suppress NF-κB protein expression. Both EO and HO possessed anti-inflammatory effects since they could significantly suppress the NF- $\kappa$ B expression (P < 0.01). Curcumin also possesses good anti-inflammatory properties in HO. Our results are in line with those of a previous study showing that NF-kB expression is suppressed by curcumin (Surh et al., 2001). The antiinflammatory effect of curcumin is well-known (Maheshwari et al., 2006; Menon & Sudheer, 2007). Beside NF-kB suppression, it could inhibit different molecules involved in the inflammation process, including phospholipase, lipooxygenase, cyclooxygenase leukotrienes, thromboxane, prostaglandins, nitric oxide, collagenase, elastase, hyaluronidase, monocyte chemoattractant protein-1, interferon-inducible protein, tumor necrosis factor, and interleukin-12 (Chainani-Wu, 2003). However, the NF-κB suppression by curcumin was less pronounced than that of HO. Therefore, the anti-inflammatory effects of HO may be due at least in part to compounds besides curcumin. There are additional constituents of Z. cassumunar rhizome extracts that act as potent anti-inflammatory agents, such as cassumunarins, phenylbutenoids, zerumbone, (E)-4-(3',4'-dimethoxyphenyl)but-3-en-2-ol, (E)-1-(3,4-dimethoxyphenyl) butadiene, (E)-4-(30,40-dimethoxyphenyl) but-3-en-l-ol, etc. (Masuda et al., 1995; Han et al., 2005; Masuda and Jitoe, 1995; Murakami et al., 2004; Panthong et al., 1997; Chaiwongsa et al., 2013; Jeenapongsa et al., 2003; Pongprayoon et al., 1997; Suksaeree et al., 2015). Some of these compounds may be extracted by the hot infusion method and included in HO, but in small amounts not detectable by HPLC. Due to their potent anti-inflammatory effects, small amounts of any of the latter compounds could produce anti-inflammatory properties of HO.

Sabinene and terpinen-4-ol, the major constituents of EO, showed potent antiinflammatory effects. The NF- $\kappa$ B suppression of terpinen-4-ol was comparable to that of indomethacin. This suggests that the active constituents responsible for anti-inflammatory activity of EO were terpinen-4-ol and sabinene. In addition, terpinen-4-ol was found to suppress the production of several pro-inflammatory mediators, such as tumor necrosis factor  $\alpha$  (TNF $\alpha$ ), interleukin-1 $\beta$ , interleukin-8, interleukin-10, prostaglandin E<sub>2</sub>, and reduced superoxide production by neutrophils and monocytes stimulated with *N*-formyl-methionylleucyl-phenylalanine and lipopolysaccharide (Hart et al., 2000; Brand et al., 2001). Moreover, it significantly inhibited edema formation in the test of carrageenan-induced hind paw edema in rats (Pongprayoon et al., 1997). Thus there are different pathways of inflammation affected by terpinen-4-ol.

Similarly, sabinene has demonstrated anti-inflammatory activity through various mechanisms. It inhibited nitric oxide ion production in lipopolysaccharide plus interferon-γ triggered macrophages (Valente et al., 2013). However, sabinene was ineffective as a topical anti-inflammatory agent in the model of carrageenan-induced hind paw edema in rats (Pongprayoon et al., 1997).

IL-6 is involved in the inflammation process due to its ability to regulate the transition from neutrophil to monocyte recruitment, which is the hallmark of acute inflammation (Kaplanski et al., 2003). In chronic inflammation, IL-6 might increase the mononuclear-cell infiltrate and participate in disease pathogenesis (Kaplanski et al., 2003). Therefore, a compound that could reduce or inhibit IL-6 secretion would possess anti-inflammatory effects. Our present study indicated that terpinen-4-ol and sabinene, the major constituents of EO, significantly reduced IL-6 secretion, which supported the conclusion concerning the anti-inflammatory effects of EO. As there are higher amounts of terpinen-4-ol and sabinene in the essential oil of *Z. cassumunar* compared to other Zingiberaceous plants (Natta et al., 2008),

this supports the extensive use of *Z. cassumunar* in folk remedies as an anti-inflammatory medicine and analgesic.

# **Conclusions**

The present study proposed several mechanisms of action to explain the antiinflammatory activity of the native oils and their major constituents. The major constituents of EO were terpinen-4-ol (40.5  $\pm$  6.6%) and sabinene (17.4  $\pm$  1.4%), whereas that of HO was curcumin. EO and HO had significant anti-inflammatory effects and were shown to be safe for human use. The anti-inflammatory effects of both oils were demonstrated by an albumin denaturation assay, in which they produced equivalent effects to those of indomethacin. NFκB suppression by EO was more pronounced than HO. The relevant pure major compounds were examined to compare their activities to both HO and EO. Curcumin had antiinflammatory effects in the BSA denaturation test and a slight effect on NF-κB suppression and IL-6 inhibition. Terpinen-4-ol and sabinene showed a strong anti-inflammatory effect in all assays. Therefore, the anti-inflammatory activity of EO was correlated to the presence of terpinen-4-ol and sabinene. Moreover, 50 µg/mL terpinen-4-ol and sabinene significantly reduced IL-6 secretion levels. This indicates that the anti-inflammatory activity produced by Z. cassumunar oil appears to be mainly attributable to the volatile compounds. EO is a promising plant for further development of topical treatments of various conditions associated with inflammation.

# Acknowledgments

This work was supported by Thailand Research Fund under Grant number TRG 5780029 and Austrian Academic Exchange Service (ÖAD).

#### References

- Adams MM, Anslyn EV. Differential sensing using proteins: exploiting the cross-reactivity of serum albumin to pattern individual terpenes and terpenes in perfume. J Am Chem Soc. 2009; 131: 17068-9.
- Adams RP. Quadrupole mass spectra of compounds listed in order of their retention time on DB-5. In: Identification of essential oils components by gas chromatography/ quadrupole mass spectroscopy. (ed.) Allured Publishing Corporation, Carol. Stream, IL, USA, 2001.
- Balsinde J, Mollinedo F. Specific activation by concanavalin A of the superoxide anion generation capacity during U937 differentiation. Biochem Biophys Res Commun. 1988; 151: 802-8.
- Bordoloi AK, Sperkova J, Leclercq PA. Essential oils of Zingiber cassumunar Roxb. from northeast India. J Essent Oil Res. 1999; 11: 441-5.
- Bhuiyan MNI., Chowdhury JU, Begum J. Volatile constituents of essential oils isolated from leaf and rhizome of *Zingiber cassumunar* Roxb. Bangladesh J Pharmacol. 2008; 3: 69-73.
- Brand C, Ferrante A, Prager RH, Riley TV, Carson CF, Finlay-Jones JJ, Hart PH. The water-soluble components of the essential oil of *Melaleuca alternifolia* (tea tree oil) suppress the production of superoxide by human monocytes, but not neutrophils, activated *in vitro*. Inflamm Res. 2001; 50: 213-9.
- Chainani-Wu N. Safety and anti-inflammatory activity of curcumin: a component of tumeric (*Curcuma longa*). J Altern Complem Med. 2003; 9: 161-8.
- Chaiwongsa R, Ongchai S, Boonsing P, Kongtawelert P, Panthong A, Reutrakul V. Active compound of *Zingiber cassumunar* Roxb. down-regulates the expression of genes

- involved in joint erosion in a human synovial fibroblast cell line. Afr J Tradit Complement Altern Med. 2013; 10: 40-8.
- Chaiyana W, Phongpradist R, Leelapornpisid P, Anuchapreeda S. Microemulsion-based hydrogel for topical delivery of indomethacin. Int J Pharm Pharm Sci. 2014; 7: 213-9.
- Dymerski T, Namieśnik J, Vearasilp K, Arancibia-Avila P, Toledo F, Weisz M, Katrich E, Gorinstein S. Comprehensive two-dimensional gas chromatography and three-dimensional fluorometry for detection of volatile and bioactive substances in some berries. Talanta. 2015; 134: 460-7.
- Dymerski T, Namieśnik J, Vearasilp K, Arancibia-Avila P, Toledo F, Weisz M, Katrich E, Gorinstein S. Comprehensive two-dimensional gas chromatography and three-dimensional fluorometry for detection of volatile and bioactive substances in some berries. Talanta. 2015; 134: 460-7.
- Ferrero-Miliani L, Nielsen OH, Andersen PS, Girardin SE. Chronic inflammation: importance of NOD2 and NALP3 in interleukin-1β generation. Clin Exp Immunol. 2007; 147: 227-35.
- Ghosh S, May MJ, Kopp EB. NF-κB and Rel proteins: evolutionarily conserved mediators of immune responses. Annu Rev Immunol. 1998; 16: 225-60.
- Gilroy DW, Colville-Nash PR, Willis D, Chivers J, Paul-Clark MJ, Willoughby DA.

  Inducible cyclooxygenase may have anti-inflammatory properties. Nat Med. 1999; 5: 698-701.
- Gopinath D, Ahmed MR, Gomathi K, Chitra K, Sehgal PK, Jayakumar R. Dermal wound healing processes with curcumin incorporated collagen films. Biomaterials. 2004; 25: 1911-7.

- Habsah M, Amran M, Mackeen MM, Lajis NH, Kikuzaki H, Nakatani N, Rahman AA, Ali AM. Screening of Zingiberaceae extracts for antimicrobial and antioxidant activities. J Ethnopharmacol. 2000; 72: 403-10.
- Han AR, Kim MS, Jeong YH, Lee SK, Seo EK. Cyclooxygenase-2 inhibitory phenylbutenoids from the rhizomes of *Zingiber cassumunar*. Chem Pharm Bull. 2005; 53: 1466-8.
- Hart PH, Brand C, Carson CF, Riley TV, Prager RH, Finlay-Jones JJ. Terpinen-4-ol, the main component of the essential oil of *Melaleuca alternifolia* (tea tree oil), suppresses inflammatory mediator production by activated human monocytes. Inflamm Res. 2000; 49: 619-26.
- Jeenapongsa R, Yoovathaworn K, Sriwatanakul KM, Pongprayoon U, Sriwatanakul K. Anti-inflammatory activity of (E)-1-(3, 4-dimethoxyphenyl) butadiene from *Zingiber* cassumunar Roxb. J Tthnopharmacol. 2003; 87: 143-8.
- Kaplanski G, Marin V, Montero-Julian F, Mantovani A, Farnarier C. IL-6: a regulator of the transition from neutrophil to monocyte recruitment during inflammation. Trends Immunol. 2003; 24: 25-9.
- Kapoor S, Priyadarsini KI. Protection of radiation-induced protein damage by curcumin. Biophys Chem. 2001; 92: 119-26.
- Lee KM, Kang BS, Lee HL, Son SJ, Hwang SH, Kim DS, Park JS, Cho HJ. Spinal NF-kB activation induces COX-2 upregulation and contributes to inflammatory pain hypersensitivity. Eur J Neurosci. 2004; 19: 3375-81.
- Maheshwari RK, Singh AK, Gaddipati J, Srimal RC. Multiple biological activities of curcumin: a short review. Life Sci. 2006; 78: 2081-7.
- Maroon JC, Bost JW, Borden MK, Lorenz KM, Ros NA. Natural antiinflammatory agents for pain relief in athletes. Neurosurg Focus. 2005; 21: E11.

- Masuda T, Jitoe A. Antioxidative and antiinflammatory compounds from tropical gingers: isolation, structure determination, and activities of cassumunins A, B, and C, new complex curcuminoids from *Zingiber cassumunar*. J Agric Food Chem. 1994; 42: 1850-6.
- Masuda T, Jitoe A. Phenylbutenoid monomers from the rhizomes of *Zingiber* cassumunar. Phytochem. 1995; 39: 459-61.
- Masuda T, Jitoe A, Mabry TJ. Isolation and structure determination of cassumunarins A, B, and C: new anti-inflammatory antioxidants from a tropical ginger, *Zingiber cassumunar*. J Am Oil Chem Soc. 1995; 72: 1053-7.
- Menon VP, Sudheer AR. Antioxidant and anti-inflammatory properties of curcumin. In The molecular targets and therapeutic uses of curcumin in health and disease. (ed.). Springer, US, 2007, pp. 105-25.
- Mizushima Y, Kobayashi M. Interaction of anti-inflammatory drugs with serum proteins, especially with some biologically active proteins. J Pharm Pharmacol. 1968; 20: 169-73.
- Murakami A, Miyamoto M, Ohigashi H. Zerumbone, an anti-inflammatory phytochemical, induces expression of proinflammatory cytokine genes in human colon adenocarcinoma cell lines. Biofactors. 2004; 21: 95-101.
- Mueller M, Hobiger S, Jungbauer A. Anti-inflammatory activity of extracts from fruits, herbs and spices. Food Chem. 2010; 122(4): 987-996.
- Nagpal M, Sood S. Role of curcumin in systemic and oral health: An overview. J Nat Sc Biol Med. 2013; 4: 3-7.
- Nandhasri P, Pawa KK. Quality control of luk prakop, a Thai herbal combination. In III WOCMAP Congress on Medicinal and Aromatic Plants-Volume 5: Quality, Efficacy, Safety, Processing and Trade in Medicinal 679, 2003, pp. 131-6.

- Natta L, Krittik N, Pantip B, Orapin K. Essential Oil from Five Zingiberaceae For Anti Food-Borne Bacteria. Int Food Res J. 2008; 15: 1-10.
- Padmanabhan P, Jangle SN. Evaluation of in-vitro anti-inflammatory activity of herbal preparation, a combination of four medicinal plants. Int J App Basic Med Res. 2012; 2: 109-16.
- Panthong A, Kanjanapothi D, Niwatananant W, Tuntiwachwuttikul P, Reutrakul V. Anti-inflammatory activity of compound D {(E)-4-(3', 4'-dimethoxyphenyl) but-3-en-2-ol} isolated from *Zingiber cassumunar* Roxb. Phytomed. 1997; 4: 207-12.
- Phongpradist R, Chaiyana W, Anuchapreeda S. Curcumin-loaded multi-valent ligands conjugated-nanoparticles for anti-inflammatory. Int J Pharm Pharm Sci. 2015; 7: 203-8.
- Phongpradist R, Chittasupho C, Okonogi S, Siahaan T, Anuchapreeda S, Ampasavate C, Berkland C. LFA-1 on leukemic cells as a target for therapy or drug delivery. Curr Pharm Des. 2010; 16: 2321-30.
- Pongprayoon U, Soontornsaratune P, Jarikasem S, Sematong T, Wasuwat S, Claeson P. Topical antiinflammatory activity of the major lipophilic constituents of the rhizome of *Zingiber cassumunar*. Part I: The essential oil. Phytomed. 1997; 3: 319-22.
- Pithayanukul P, Tubprasert J, Wuthi-Udomlert M. *In vitro* antimicrobial activity of *Zingiber* cassumunar (Plai) oil and a 5% Plai oil gel. Phytother Res. 2007; 21: 164-9.
- Rahman H, Eswaraiah MC, Dutta AM. *In-vitro* anti-inflammatory and anti-arthritic activity of *Oryza sativa* Var. Joha rice (an aromatic indigenous rice of assam) Am Eurasian J Agric Environ Sci. 2015; 15: 115-21.
- Ryan GB, Majno G. Acute inflammation. A review. Am J Pathol. 1977; 86: 183-276.
- Sakat S, Juvekar AR, Gambhire MN. *In vitro* antioxidant and anti-inflammatory activity of methanol extract of Oxalis corniculata Linn. Int J Pharm Pharm Sci. 2010; 2: 146-55.

- Shendkar AK, Chaudhari SG, Shendkar YK. *In vitro* antiartthritic activity of *Withania* coagulans Dunal fruits. Indo Am J Pharm Res. 2014; 4: 915-24.
- Shishodia S, Amin HM, Lai R, Aggarwal BB. Curcumin (diferuloylmethane) inhibits constitutive NF-κB activation, induces G1/S arrest, suppresses proliferation, and induces apoptosis in mantle cell lymphoma. Biochem Pharmacol. 2005; 70: 700-13.
- Sukatta U, Rugthaworn P, Punjee P, Chidchenchey S, Keeratinijakal V. Chemical composition and physical properties of oil from Plai (*Zingiber cassumunar* Roxb.) obtained by hydro distillation and hexane extraction. Kasetsart J Nat Sci. 2009; 43: 212-7.
- Suksaeree J, Charoenchai L, Madaka F, Monton C, Sakunpak A, Charoonratana T, Pichayakorn W. *Zingiber cassumunar* blended patches for skin application: Formulation, physicochemical properties, and in vitro studies. Asian J Pharm Sci. 2015; 10: 341-9.
- Surh YJ, Chun KS, Cha HH, Han SS, Keum YS, Park KK, Lee SS. Molecular mechanisms underlying chemopreventive activities of anti-inflammatory phytochemicals: down-regulation of COX-2 and iNOS through suppression of NF-κB activation. Mutat Res Fund Mol M. 2001; 480: 243-68.
- Tuntiwachwuttikul P, Pancharoen O, Jaipetch T, Reutrakul V. Phenylbutanoids from *Zingiber cassumunar*. Phytochem, 1981; 20: 1164-5.
- Valente J, Zuzarte M, Goncalves MJ, Lopes MC, Cavaleiro C, Salgueiro L, Cruz MT.

  Antifungal, antioxidant and anti-inflammatory activities of *Oenanthe crocata* L.

  essential oil. Food Chem Toxicol. 2013; 62: 349-54.
- Vane JR, Botting RM. New insights into the mode of action of anti-inflammatory drugs. Inflamm Res. 1995; 44: 1-10.

Table I

Percentage of constituents in EO identified by GC-MS analysis

| No.   | RT <sup>a</sup> | Compound <sup>b</sup>   | % Area         | KI     |                  | O1d                 |
|-------|-----------------|-------------------------|----------------|--------|------------------|---------------------|
|       |                 |                         |                | Sample | Ref <sup>c</sup> | - Qual <sup>d</sup> |
| 1     | 3.98            | alpha-thujene           | $1.8 \pm 1.9$  | 931    | 930              | 94                  |
| 2     | 4.13            | alpha-pipene            | $1.6 \pm 0.7$  | 938    | 939              | 97                  |
| 3     | 4.46            | camphene                | $0.1 \pm 0.0$  | 954    | 954              | 96                  |
| 4     | 5.06            | sabinene                | $17.4 \pm 1.4$ | 978    | 975              | 96                  |
| 5     | 5.13            | beta-pinene             | $2.7 \pm 0.6$  | 981    | 979              | 97                  |
| 6     | 5.42            | beta-myrcene            | $1.4 \pm 0.3$  | 993    | 991              | 97                  |
| 7     | 5.81            | alpha-phellandrene      | $0.6 \pm 0.3$  | 1008   | 1003             | 97                  |
| 8     | 6.17            | alpha-terpipene         | $6.4 \pm 4.2$  | 1021   | 1017             | 98                  |
| 9     | 6.43            | para-cymene             | $2.2 \pm 3.6$  | 1031   | 1025             | 95                  |
| 10    | 6.54            | beta-phellandrene       | $1.8 \pm 1.4$  | 1034   | 1030             | 94                  |
| 11    | 6.60            | 1,8-cineole             | $0.3 \pm 0.1$  | 1036   | 1031             | 97                  |
| 12    | 7.11            | trans-beta-ocimene      | $0.1 \pm 0.1$  | 1053   | 1050             | 92                  |
| 13    | 7.50            | gamma-terpinene         | $5.8 \pm 3.0$  | 1065   | 1060             | 97                  |
| 14    | 7.85            | cis-sabinene hydrate    | $0.5 \pm 1.2$  | 1075   | 1070             | 98                  |
| 15    | 8.46            | terpinolene             | $2.2\pm2.5$    | 1091   | 1089             | 98                  |
| 16    | 8.96            | trans-sabinene hydrate  | $0.5 \pm 1.0$  | 1104   | 1098             | 96                  |
| 17    | 10.53           | 1-terpineol             | $1.0 \pm 0.3$  | 1140   | 1134             | 96                  |
| 18    | 12.26           | terpinen-4-ol           | $40.5 \pm 6.6$ | 1173   | 1177             | 98                  |
| 19    | 12.63           | gamma-terpineol         | $1.6\pm0.2$    | 1199   | 1199             | 91                  |
| 20    | 12.75           | cis-piperitol           | $0.5 \pm 0.0$  | 1202   | 1196             | 97                  |
| 21    | 13.27           | trans-piperitol         | $0.5 \pm 0.1$  | 1212   | 1208             | 91                  |
| 23    | 23.29           | trans-beta-farnesene    | $0.2 \pm 0.4$  | 1460   | 1457             | 90                  |
| 24    | 24.81           | zingiberene             | $0.1 \pm 0.1$  | 1496   | 1494             | 94                  |
| 25    | 25.31           | beta-bisabolene         | $0.1 \pm 0.0$  | 1508   | 1506             | 93                  |
| 26    | 25.92           | beta-sesquiphellandrene | $0.8 \pm 0.0$  | 1521   | 1523             | 99                  |
| Total |                 |                         | $90.5 \pm 1.3$ |        |                  |                     |

 $\mathbf{RT}$  = Retention time;  $\mathbf{a}$  = Compounds are listed in the order of their elution from a DB-5 column;  $\mathbf{b}$  = Peak identifications are based on MS comparisons with file spectra and relative retention time (KI);  $\mathbf{c}$  = KI from Sparkman;  $\mathbf{d}$  = database of WILEY275

#### Figures with labels

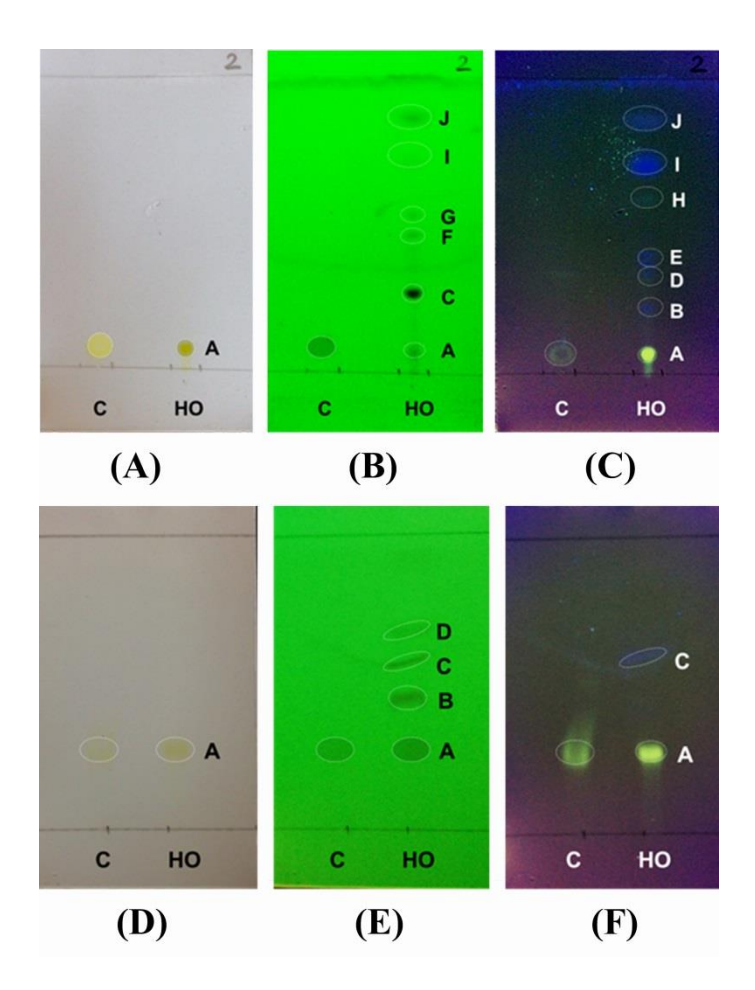


**Figure 1:** TLC chromatograms of curcumin (C) and HO after developing with ethanol and hexane in the ratio of 2:8 (**System I**) and detected under visible light (**A**), short-wave (254 nm) UV light (**B**), and long-wave (366 nm) UV light (**C**) and after developing with ethanol and hexane in the ratio of 4:6 (**System II**) and detected under visible light (**D**), short-wave (254 nm) UV light (**E**), and long-wave (366 nm) UV light (**F**)

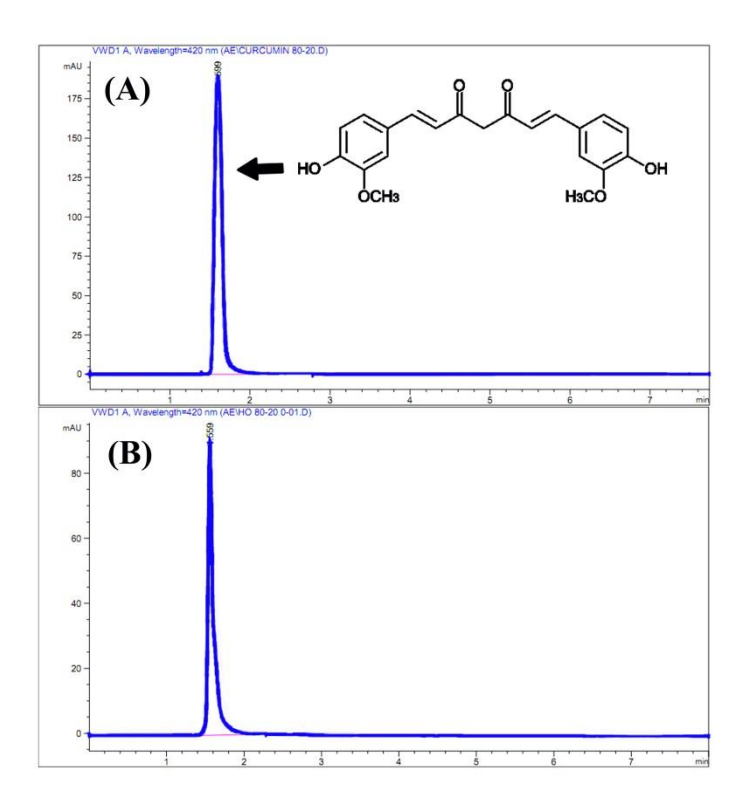
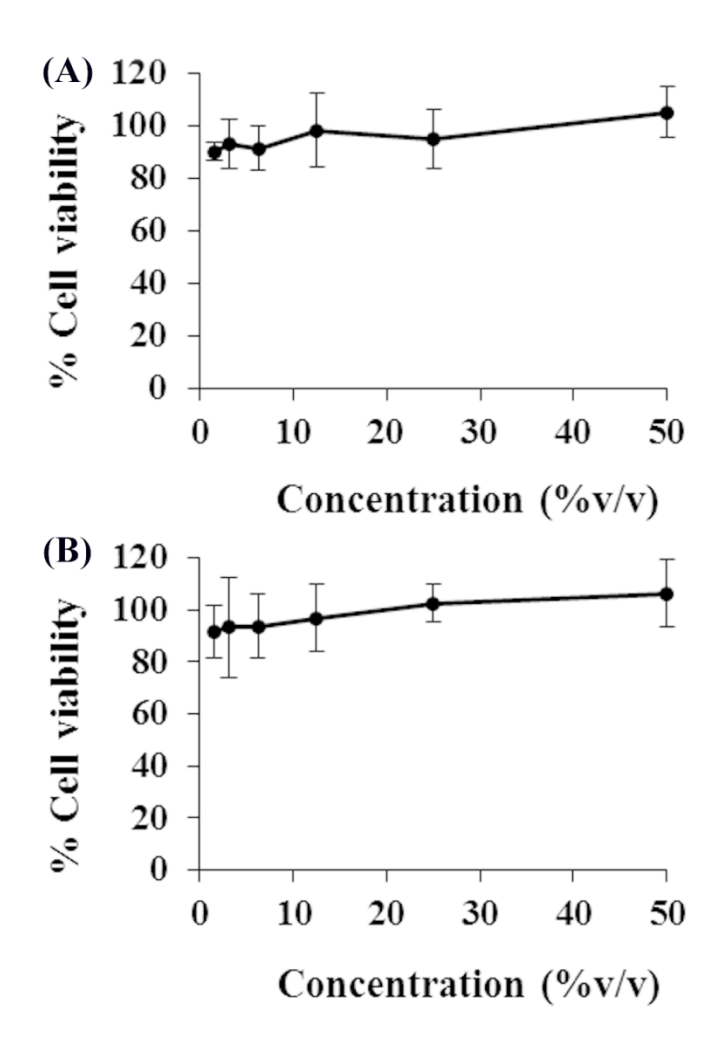
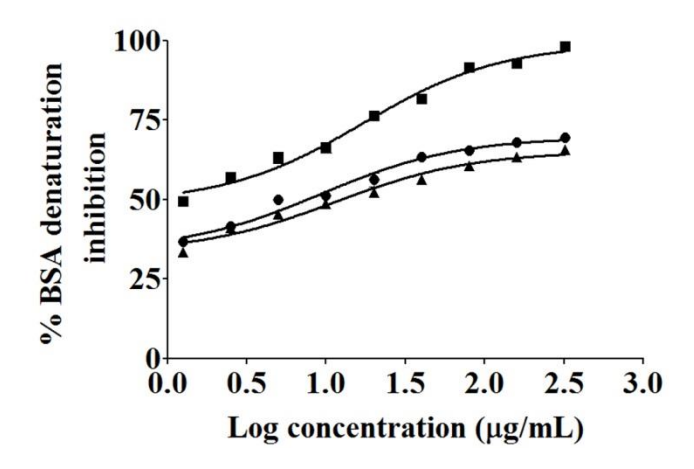


Figure 2: HPLC chromatograms of curcumin standard (A) and HO (B)



**Figure 3:** Dose-response curve of viability of PBMCs versus concentrations of EO (**A**) and HO (**B**) (n = 3)



**Figure 4:** Effect of various concentrations of indomethacin ( $\blacksquare$ ), EO ( $\blacktriangle$ ), and HO ( $\bullet$ ) on inhibition of BSA denaturation

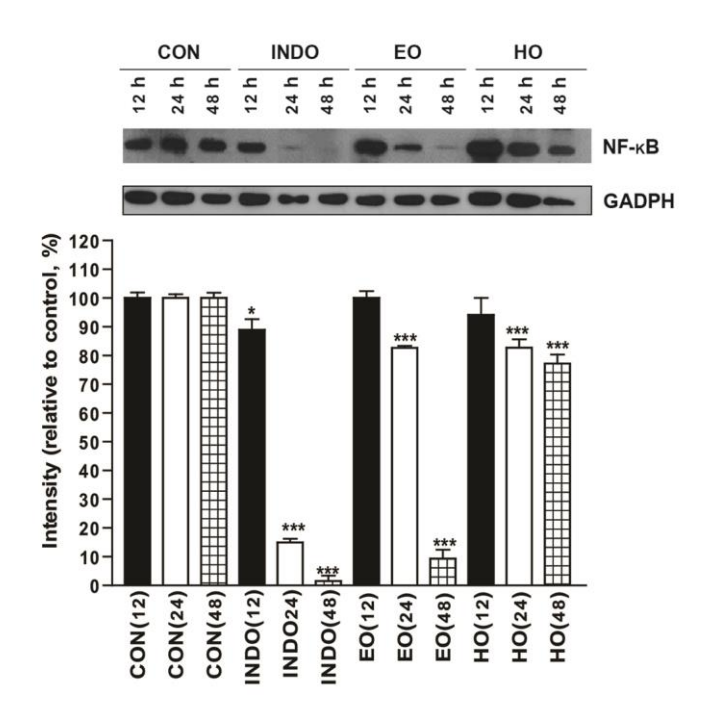


**Figure 5:** Western blotting of NF-κB from U937 cells treated with 7.8  $\mu$ g/mL indomethacin (IND), control (CON), 7.8  $\mu$ g/mL EO, and 7.8  $\mu$ g/mL HO at 12 h (black), 24 h (white), and 48 h (grid) (n = 3, \* denotes P < 0.05, \*\* denotes P < 0.01, \*\*\* denotes P < 0.001)

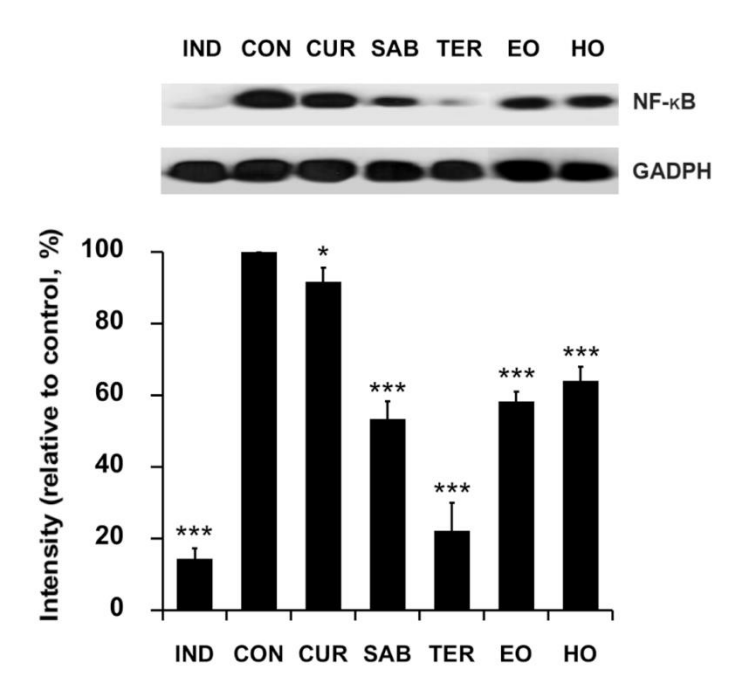


**Figure 6:** Western blotting of NF-κB from U937 cells treated with 7.8 μg/mL indomethacin (IND), control (CON), 7.8 μg/mL curcumin (CUR), 7.8 μg/mL sabinene (SAB), 7.8 μg/mL terpinen-4-ol (TER), 7.8 μg/mL EO, and 7.8 μg/mL HO (n = 3, \* denotes P < 0.05, \*\* denotes P < 0.01, \*\*\* denotes P < 0.001)

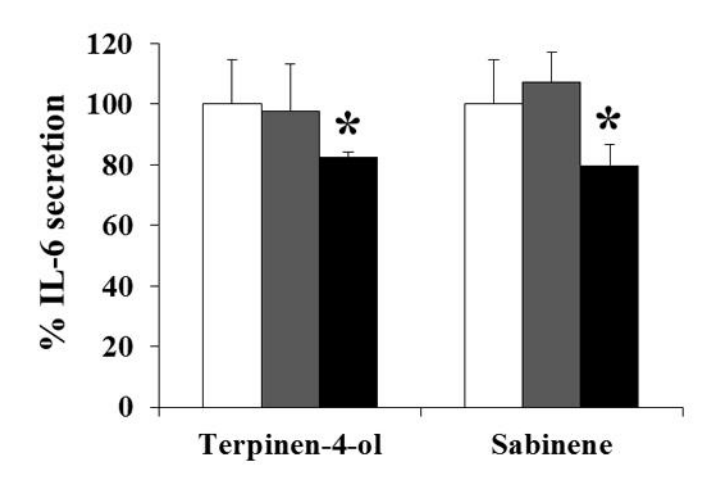


**Figure 7:** IL-6 secretion by the RAW 264.7 cell line after being treated with terpinen-4-ol and sabinene at the concentrations of 5  $\mu$ g/mL (gray) and 50  $\mu$ g/mL (black) compared to control (white) (n = 3, \* denotes P < 0.05)



### การพัฒนาตำรับไมโครอิมัลขันเจลอินโดเมทาซินจากน้ำมันไพลทอด

#### Development of Indomethacin Microemulsion-Based Gel from Hot Extract of Plai



ผู้ทำการวิจัย นศภ. จินตภา วิชญาณรัคน์ และ นศภ. ชวการ สุขเคโชสว่าง อาจารย์ที่ปรึกษา อ.ศร.ภญ. วรรธิดา ขัยญาณะ ภาควิชาวิทยาศาสตร์เภสัชกรรม คณะเภสัชศาสตร์ มหาวิทยาลัยเชียงใหม่

#### ที่มาและความสำคัญ



ไพล (Zingiber cassumunar Roxb.) เป็นพืชสมุนไพรที่มีการใช้สำหรับบรรเทาอาการปวดเมื่อยกล้ามเนื้อมาอย่างยาวนานในประเทศไทย ตามภูมิปัญญาท้องถิ่นมีการใช้ น้ำมันมะพร้าวในการสกัดสารจากเหง้าไพลเพื่อให้ได้น้ำมันไพลทอด แต่มีข้อจำกัดในด้านความไม่สะดวกในการใช้ ล้างออกยาก เหนอะหนะเมื่อทาบนผิว และมีกลิ่นไม่พึงประสงค์ คณะ นักวิจัยจึงมีความสนใจที่จะพัฒนา ผลิตภัณฑ์จากน้ำมันไพลทอดที่มีคุณลักษณะและความคงตัวดี ทั้งยังใช้ได้สะดวก โดยเดรียมเป็นไมโครอิมัลชันเจล เนื่องจากมีข้อดีหลายอย่าง ได้แก่ การเดรียมที่ง่าย ความคงตัวสูง และสามารถนำส่งตัวยาผ่านผิวหนังได้ดี ซึ่งในการศึกษานี้ใช้ตัวยา อินโดเมทาชิน (Indomethacin) เป็นตัวยาสำคัญ

#### > วัตถประสงค์

- 1. เพื่อสกัดสารออกฤทธิ์จากไพลโดยการสกัดร้อนตามวิธีของคนไทยโบราณ
- 2. เพื่อพัฒนาตำรับไมโครอิมัลชันเจลจากน้ำมันไพลสกัดร้อนสำหรับนำส่งตัวยาอินโดเมทาชินที่มีประสิทธิภาพและมีความคงตัวดี
- เพื่อศึกษาการปลดปล่อยตัวยาอินโดเมทาซินจากตำรับไมโครอิมัลชันเจลของน้ำมันไพลสกัดร้อน

#### > คำสำคัญ

ไพล, อินโดเมทาซิน, ไมโครอิมัลซัน, ไมโครอิมัลซันเจล, แผนผังวัฏภาค

# ## Phase diagram ME : Characterization, Stability study ME-I : Characterization, Stability study, Release ME gel : Characterization, Stability study

#### ผลการทดลอง

Pseudoternary phase diagrams

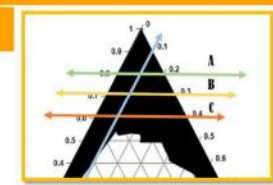


รูปที่ 1 Pseudotemory phase diagrams โดยมีลัดส่วน รัฏภาคน้ำมัน ดังนี้ P:C (1:1) (ก.) , P:C (2:1) (ฆ.) , P:C (1:2) (ค.) , P:C (3:3) (ҳ.) , P:C (3:1) (ฆ.) , P:C (3:2) (ฉ.) , P:C:O (2:1:1) (ฆ.) , P:C:O (3:2:2) (ฆ.)



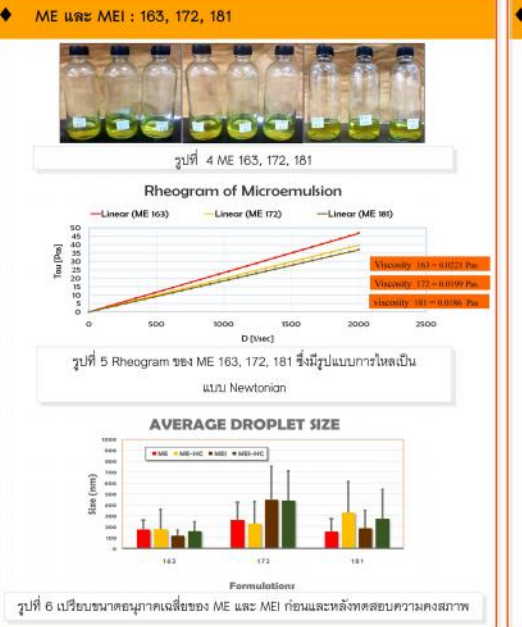
ผลของสารลดแรงตึงผิวผสม

รูปที่ 2 Pseudotemary phase diagrams โดยมีตัดส่วนรัฏภาคตารลด แรงสิงผิวผสม ดังนี้ TX-114 : PEG 400 (3:2) (ก.) , TX-114 : EtOH (3:2) (ข.) , TX-114 : PG (3:2) (ค.) , TX-114 : IPA (3:2) (ง.)

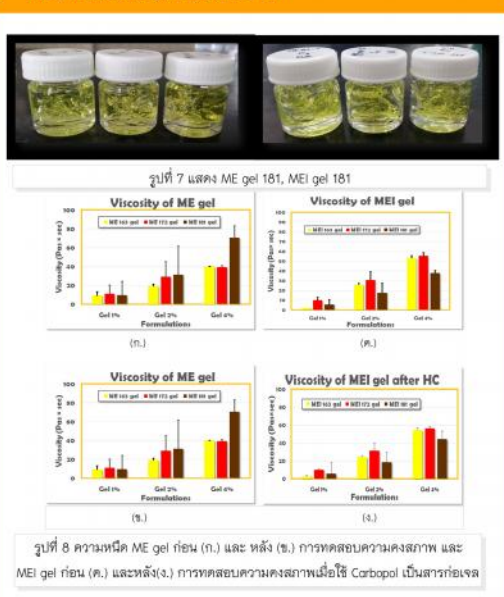


รูปที่ 3 Pseudotemary phase diagrams แสดงคำรับไม่โครยิมัลซัน A.B.C ที่มีลัดส่วน รัฏภาคน้ำ : สารลดแรงตึงผิวผสม : น้ำมัน เท่ากับ 1:6:3, 1:7:2, 1:8:1 ตามสำคับ

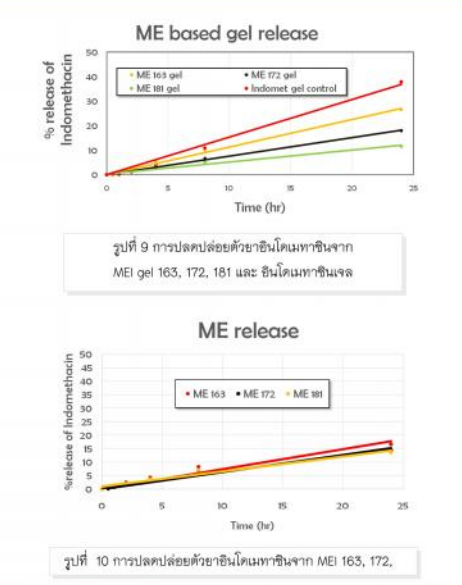
#### ผลการทดลอง



♦ ME gel และ MEI gel : 163, 172, 181



#### 🔷 การทดสอบปลดปล่อยตัวยาอินโดเมทาซินด้วย Dialysis bag



#### สรุปการทดลอง

ตำรับไมโครอิมัลขันเจลอินโดเมทาชินที่ใช้น้ำมันไพลทอดเป็นวัฏภาคน้ำมัน สามารถใช้เป็นระบบนำส่งยาทางผิวหนังได้ เนื่องจากมี คุณลักษณะทางกายภาพที่ดี มีความคงตัวดี ไม่เหนอะหนะ มีความหนีดเหมาะสม สามารถแผ่กระจายบนผิวหนังได้ดี ล้างออกได้ง่าย และตำรับ ที่สามารถปลดปล่อยยาอินโดเมทาชินได้ดีที่สุด คือ ตำรับ MEI gel 163

#### ➤ เอกสารอ้างอิง

- เหลาห สุขการรัฐเกต. น้ำนั้นโดยพระท่างจากน้ำนั้นโดยกันเข่าน้ำว. (2555). (Critine). Available at URL: http://www.phamacy.mahidol.ac.th/thai knowledgenio.phg/id=109. Accessed August 10, 2557.
- Swapnil, suresh valleker, NB,Wankhade, GS,Deoker, "Microemulsion bases get system: A novel approach for topical drug delivery". An internation Journal of Advances in Pharmaceutical Sciences, S. (2014): 1776-1782



## Anti-inflammatory activity of essential oil

and hot infusion oil from Plai rhizome



Chaiyana, W.1\*, Phongpradist, R.1, Anuchapreeda S.2

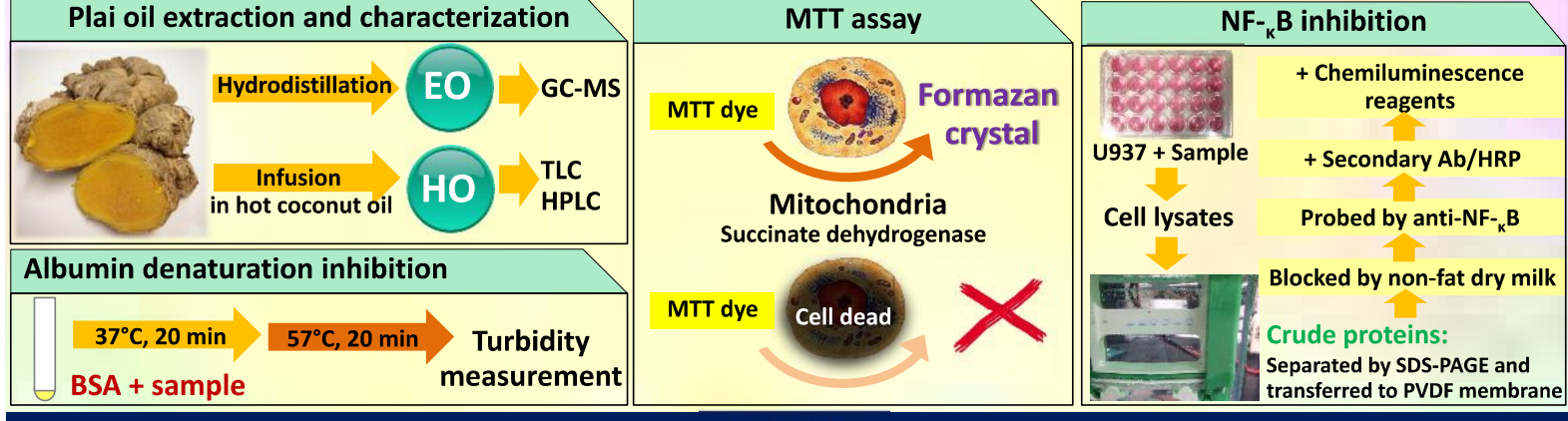
 $^1$ Department of Pharmaceutical Science, Faculty of Pharmacy, Chiang Mai University, Chiang Mai, Thailand <sup>2</sup>Division of Clinical Microscopy, Department of Medical Technology, Faculty of Associated Medical Sciences, Chiang Mai University, Chiang Mai, Thailand

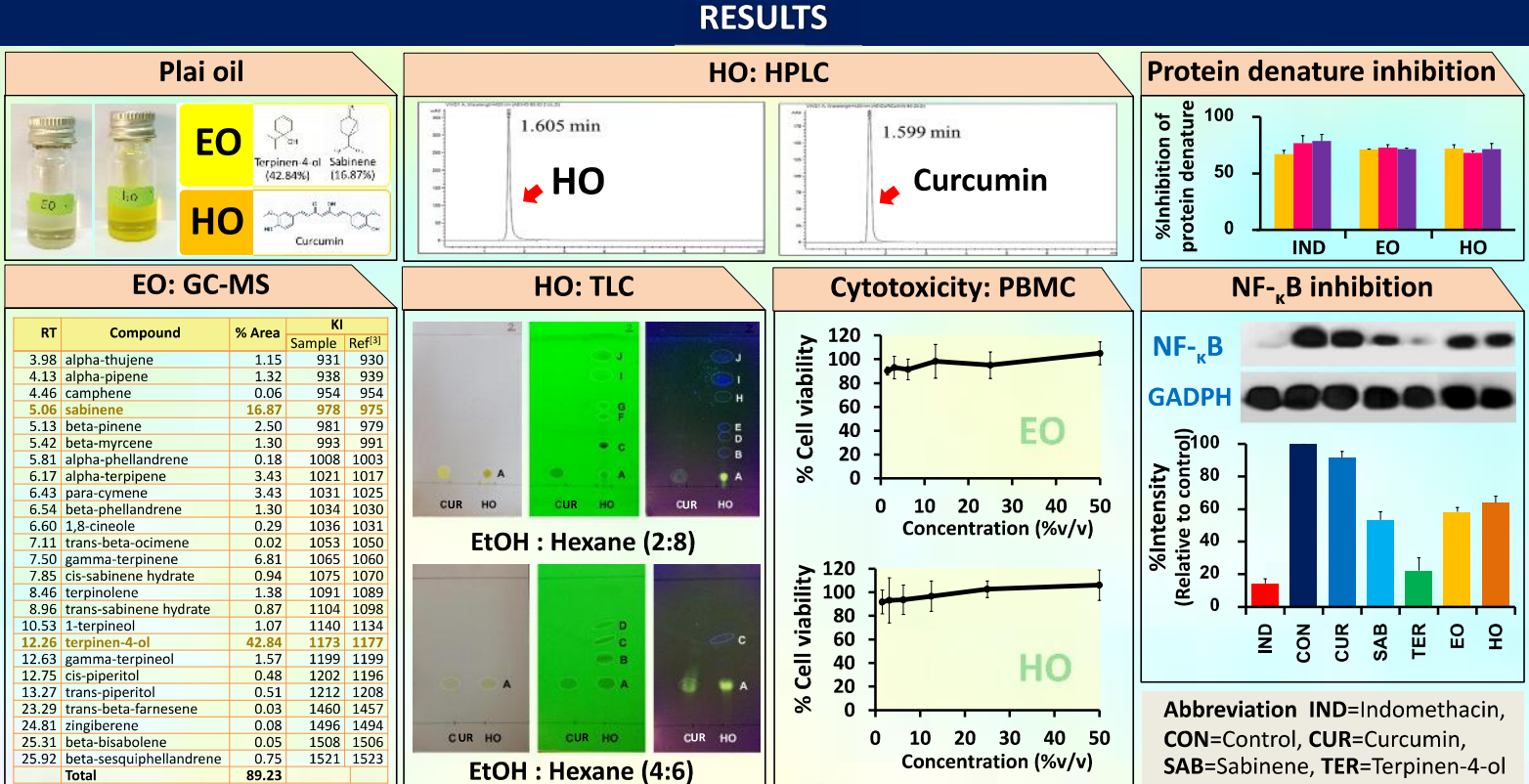
\*e-mail: Aa Rx105@hotmail.com

#### INTRODUCTION

Zingiber cassumunar Roxb. (Plai) is an aromatic plant which is widely distributed in various parts of Thailand. It was used in folklore remedies, especially rheumatism and muscular pain [1]. The rhizome of Z. cassumunar has been used as a component in herbal compress balls and massage oil for muscular pain relief since the ancient time [2]. The aims of the present study were to investigate anti-inflammatory activity and cytotoxicity of Plai oils.

#### **EXPERIMENTALS**





#### CONCLUSION

The major constituents of EO were terpinen-4-ol and sabinene, whereas, curcumin was a major constituent of HO. HO and EO had no toxic effect on human PBMCs and possessed anti-inflammatory activity since they can protect bovine serum albumin against heat denaturation and prevent NF-KB activation. Therefore, both HO and EO are promising oils for the further antianalgesic product development.

#### **ACKNOWLEDGEMENT**

The authors are grateful for financial support received from Thailand [1] Pithayanukul, et. al. 2007. Phytother. Res. 21, 164-169. Research Fund through the TRF grant for new researcher (No. TRG [2] Panthong, et. al. 1997. Phytomedicine, 4, 207-212. 5780029) and Chiang Mai University Grant for New Researcher.

#### **REFERENCES**

- [3] Adams RP. Allured Publishing Co, Carol Stream, IL, USA; 2001.